Studies on interactions of Sarco/Endoplasmic Reticulum Ca^{2+}-ATPase (SERCA) with anti apoptotic protein Bcl-2.

By

C2008

Geetha S. Hewawasam

Submitted to the Department of Chemistry and the Faculty of the Graduate School of the University of Kansas in partial fulfillment of the requirements for the degree of Doctor of Philosophy

Committee members:

_____
George S. Wilson (Chairperson)

_____
Christian Schöneich

_____
Richard Givens

_____
Robert Dunn

_____
Heather Desaire

Date Defended: March 14, 2008

The Dissertation Committee for Geetha S. Hewawasam certifies that this is the approved version of the following dissertation:

Studies on interactions of Sarco/Endoplasmic Reticulum Ca^{2+}-ATPase (SERCA) with anti apoptotic protein Bcl-2.

Committee:

_____
George S. Wilson (Chairperson)

_____
Christian Schöneich

_____
Richard Givens

_____
Robert Dunn

_____
Heather Desaire

Date Approved: March 14, 2008

ABSTRACT:

Bcl-2, an anti-apoptotic member of the Bcl-2 family of proteins, plays a major role in apoptosis regulation at the level of endoplasmic reticulum (ER) by controlling luminal Ca^{2+} concentration of ER through different mechanisms. It has been reported by Dremina et al. that Bcl-2 can directly interact with Sarcoplasmic/Endoplasmic Reticulum Calcium ATPase (SERCA), the Ca^{2+} pump in SR/ER membrane which transports Ca^{2+} from cytoplasm to the lumen of SR/ER, causing inactivation and also translocation of SERCA from Caveolae-Related Domains (CRD) of the SR/ER membrane.

The work reported here are the important characteristics of the SERCA/Bcl-2 interactions using wild type and three mutants, G145E, S24C/C158S and S205C/C158S, of the C-terminal truncated protein, Bcl-2Δ21. Photo and chemical cross-linking of the interacting proteins, Ca^{2+}-ATPase activity assay of SERCA, Sucrose Density Gradient (SDG) fractionation of the SR membrane, immunoprecipitation and the fusion protein GST-Bcl-2Δ21 (GST stands for Glutathione-S-Transferase) binding assay are the approaches used to examine the interaction. Based on the cross-linking studies the two proteins can interact with both 1:1 and 2:1 (Bcl-2Δ21: SERCA) molar ratios. The distance between the interface/interfaces of the Bcl-2Δ21/SERCA complex can range from ~6-14Å. BH1 and BH2 domains (BH stands for Bcl-2 Homology domains which are the conserved domains found in the Bcl-2 family), hence the hydrophobic surface groove of Bcl-2Δ21 is identified as directly involved in the interactions with SERCA whereas the

BH4 domain of Bcl-2Δ21 does not belong to the interface of the Bcl-2Δ21/SERCA complex. Based on mass spectrometric findings, the BH1 domain of Bcl-2Δ21 interacts with the ATP binding domain of SERCA.

According to the immunoprecipitation and GST-Bcl-2Δ21 binding assay experiments all the three mutants, S24C/C158S, S205C/C158S and G145E of Bcl-2Δ21 studied can directly associate with SERCA. However, the G145E mutant is a loss-of-function whereas the two Cys-mutants, S24C/C158S and S205C/C158S, are gain-of-function on SERCA inactivation and translocation, as revealed by Ca^{2+}-ATPase activity assay and Sucrose Density Gradient (SDG) fractionation experiments. Therefore the conserved residue G145 is a critical hot spot for the Bcl-2Δ21-mediated inactivation and translocation of SERCA.

Mitsugumin-29 (Mg29) is a recently found protein expressed in the triad-junction complex which connects the cell surface to the SR membrane of skeletal muscle. Some evidence on the involvement of Mg29 in this Bcl-2Δ21/SERCA interaction and also on the effect of aging in Bcl-2Δ21/SERCA association is reported here. These findings support Bcl-2/SERCA interactions as a possible mechanism of apoptosis control by Bcl-2 through regulation of Ca^{2+} homeostasis at the ER.

Dedicated to my parents

Mr. Ananda S. Hewawasam & Mrs. K. D. Kalyani Waidyarathne

ACKNOWLEDGEMENTS:

When I stop for a moment to look back, at this biggest milestone in my life, there are number of people who helped and inspired me to be the individual who I am today.

First, I would like to express my deep and sincere thanks to my supervisors, Professor George S. Wilson, Department of Chemistry and Professor Christian Schöneich, Department of Pharmaceutical Chemistry of the University of Kansas. Your valuable advice, guidance and support throughout my years in graduate school are greatly appreciated. I never ran into a stressful situation while working with you, since you never pressured me. I always admire this. You both gave me the freedom to explore on my own. It broadened my knowledge a lot and also has had a remarkable impact on my entire carrier. I specially thank you for your comments and advise on preparing my talks. It helped me a lot to improve my presentation skills. The wonderful experience I gained as a graduate student under the supervision of both of you is a great part of my life.

I wish to thank former and present Wilson and Schöneich group members for their tremendous support in many different ways. Because of you I had a nice working environment around me and it made my research life smooth and convenient. In particular, many thanks to Dr. Elena S. Dremina for her important assistance throughout my research work. You were always willing to help me whenever I needed comments and suggestions. In addition, thank to you, I have earned lot of technical skills and I will remember you whenever I make use of those

skills. Also Dr. Giridharan Gokulrangan, former Schöneich group member and Dr. Nadya Galeva, Structural Biology Center of KU, should be thanked for their help in Mass Spectrometry.

Professors Richard Givens, Robert Dunn and Heather Desaire deserve special thanks as thesis committee members. Also I would like to thank the staff members of the Departments of Chemistry and Pharmaceutical Chemistry of KU. Especially, Sonjia Payne, Jan Akers and Beverly Johnson are thanked for all their kind support. The University of Kansas is acknowledged for offering me the opportunity to complete my graduate studies.

Furthermore, I am grateful to the faculty members of the Department of Chemistry of the University of Peradeniya, Sri Lanka, where I completed my undergraduate studies. Specially, Professors D. T. B. Thennakoon, Anura Wickramasinghe and O. A. Ileperuma should be thanked for their encouragement to pursue higher studies in U.S.A. I am also deeply thankful to Professor Veranja Karunarathne and Dr. Nedra Karunarathne for their excellent support while I was trying to adjust to the American culture, during my very first year in the U.S.A.

I owe my sincere gratitude to my aunts, uncles and grand parents (specially, Chuti Punchi, Nona Punchi, Maddu, Hamine Punchi, Thilak Mama, Shom Mama and Jamburegoda Achchi) who have been a tremendous support especially during my childhood. I know how you struggled to raise me while my parents were facing the hardest time in their lives. Thank you so much for loving and caring for me. Also my late grandma, Weligama Achchi (my father's mom) was a big hand during my

elementary education. Anura Bappa (my father's only brother who died of cancer in his early twenties), even though I missed you after I was ten years old, I still remember how you loved me and my siblings. I always believed that your spirit is behind me in all my achievements.

I would like to thank my schools (Sri Sumangala College, Weligama and Sangamitta College, Galle, Sri Lanka) and also my teachers from elementary level to the university entrance level. Without the great educational foundation you have laid, I would not be able to come so far. My loving country, Sri Lanka deserves a special mention. Without the free educational system in Sri Lanka, it would have been impossible for me to be successful in studies. Also many thanks to the Mahapola Higher Education Scholarship, which supported me during my undergraduate years.

Thank you all my friends for cheering me up and for sharing my ups and downs with me. I owe special thanks to my three sisters, Chamila, Dinesha and Ineesha and my brother, Charitha. Loving and entertaining environment you created at home was extremely helpful in my studies. Also thank you for believing in me. It always has been an extra support and a motivation for my life.

I am grateful to my mother-in-law for all her support throughout my thesis-writing period. You took good care of my two kids and also cooked delicious food while letting me concentrate on my thesis.

My special thank goes to loving husband, Mr. Anuruddha Liyanawaduge. Without your understanding, support, loving and caring, encouragements and emotional support none of these accomplishments would have been possible. I cannot

forget my precious daughter, Gagani and son, Chamiru who always brought me a smile when I was tired.

Lastly and most importantly, my deepest gratitude is for my loving parents, Mr. A.S. Hewawasam and Mrs. K.D.K. Waidyarathne. Despite all the hardships, you decided to send me to Sangamitta College, one of the best schools in Sri Lanka. Sound educational foundation I had there drew me to the position where I am today. Ammi, I was always inspired by your determination and strong nature. It helped me to go for my goals and face all ups and downs in my life. Thaththi, your willingness to help anybody, anytime, set a good example for me to interact nicely with people I meet. Dear Ammi and Thaththi, thank you for every thing. I dedicate this thesis to you.

TABLE OF CONTENTS:

Chapter 1:

Introduction, significance and objectives.

1.1: Apoptosis, Bcl-2 family and Bcl-2…….....1

1.2: Ca^{2+} signaling and SERCA……8

1.3: ER/MC apoptotic cross-talk and involvement of Bcl-2……...14

1.4: SRECA/Bcl-2 interactions and objectives of this work…….....16

1.5: References…….....18

Chapter 2:

Interactions of Bcl-2 with SERCA; Using wild type Bcl-2.

2.1: Introduction to the analytical strategies.

2.1.1: Cross-linking in protein-protein interaction studies……27

(a)Photo cross-linking……..28

(b)Chemical cross-linking…...…….....32

2.1.2: Bcl-2Δ21 and His_6-Bcl-2Δ17……..32

2.1.3: Monitoring cysteine derivatization efficiency of Bcl-2Δ21……...33

2.1.4: Analysis of cross-linked products……33

(a) Mass spectrometry in cross-linking studies……33

(b) Western blotting in cross-linking studies……35

2.1.5: GST-Bcl-2Δ21 binding assay……..35

2.2: Materials and methods.

2.2.1: Bcl-2Δ21 expression and purification.

(a) Expression of Bcl-2Δ21……36

(b) Purification of Bcl-2Δ21……..…37

(c) Bcl-2Δ21 Storage Conditions ……38
2.2.2: Isolation of SR Vesicles……...38
2.2.3: Optimization of BPM labeling reaction conditions.
(a) Optimum reaction time……39
(b) Effect of the redox status of Bcl-2Δ2 cysteine……39
(c) Effect of native and denatured Bcl-2Δ21……40
(d) Effect of mild denaturing agents……40
(e) Lowest effective concentration of SDS……41
(f) Comparison of Bcl-2Δ2 and His_6-Bcl-2Δ17 in cysteine derivatization...41
2.2.4: Labeling Cys158 of Bcl-2Δ21/ His_6-Bcl-2Δ17 using optimized conditions……41
2.2.5: Characterization of BPM labeling reaction samples.
(a) RP-HPLC Separation of BPM Labeling Reaction Mixture……42
(b) Mass spectrometric analysis of BPM Labeling Reaction Mixture……..42
(c) Effect of BPM treated Bcl-2Δ21 on Ca^{2+}-ATPase activity of SERCA……...43
2.2.6: Optimization of photo cross-linking reaction conditions
(a) Molar ratio between SERCA and Bcl-2Δ21……44
(b) Incubation time for SERCA and Bcl-2Δ21……..44
2.2.7: Photo cross-linking of BPM treated Bcl-2Δ21/His_6-Bcl-2Δ17 with SERCA using optimized reaction conditions……...…45
2.2.8: Ni^{2+} Affinity Purification of Photo Cross-Linked Products of BPM-His_6-Bcl2Δ17……..46
2.2.9: Chemical Cross-Linking of Bcl-2Δ21 with SERCA.
(a) Starting with Bcl-2 Δ21……...47
(b) Starting with SERCA……...48
2.2.10: Analysis of other possible SR proteins associated with Bcl-2 or SERCA.
(a)Using western blotting……49

(b)Using GST- Bcl-2Δ21 binding assay……49
2.2.11: Comparison of young and old SERCA in photo cross-linking with Bcl-2Δ21……50
2.2.12: Details of SDS-PAGE and western blotting……..……51
2.2.13: Antibodies……..51
2.2.14: In-gel tryptic digestion procedure…….....52

2.3: Results and Discussion.
2.3.1: Expression and purification of Bcl-2Δ21……52
2.3.2: Optimization of BPM labeling reaction conditions.
(a) Optimum reaction time……54
(b) Effect of the redox status of Bcl-2Δ2 cysteine…….54
(c) Effect of native and denatured Bcl-2Δ21…….56
(d) Comparison of Bcl-2Δ2 and His_6-Bcl-2Δ17 in cysteine derivatization...58
2.3.3: Characterization of BPM labeling reaction sample.
(a) RP-HPLC Separation of BPM Labeling Reaction Mixture……59
(b) Mass spectrometric analysis of BPM Labeling Reaction Mixture……..62
(c) Effect of BPM-Bcl-2Δ21 on Ca^{2+}-ATPase activity of SERCA……...63
2.3.4: Photo cross-linking of Bcl-2Δ21 with SERCA……...65
2.3.5: Photo cross-linking of His_6-Bcl-2Δ17 with SERCA……...70
2.3.6: Chemical cross-linking of Bcl-2 Δ21 with SERCA……73
2.3.7: Mass spectrometric analysis of photo cross-linked SERCA/Bcl-2Δ21…..77
2.3.8: Other possible SR proteins associated with Bcl-2Δ21 or SERCA……..87
2.3.9: Comparison of young and old SERCA in photo cross-linking with Bcl-2Δ21……92
2.4: Conclusions……94
2.5: References……...94

Chapter 3:

Effect of Bcl-2 mutants on the interaction with SERCA.

3.1: Introduction to the analytical strategies.

3.1.1: Mutants of Bcl-2Δ21……...…97

3.1.2: Sucrose Density Gradient (SDG) fractionation of SR membranes…….98

3.1.3: Ca^{2+}-ATPase activity assay…….98

3.1.4: Immunoprecipitation and GST-Bcl-2Δ21 binding assay……99

3.1.5: Photo cross-linking of mutants of Bcl-2Δ21with SERCA……100

3.2: Materials and methods.

3.2.1: Site directed mutagenesis of Bcl-2Δ21……..100

3.2.2: Protein expression and purification……...101

3.2.3: Ca^{2+}-ATPase activity assay in the presence of Bcl-2Δ21 mutants……101

3.2.4: Sucrose Density Gradient (SDG) fractionation of SR in the presence of Bcl-2Δ21 mutants……...103

3.2.5: Immunoprecipitation and GST- Bcl-2Δ21 binding assay…….104

3.2.6: Comparison of WT and Cys-mutants of Bcl-2Δ21 in cysteine derivatization……105

3.2.7: Photo cross-linking of Bcl-2Δ21 mutants with SERCA using BPM…….105

3.2.8: Details of SDS-PAGE and Western Blotting……105

3.3: Results and Discussion.

3.3.1: Mutants of Bcl-2Δ21…….106

3.3.2: Effect of mutants of Bcl-2Δ21 on Ca^{2+}-ATPase activity of SERCA……109

3.3.3: Effect of mutants of Bcl-2Δ21 on Sucrose Density Gradient (SDG) fractionation of SR……..113

3.3.4: Association of SERCA with mutants of Bcl-2Δ21; Using GST-Bcl-2Δ21 binding assay and immunoprecipitation…….116

3.3.5: Comparison of WT and Cys-mutants of Bcl-2Δ21 in cysteine derivatization……...120
3.3.6: Mutants of Bcl-2Δ21 in photo cross-linking with SERCA……...122
3.4: Conclusions……127
3.5: References……..127

Chapter 4:

Overall discussion, conclusions and future experiments.

4.1: Overall discussion and conclusions……129
4.2: Future experiments.
4.2.1: Improvement of mass spectrometric identification of cross-linked peptides……137
4.2.2: Effect of W188 of Bcl-2Δ21 on inactivation and translocation of SERCA……...139
4.2.3: Other proteins involved in the interactions of SERCA/Bcl-2Δ21…….141
4.3: References……..142

Chapter 5:

Unresolved issues related to the SERCA/Bcl-2Δ21 investigations ...146
5.1: Derivatization of Cys158 of Bcl-2Δ21 using Benzophenone-4-maleimide (BPM)……...146
5.2: Photo and chemical cross-linking reactions……..147
5.3: Mass spectrometric analysis of cross-linked products……148
5.4: Mutants of Bcl-2Δ21……149

INDEX OF FIGURES:

FIGURE 1.1: Bcl-2 family proteins……3

FIGURE 1.2: Ribbon depiction of the structure of Bcl-2……5

FIGURE 1.3: Topology of Bcl-2……6

FIGURE 1.4: Structure of sarcoplasmic reticulum Ca^{2+}-ATPase (SERCA) from two different angles……...12

FIGURE 2.1: Photo cross-linking of interacting proteins using BPM……...30

FIGURE 2.2: Bottom-up strategy for the analysis of protein cross-links……..34

FIGURE 2.3: Simulated western blots of SERCA/Bcl-2 cross-linking reaction samples……36

FIGURE 2.4: Expression and purification of Bcl-2Δ21……..……..53

FIGURE 2.5: Optimum reaction time for BPM labeling of Bcl-2Δ21 as determined by ThioGlo1 labeling of free cysteine residues……...55

FIGURE 2.6: Redox status of cysteine of Bcl-2Δ21 as determined by ThioGlo1 labeling of free cysteine residues……55

FIGURE 2.7: Comparison of native and denatured Bcl-2Δ21 in BPM labeling, as determined by ThioGlo1 labeling of free cysteine residues……...57

FIGURE 2.8: Comparison of Bcl-2Δ2 and His_6-Bcl-2Δ17 in cysteine derivatization, as determined by ThioGlo1 labeling of free cysteine residues……...58

FIGURE 2.9: Determination of BPM-Bcl-2Δ21 using RP-HPLC separation of the reaction mixture; Chromatograms recorded at 280 nm……..59

FIGURE 2.10: Determination of BPM-Bcl-2Δ21 using RP-HPLC separation of the reaction mixture; Chromatograms recorded at 260 nm……..60

FIGURE 2.11: RP-HPLC separation of BPM labeling reaction mixture after BPM spiking; Chromatograms recorded at 260 nm……...61

FIGURE 2.12: MS/MS spectrum of BPM labeled peptide of Bcl-2Δ21……...62

FIGURE 2.13: Effect of BPM treated Bcl-2Δ21 on Ca^{2+}-ATPase activity of SERCA……...64

Figure 2.14: Photo cross-linking of Bcl-2Δ21 with SERCA……...67

FIGURE 2.15: Photo cross-linking of His_6-Bcl-2Δ17 with SERCA…….70
FIGURE 2.16: Photo cross-linking of His_6-Bcl-2Δ17 with SERCA…….72
FIGURE 2.17: Chemical cross-linking of Bcl-2Δ21 with SERCA……...75
FIGURE 2.18: Chemical cross-linking of Bcl-2Δ21 with SERCA……...77
FIGURE 2.19: Mass Spectrum of $[M+4H]^{+4}$ of the cross-linked SERCA-Bcl-2Δ21 dipeptide……...82
FIGURE 2.20: Mass Spectrum of $[M+3H]^{+3}$ of the cross-linked SERCA-Bcl-2Δ21 dipeptide……...83
FIGURE 2.21: Intensities of the isotopic peaks of $[M+4H]^{+4}$ relative to the control samples……...84
FIGURE 2.22: The 3-D structure of SERCA showing the peptide cross-linked to Bcl-2Δ21…….85
FIGURE 2.23: Affinity purified fractions of photo cross-linking reaction samples…..89
FIGURE 2.24: GST-Bcl-2Δ21 binding assay samples……..91
FIGURE 2.25: Young and old SERCA in photo cross-linking with Bcl-2Δ21…….93
FIGURE 3.1: Mutants of Bcl-2Δ21……..107
FIGURE 3.2: Wild type and mutants of Bcl-2Δ21 analyzed by western blotting with Bcl-2 antibody……...109
FIGURE 3.3: Effect of G145E mutant of Bcl-2Δ21 on the activity of SERCA……..110
FIGURE 3.4: Effect of the Cys-mutants of Bcl-2Δ21 on the activity of SERCA…...112
FIGURE 3.5: Simulated sucrose gradient after fractionation of SR……113
FIGURE 3.6: Location of SERCA in SR/ER membrane…….114
FIGURE 3.7: Effect of mutants of Bcl-2Δ21 on Sucrose Density Gradient (SDG) fractionation of SR……...……115
FIGURE 3.8: Association of SERCA with mutants of Bcl-2Δ21; Using GST-Bcl-2Δ21 binding assay…….118
FIGURE 3.9: Association of SERCA with mutants of Bcl-2Δ21; Using immunoprecipitation……..119

FIGURE 3.10: Comparison of the Cys-mutants with wild type
Bcl-2Δ21 (without SDS) for cysteine derivatization,
as determined by ThioGlo1-Cystein adduct formation…….121
FIGURE 3.11: Comparison of the Cys-mutants with wild type
Bcl-2Δ21 (with SDS) for cysteine derivatization,
as determined by ThioGlo1-Cystein adduct formation…….121
FIGURE 3.12: Bcl-2 antibody western blot of photo cross-linked samples……123
FIGURE 3.13: SERCA antibody western blot of photo cross-linked samples……126
FIGURE 4.1: Effect of W188A mutant of Bcl-2Δ21 on Ca^{2+}-ATPase activity of
SERCA……..140
FIGURE 4.2: Effect of W188A mutant of Bcl-2Δ21 on Sucrose Density Gradient
(SDG) fractionation of SR……141

INDEX OF TABLES AND SCHEMES:

TABLE 2.1: Summery of mass spectrometric results……79
SCHEME 2.1: Benzophenone-4-maleimide (BPM)……...29
SCHEME 2.2: Chemical cross-linking reagents…….31
SCHEME 3.1: Amino acid sequence of wild type Bcl-2Δ21……...106
SCHEME 4.1: *N*-((2-pyridyldithio)ethyl)-4-azidosalicylamide (PEAS)……..138

ABBREVIATIONS:

BH	Bcl-2 homology domains
BMPS	N-[β-maleimidopropyloxy]succinimide ester
BPM	Benzophenone-4-maleimide
CRD	Caveolae-Related Domains
DTT	dithiothreitol
ER	Endoplasmic reticulum
GSH	glutathione
GST	glutathione-S-transferase
His_6	hexahistidine
HSP70	heat shock protein 70
Im	imidazole
IMM	inner mitochondrial membrane
IP	immunoprecipitation
IP_3R	Inositol tris phosphate receptor
IPTG	Isopropyl β-D-thiogalactoside
IRS	Insulin Receptor Substrate
LB	Luria-Bertani medium
MBS	m-maleimidobenzoyl-N-hydroxysuccinimide ester
MC	Mitochondria
mCU	mitochondrial Ca^{2+} uniporters
Mg29	Mitsugumin-29
NHS	N-hydroxysuccinimide
O	old
PCR	Polymerase Chain Reaction
PDB	protein data bank
PEAS	N-((2-pyridyldithio)ethyl)-4-azidosalicylamide
PLN	phospholamban
PMSF	Phenylmethylsulfonyl fluoride

PTP	permeability transition pore
RyR	Ryanodine receptor
SDG	Sucrose Density Gradient
SDS-PAGE	sodium dodecyl sulfate-polyacrylamide gel electrophoresis
SERCA	sarco/endoplasmic reticulum Ca^{2+}-ATPase
SLN	Sarcolipin
SMCC	Succinimidyl 4-(N-maleimidomethyl)cyclohexane-1-carboxylate
SMPH	Succinimidyl-6-[(β-maleimidopropionamido)hexanoate
SR	sarcoplasmic reticulum
STE buffer	Tris-buffered saline containing 7.5 mM Tris (pH 8.0), 150 mM NaCl and 3 mM EDTA
TG	thapsigargin
TM	trans-membrane domain
WB	western blot/blotting
WT	wild type
Y	young

Chapter 1:

Introduction, Significance and Objectives.

1.1: Apoptosis, Bcl-2 family and Bcl-2.

Apoptosis or programmed cell death is an evolutionarily conserved biological process. Proper apoptosis machinery is vital in physiological processes such as fetal development, tissue homeostasis and also in cellular defense mechanisms against pathologies (*1-7*). Impaired apoptosis regulation contributes to numerous diseases including cancer, stroke, heart failure, AIDS, neurodegenerative disorders and auto immune diseases (*1-9*). Molecular mechanisms involved in this programmed cell death machinery are well characterized to date and investigation of underlying mechanisms is important to discover therapeutics to cure diseases associated with altered apoptosis.

There are two well known pathways, intrinsic and extrinsic, for apoptosis. The intrinsic pathway is triggered by intracellularly originated death stimuli whereas in the extrinsic pathway the death stimulus is extracellular. Both these pathways direct the apoptotic cell to undergo number of morphological and biochemical changes. Caspases, a family of intracellular proteases, are directly or indirectly responsible for all these changes. Caspase activation is directly or indirectly regulated by other apoptosis associated intracellular proteins, which act by either activating or inhibiting caspases (*1-7*). Participation of mitochondria in caspase activation in the intrinsic apoptosis pathway is well characterized (*1-7, 10, 11*). Endoplasmic reticulum (ER)

stress-induced caspase activation and also caspase-independent apoptosis are two other newly emerging apoptosis mechanisms (*7*).

Among the various modulators of apoptosis, Bcl-2 family members are well known for their involvement in the mitochondrially-initiated intrinsic apoptosis pathway (*10-19*). The Bcl-2 family is conserved in metazoans and consists of more than two dozens of members (*1-7, 10-16*). Comparison of primary structures of members reveals four conserved amino acid sequence stretches found within the family and each member contains at least one of these four homology motifs known as Bcl-2 homology domains or BH1, BH2, BH3 and BH4. Functionally, Bcl-2 family members are either pro-apoptotic or anti-apoptotic. The balance between pro- and anti-apoptotic members in a cell is important in determining the cell fate. Based on structural and functional similarities, Bcl-2 family can be divided into three sub families; (1) Anti-apoptotic (Pro-survival) members have all four Bcl-2 homology domains (eg. Bcl-2, Bcl-x_L), (2) Multidomain pro-apoptotic members (Bax family) posses BH1, BH2 and BH3 but lacks BH4 (eg.Bax, Bak), (3) BH3-only pro-apoptotic members (eg. Bid, Bad) (*12-16*). Figure 1.1 is a schematic of these three Bcl-2 sub families.

Anti-apoptotic member Bcl-2 is the founding member of the Bcl-2 family in mammals. Since the discovery of Bcl-2, at least 20 Bcl-2 family members have been identified in mammals (*12*). The Bcl-2 gene was found activated by chromosome translocation and the protein was found over expressed in human B-cell lymphomas (*20*). Thereafter, over expressed Bcl-2 was identified in many lymphomas and solid

tumors and Bcl-2 over expression makes those abnormal cells resistant to chemo- and radio-therapy (*21, 22*). This led researchers to investigate cytoprotective mechanisms of Bcl-2.

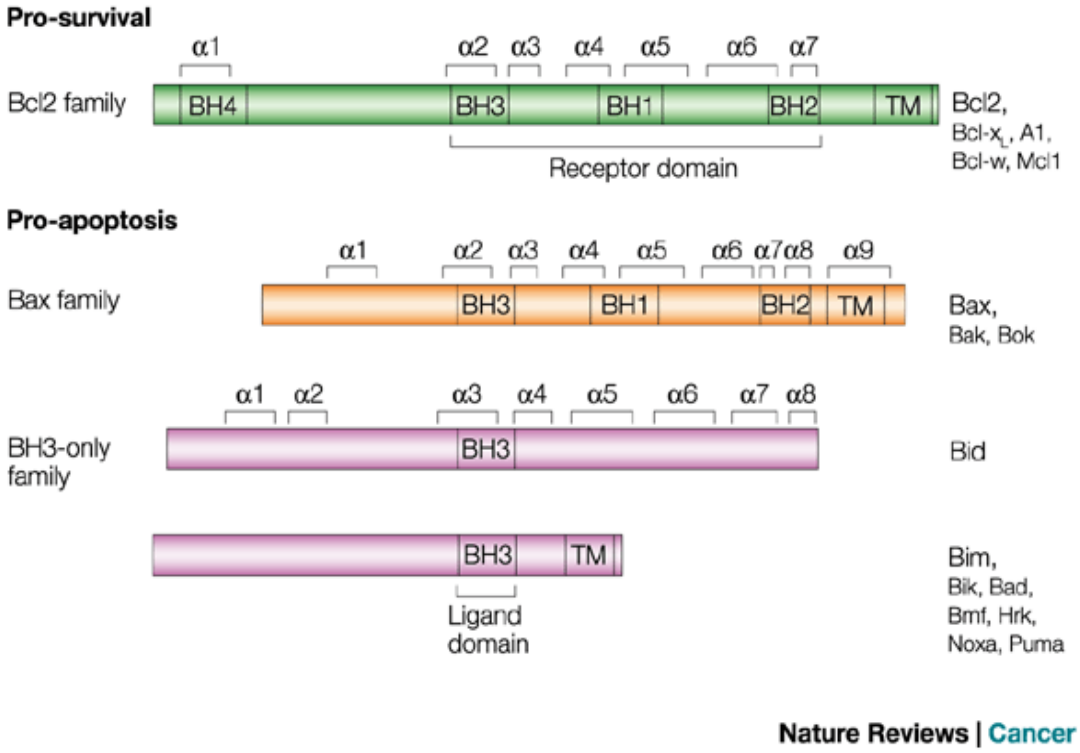

FIGURE 1.1: Bcl-2 family proteins: Bcl-2 family can be divided into three sub families; (1) Anti-apoptotic (Pro-survival) members have all four Bcl-2 homology domains. (2) Multidomain pro-apoptotic members (Bax family) posses BH1, BH2 and BH3 but lacks BH4. (3) BH3-only pro-apoptotic members. (Adapted from Cory, S., and Adams, J.M. (2002) *Nat. Rev. Cancer 2(9),* 647-656.)

Bcl-2 is an integral membrane protein. It contains nine α helices and a long unstructured loop between α1 and α2. The structure of Bcl-2 was first determined using a chimeric protein in which a part of unstructured loop of Bcl-2 was replaced with a part of Bcl-x_L loop. As revealed by this NMR spectroscopic study, Bcl-2 contains two central hydrophobic α helices, α5 and α6, which are surrounded by five other amphipathic helices (*23*). Ribbon depiction of the structure of Bcl-2ΔTM, transmembrane domain truncated Bcl-2, is shown in figure 2. Important feature of this structure is that it has an elongated hydrophobic surface groove formed by α helices in conserved motifs BH1, BH2 and BH3 (*23,24*). The C-terminal hydrophobic helix α9 forms the transmembrane (TM) domain which helps the molecule to anchor to membranes (*24-26*). The two central hydrophobic helices, α5 and α6, are also reported to have membrane insertion properties (*27*). Figure 3 is a cartoon of Bcl-2 indicating different regions and known functions/importance associated with those regions.

Bcl-2 is a multifunctional protein which can insert its cytoprotective action through numerous mechanisms. Some of these mechanisms are well established whereas others are poorly understood or not identified yet. Bcl-2 localizes and plays its cell protective role in different subcellular compartments such as the mitochondrial, endoplasmic reticulum (ER) and nuclear membrane (*28-30*). Role of Bcl-2 at the level of mitochondria is well known (*10-18*) where as its role at the level of the ER is poorly understood and currently under investigation (*31-58*). Currently

known information about the Bcl-2's anti apoptotic activity in the ER will be discussed in detail in section 1.3 of this chapter.

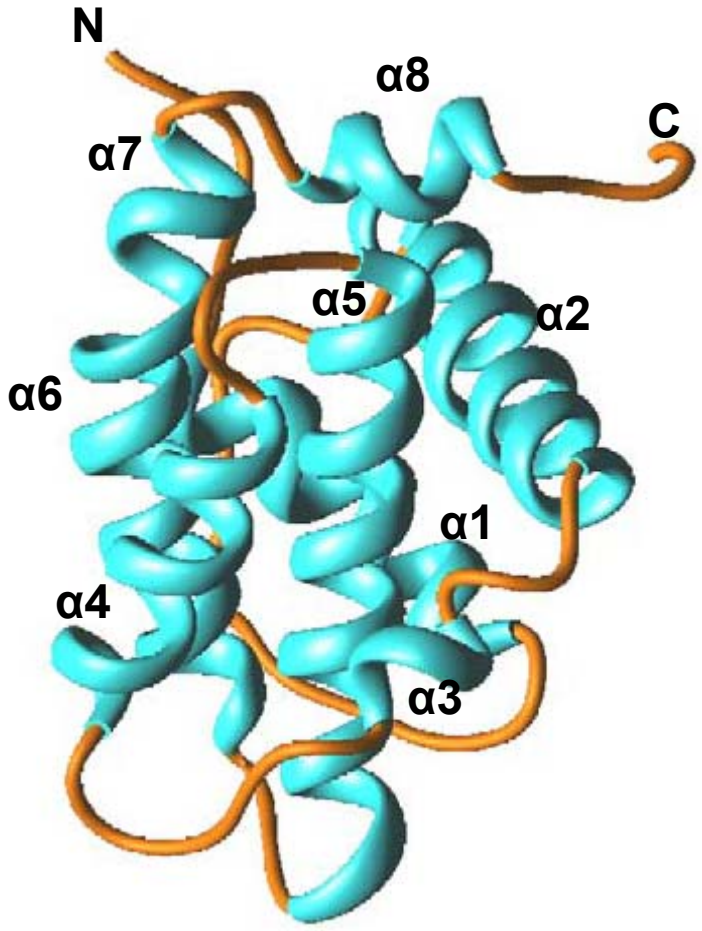

FIGURE 1.2: Ribbon depiction of the structure of Bcl-2: Structure of Bcl-2 was first determined using a truncated Bcl-2/Bcl-x_L chimeric protein in which a part of the unstructured loop of Bcl-2 was replaced with a part of Bcl-x_L loop and the C-terminal 21 amino acids were truncated (23). (Modified from Petros, A.M., Olejniczak, E.T., and Fesik, S.W. (2004) *Biochim. Biophys. Acta. 1644(2-3),* 83-94.)

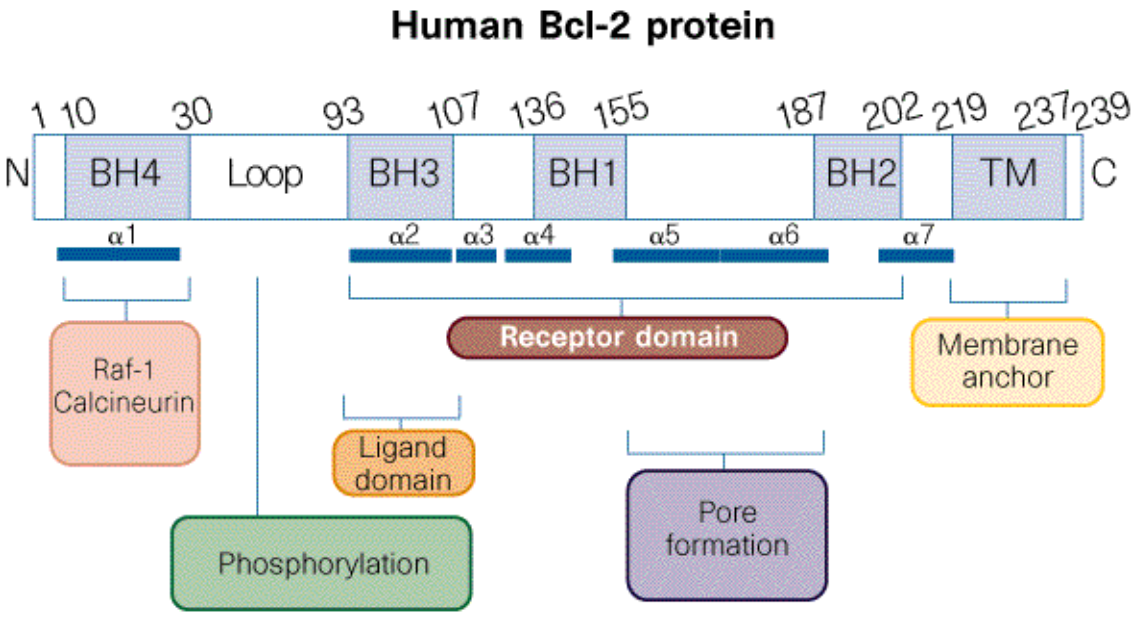

FIGURE 1.3: Topology of Bcl-2: Different helices, domains and associated functions/importance of different regions are indicated. The BH4 domain is known to participate in binding with Raf-1 and Calcineurin, two well known binding partners of Bcl-2. Important phosphorylation sites which regulate activity of Bcl-2 are located in unstructured loop region. The BH3 domain helps in homodimerization and also in hetero dimerization with other Bcl-2 family members. The BH1, BH2 and BH3 domains collectively form the hydrophobic surface groove which acts as the receptor domain for dimerization. Membrane anchoring TM domain includes helices 8 and 9. (Adapted from Reed, J.C. (1997) *Nature 387(6635)*, 773-776.)

Bcl-2 protects mitochondrial membrane integrity while residing on the membrane. Pro-apoptotic BH3-only members can heterodimerize with Bcl-2 and neutralize it by binding to the hydrophobic surface groove of Bcl-2. This leads other pro-apoptotic multi-domain members such as Bax and Bak to homodimerize and form channels on the mitochondrial membrane, disturbing the membrane integrity and releasing cytochrome-c, which in turn activates caspases (*10-19, 25, 26, 28*). Heterodimerization of Bcl-2 with Bax and Bak is also suggested as an explanation for protected mitochondrial membrane integrity by Bcl-2 (*59-63*). However, a direct physical interaction was not revealed by cross-linking (*64*). Bcl-2 is also reported to inhibit opening of permeability transition pore (PTP) in the inner mitochondrial membrane (IMM) preventing cyt-c release through those channels (*10, 11, 14, 15, 17, 65*).

Ability to form ion channels in membranes is another fascinating feature of Bcl-2 in apoptosis regulation (*11, 15, 49, 66-68*). Bcl-x_L, a structural homolog of Bcl-2, shows structural similarity to pore forming domains of bacterial toxins such as diphtheria toxin (69). This suggests that Bcl-x_L / Bcl-2 might form ion channels in membranes regulating ion exchange. In fact they are reported to form ion channels in synthetic membranes in vitro (*11, 70*). Phosphorylation/dephosphorylation status of Bcl-2 is also important in apoptosis regulation. Several serine and threonine residues located in unstructured loop region of Bcl-2 have been identified as phosphorylation sites which affect activity and conformation of Bcl-2 upon phosphorylation. There are reports on altered anti-apoptotic activity due to phosphorylation of Bcl-2 and

physiological kinases and phosphatases involved have been identified (*15, 71-82*). Another anti-apoptotic property of Bcl-2 includes its antioxidative function. Cellular antioxidant capacity is reported to be elevated in Bcl-2 over expressing cells (*10, 73, 83, 84*). Physical and/or functional interactions of Bcl-2 with other non related protein partners is another emerging side of Bcl-2 involvement in apoptosis regulation (*15, 35, 50-58, 68, 76*).

Broadened knowledge of apoptosis-suppression by Bcl-2 helps discovery of new or more effective approaches to treat pathologies such as cancer (*22*). In one approach, Bcl-2 expression in cancer cells is suppressed using anti-sense oligonucleotides and this approach has advanced to Phase III trials (*85*). Also there are several reports of small organic molecules which bind to the hydrophobic groove of Bcl-2 mimicking the binding of BH3 peptides to the groove thus inducing cell viability (*86-89*). New pro-apoptotic drug delivery system including a synthetic BH3 domain peptide was also reported recently (*90*).

1.2: Ca^{2+} signaling and SERCA.

Ca^{2+} is an essential second messenger throughout the lifespan of the cell. Fertilization, proliferation and differentiation, development, learning and memory, contraction, secretion, metabolism and apoptosis are among the important cellular processes which are controlled by Ca^{2+} ions. Cellular Ca^{2+} signaling is a complex network of underlying signaling mechanisms that are tissue specific making the network more complex. Basically this network consists of internally or externally

generated Ca^{2+}–mobilizing signals, ON/OFF mechanisms to control entry and removal of Ca^{2+} ions to and from the cytoplasm, respectively, and various Ca^{2+}-sensitive processes which are triggered by Ca^{2+} changes within the cell. Proper control of Ca^{2+} signaling is of vital importance for healthy life and various receptors, ion channels, pumps, exchangers and Ca^{2+} binding proteins which act as buffers, are important participants in controlling Ca^{2+} signaling (*91-93*).

The endoplasmic reticulum (ER) (sarcoplasmic reticulum (SR) in muscle cells) is the cellular Ca^{2+} storage compartment. ER/SR has the ability to hold Ca^{2+} within the concentration range of 100-1000μM and this $[Ca^{2+}]_{ER/SR}$ is 10^3-10^4 times higher compared to $[Ca^{2+}]_C$, cytosolic free Ca^{2+} concentration, which is about 0.1 μM (*94*). ER/SR Ca^{2+} uptake, storage and release is controlled by three major classes of Ca^{2+}-regulatory proteins. Luminal Ca^{2+}-binding proteins such as calsequestrin and calreticulin help Ca^{2+}-storage. Ca^{2+}-release channels such as Ryanodine receptor (RyR) and Inositol tris phosphate receptor (IP_3R) help Ca^{2+}-release whereas sarco/endoplasmic reticulum Ca^{2+}-ATPase (SERCA), the calcium pump, helps uptake of Ca^{2+}(*95,96*).

More than ten isoforms of SERCA have been identified to date which are generated by alternative splicing of three separate genes SERCA1, 2 and 3. Fast-twitch skeletal muscle isoforms, SERCA1a and SERCA1b are found in adult and fetal tissue, respectively. Cardiac and slow-twitch skeletal muscle isoform is SERCA2a. Both non-muscle tissues and smooth muscles contain SERCA2b. SERCA2c and SERCA2d are relatively rare isoforms. SERCA3a, SERCA3b and

SERCA3c are found in non muscle cells such as platelets, lymphoid cells and endothelial cells while SERCA3d-SERCA3f are detected only at the mRNA level (*96, 97*). Even though these SERCA isoforms show significant similarities in primary structure, they have evolved for specialized functions depending on the cellular environment (*98-102*).

SERCA is a monomeric transmembrane protein of 110 kDa and its a P-type Ca^{2+}-ATPase. It hydrolyses ATP and undergoes autophosphorylation of a conserved aspartate residue, upon Ca^{2+} transport. The energy derived from hydrolysis of one ATP molecule is used to transport two Ca^{2+} ions from the cytoplasm to the lumen against a concentration gradient across the ER/SR membrane (*97, 98*). The crystal structure of SERCA reveals a transmembrane domain consisting of ten helices (M1-M10) and a cytosolic head piece of a mixture of α helices and β strands (*103,104*). The cytosolic head piece consists of three main domains: A-domain (actuator or anchor domain –residues 1-50 and 131-238), P-domain (phosphorylation domain – residues 330-359 and 605-737) and N-domain (nucleotide/ATP binding domain – residues 360-604) (*96,103*). Out of these three domains, the N-domain is the largest (~27 kDa) and A-domain is the smallest (~16 kDa) (*104*). More than half of the molecule belongs to this cytoplasmic head piece while only small loops between TM helices are exposed in the luminal side. The four trans membrane helices M4, M5, M6 and M8 form the Ca^{2+} ion transporting channel and coordinating residues of high affinity Ca^{2+} binding sites are also located in these four helices (*105-107*). The P and N domains together form the active site for ATP hydrolysis and Asp351 of the P-

domain is the site of autophosphorylation (*105,106*). Structure of the sarcoplasmic reticulum Ca^{2+}-ATPase is shown in Figure 4 (*104*).

According to the popular E1/E2 model for explaining the Ca^{2+} transport mechanism, SERCA switches its conformation back and forth between two different conformations, the high Ca^{2+} affinity E1 state and the low Ca^{2+} affinity E2 state. A number of sequential steps complete the transport cycle (*105,106,108*). The high affinity E1 state is achieved by binding of two Ca^{2+} ions to SERCA. Then, binding of ATP to the N-domain, hydrolysis of bound ATP and autophosphorylation of the P-domain leads to E1-P, the phosphorylated form of the E1 state. Next, ADP is dissociated and the conformation changes to E2-P, the phosphorylated form of the E2 state, resulting in dissociation of bound Ca^{2+}. Finally, hydrolytic cleavage of the phosphate group on Asp351 converts the molecule back to E2 state completing the cycle. In the E1 state, high affinity Ca^{2+} binding sites are accessible from the cytoplasmic side where as in the E2 state, low affinity Ca^{2+} binding sites are exposed to the lumen. Therefore the conformational switch from E1 to E2 results in Ca^{2+} transport from the cytoplasm to the lumen (*105,106,108*).

There are specific amino acid residues that directly contribute to the process while some residues help indirectly, by stabilizing directly involved neighboring residues. Based on mutational and structural analysis, Thr441, Glu442, Phe487, Arg489, Lys492, Lys515, Arg560 and Leu562 have been identified as critical ATP binding residues of the N-domain (*109-113*). Asp351, Thr 625, Lys 684 and Thr 353

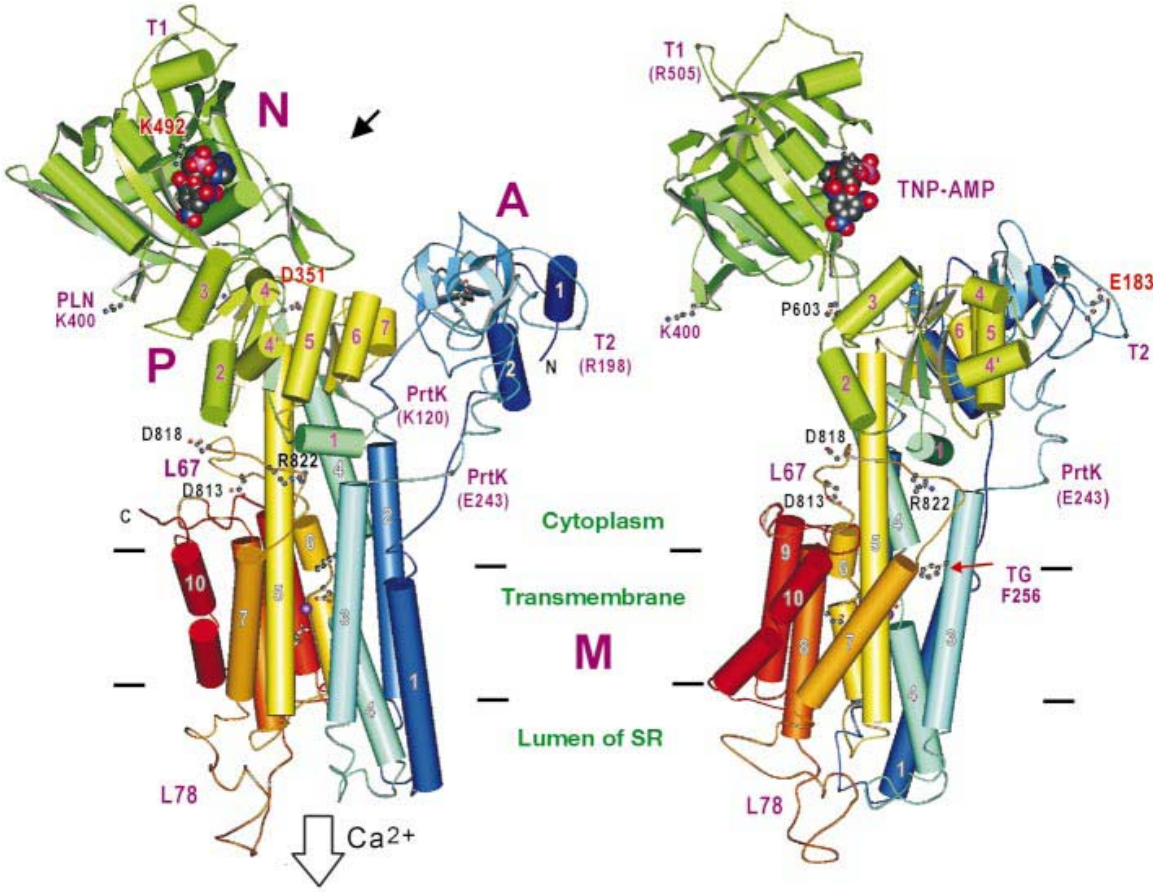

FIGURE 1.4: Structure of sarcoplasmic reticulum Ca^{2+}-ATPase (SERCA) from two different angles: Cylinders and arrows are used to represent α-helices and β-strands respectively. The N, P and A domains are labeled. The Helices in TM, A and P domains are numbered. TNP-AMP, an ATP analog, shows the ATP binding site within the N-domain. Phosphorylation site (D351), binding sites for the inhibitors phospholamban (PLN) and thapsigargin (TG), major digestion sites for trypsin (T1 and T2) and proteinase K (PrtK) are marked. (Adapted from Toyoshima, C., Nakasako, M., Nomura, H., and Ogawa, H. (2000) *Nature 405 (6787)*, 647-55.)

of the P-domain bind with phosphate (*109*). Inter-domain interactions and relative positional changes of domains play a vital role in completing the Ca^{2+} transport cycle. Arg560 of the N-domain and Asp627 of the P-domain interact with each other facilitating inter-domain interactions between the N and P domains, required for ATP binding and autophosphorylation (*109*). During the E1/E2 conformational transition, the A-domain rotates and forms hydrogen bonds with several residues in the N and P domains changing the environment around the phosphorylation residue. This in turn facilitates hydrolysis of the phosphate group on Asp351. Also these inter-domain interactions aid in opening of the luminal gate for Ca^{2+} ions (*106*). Several acidic residues located in luminal loops between transmembrane helices also participate in this Ca^{2+} transport process (*114*).

Various regulators of enzymatic activity of SERCA have been identified to date. Phospholamban (PLN) is a well characterized small protein regulator of SERCA. It can reversibly inhibit SERCA by reducing the affinity for Ca^{2+} (*115-120*). Sarcolipin (SLN) is another regulator of SERCA. This small proteolipid increases V_{max} for Ca^{2+} transport while reducing apparent Ca^{2+} affinity for SERCA. (*121*). Also SLN can regulate SERCA by association with PLN (*122,123*). Insulin Receptor Substrate (IRS) proteins, HSP70 and Phosphatidylinositol 3-kinase (PI3-kinase) are three other identified proteins which can bind with and/or regulate SERCA (*124-126*). Post translational modifications such as phosphorylation, oxidation and nitration are also considered to be involved in regulation of SERCA activity (*127-129*). Also membrane lipids might involve in regulation of SERCA activity (*130-132*).

1.3: ER/MC apoptotic cross-talk and involvement of Bcl-2.

Mitochondria (MC) and endoplasmic reticulum(ER) interact both physically and functionally regulating Ca^{2+} signaling events within the cell (*133-136*). Under normal physiological conditions Ca^{2+} ions are actively pumped into ER by SERCA. Stored Ca^{2+} is released transiently back into the cytoplasm passively by Inositol tris phosphate receptor (IP_3R) and Rynodine Receptor (RyR), Ca^{2+} release channels in ER membrane (*137*). MC sense this released Ca^{2+} and a significant fraction of it is captured using mitochondrial Ca^{2+} uniporters (mCU) (*133,137*). Release of this Ca^{2+} to cytoplasm through mitochondrial Na^{+}/Ca^{2+} exchangers allows recycling of Ca^{2+} back into the ER(*137*). This Ca^{2+} recycling process is efficient due to the close localization of the two organelles (*134,138*). Apoptosis is one of the cellular processes in which Ca^{2+} signaling plays a crucial role, especially in the mitochondrial-generated intrinsic pathway of apoptosis. Concentration of Ca^{2+} in ER determines the magnitude of Ca^{2+} signal which enters the MC and higher mitochondrial Ca^{2+} signals can trigger the mitochondrial-generated intrinsic apoptosis pathway (*1-7, 10, 11, 137*).

Cellular processes that increase $[Ca^{2+}]_{ER}$ level and/or enhance Ca^{2+} transport from ER to MC are apoptogenic. Overexpression of SERCA causes elevated $[Ca^{2+}]_{ER}$ leading to cell death (44,*137*). Bcl-2 family members are known to regulate $[Ca^{2+}]_{ER}$ level and/or Ca^{2+} transfer from the ER to MC (*31-35,45-47,137,139-144*). There are a number of reports in this regard, involving Bcl-2, an antiapoptotic member of Bcl-2 family. The very first evidence that Bcl-2 can protect cells from apoptosis by

inhibiting ER/MC Ca^{2+} cross-talk, was reported by Baffy et al. in 1993 (47). In a later study, Cyt-c release induced by BFA (cyt-c release inducing drug) is blocked by both wild type and an ER targeted variant of Bcl-2, indicating its involvement in Ca^{2+} regulated apoptotic cross-talk between the ER and MC (*31*). Jacobson et al. noticed inhibition of apoptosis by over expression of Bcl-2 in cells lacking mitochondrial DNA. This suggests a protective effect of Bcl-2, independent of mitochondrial respiration (*39*). After this, a number of groups investigated the role of Bcl-2 at the ER level. One group reported that Bcl-2 over expression reduced Ca^{2+} efflux from the ER lumen to the cytoplasm, suggesting that Bcl-2 can directly or indirectly control the Ca^{2+} flux across the ER membrane regulating apoptotic Ca^{2+} signals (*40*). Supporting this, other groups found that Bcl-2 overexpression can reduce the steady state Ca^{2+} concentration in the ER and also Ca^{2+} influx rate which is activated by Ca^{2+} store depletion while increasing the Ca^{2+} permeability of the ER membrane (34, 36, *42-44*). However others reported, that Bcl-2 can inhibit apoptosis by maintaining Ca^{2+} influx thus preserving $[Ca^{2+}]_{ER}$ in thapsigargin (Ca^{2+} pump inhibitor) treated cells (41). Overall, these studies prove the capability of Bcl-2 to control Ca^{2+} signaling thus protecting cells while residing in the ER.

Since both reduction or preservation of $[Ca^{2+}]_{ER}$ is seen, Bcl-2 should have different mechanisms to control influx/efflux of Ca^{2+} across the ER membrane depending upon the condition of the apoptotic cell. However, the underlying mechanisms are still not clear and under investigation. There are evidence that Bcl-2 can control Ca^{2+} level in ER through interaction with other Bcl-2 family members

(*36,38*).There are reports that the phosphorylation /dephosphorylation status of Bcl-2 is important in reducing the steady state Ca^{2+} concentration in the ER. Phosphorylation of Bcl-2 inhibits its ability to lower $[Ca^{2+}]_{ER}$ (*82*). Protein Phosphatase 2A (PP2A) has been identified as a regulator of phosphorylation of Bcl-2 at the ER membrane (*81*). Ability of Bcl-2 to form ion channels in membranes is believed to be another important means for controlling $[Ca^{2+}]_{ER}$ (*15,27,43,49,66-70*). However, Chami et al. found that the reduction of $[Ca^{2+}]_{ER}$ by Bcl-2 is independent of the putative pore forming domains (α5 and α6)(36). Antioxidant properties of Bcl-2 at ER are also reported (*48*). Also it is evident that Bcl-2 can regulate $[Ca^{2+}]_{ER}$ through physical and functional interactions with other ER proteins (*50-58*). Bcl-2 is reported to interact with IP_3R, calcium release channels in the ER membrane, thereby inhibiting Ca^{2+} release through the channel (*50*). Calcineurin (PP2B), a calmodulin-dependent protein phosphatase, dephosphorylates IP_3R, reducing Ca^{2+} leak and Bcl-2 is reported to directly interact with this calcineurin-IP_3R complex (*51, 52*). Another important interaction partner of Bcl-2 at ER is SERCA, the calcium pump in the ER membrane (*54-56*). This SERCA/Bcl-2 interaction is the subject of the work reported in this dissertation.

1.4: SRECA/Bcl-2 interactions and objectives of this work.

Physical interaction of Bcl-2 with SERCA was first reported by Kuo et.al. in 1998 using immunoprecipitation (*54*). Recently Dremina et al. were also able to co-immunoprecipitate SERCA1, fast-twitch skeletal muscle isoform, with both full-

length Bcl-2 and truncated form, Bcl-2Δ21. They also reported irreversible inactivation and translocation of SERCA from caveolae-related domains (CRD) of the SR membrane as a result of the interaction with Bcl-2 (*55, 56*).

Based on above mentioned studies, direct physical and functional interaction of Bcl-2 with SERCA is obvious. However, very little/nothing is known to date, about the characteristics of this interaction. Therefore characterization of SERCA/Bcl-2 interaction is undoubtedly a huge contribution to the knowledge of anti-apoptotic mechanisms of Bcl-2. This understanding would in turn be a new area of research for pharmacologists in discovering novel therapeutics for treating apoptosis resistant, Bcl-2 overexpressing pathological conditions such as cancer. This necessity of understanding SERCA/Bcl-2 interaction set the following objectives of the work reported in this dissertation;

1. Characterization of the site/sites of SERCA involved in the interaction.
2. Identification of residues/domains of Bcl-2 which are critical for this interaction.

The analytical strategies used to fulfill the above objectives and the results will be discussed in the following chapters.

1.5: References.

1. Yan, N., and Shi, Y. (2005) Mechanisms of apoptosis through structural biology, *Annu. Rev. Cell Dev. Biol. 21, 35-56.*
2. Martin, D.A., and Elkon, K.B. (2004) Mechanisms of apoptosis, *Rheum. Dis. Clin. North Am. 30(3),*441-454.
3. Kukhta, V.K., Marozkina, N.V., Sokolchik, I.G., and Bogaturova, E.V. (2003) Molecular mechanisms of apoptosis, *Ukr. Biokhim. Zh. 75(6),* 5-9.
4. Delhalle, S., Duvoix, A., Schnekenburger, M., Morceau, F., Dicato, M., and Diederich, M. (2003) An introduction to the molecular mechanisms of apoptosis, *Ann. N. Y. Acad. Sci. 1010,* 1-8.
5. Reed, J.C. (2000) Mechanisms of apoptosis. *Am. J. Pathol. 157(5),* 1415-30.
6. Saini, K.S., and Walker, N.I. (1998) Biochemical and molecular mechanisms regulating apoptosis, *Mol. Cell. Biochem. 178(1-2),* 9-25.
7. Vermeulen, K., Van Bockstaele, D.R., and Berneman, Z.N. (2005) Apoptosis: mechanisms and relevance in cancer, *Ann. Hematol. 84(10),* 627-639.
8. Allen, D.A., Yaqoob, M.M., and Harwood, S.M. (2005) Mechanisms of high glucose-induced apoptosis and its relationship to diabetic complications, *J. Nutr. Biochem. 16(12),* 705-713.
9. Narula, J., Haider, N., Arbustini, E., and Chandrashekhar, Y. (2006) Mechanisms of disease: apoptosis in heart failure--seeing hope in death, *Nat. Clin. Pract. Cardiovasc. Med. 3(12),* 681-8.
10. Mignotte, B., and Vayssiere, J.L. (1998) Mitochondria and apoptosis, *Eur. J. Biochem. 252(1),* 1-15.
11. Green, D.R., and Reed, J.C. (1998) Mitochondria and apoptosis, *Science 281(5381),* 1309-1312.
12. Cory, S., and Adams, J.M. (2002) The Bcl2 family: regulators of the cellular life-or-death switch, *Nat. Rev. Cancer 2(9),* 647-656.
13. Adams, J.M., and Cory, S. (1998) The Bcl-2 protein family: arbiters of cell survival, *Science 281(5381),* 1322-1326.
14. Reed, J.C. (1998) Bcl-2 family proteins, *Oncogene 17(25),* 3225-3236.
15. Tsujimoto, Y. (1998) Role of Bcl-2 family proteins in apoptosis: apoptosomes or mitochondria? *Genes Cells. 11,* 697-707.
16. Gross, A., McDonnell, J.M., and Korsmeyer, S. J. (1999) BCL-2 family members and the mitochondria in apoptosis, *Genes Dev. 13(15),* 1899-1911.
17. Shimizu, S., Narita, M., and Tsujimoto, Y. (1999) Bcl-2 family proteins regulate the release of apoptogenic cytochrome c by the mitochondrial channel VDAC, *Nature 399(6735),* 483-487.
18. Scorrano, L., and Korsmeyer, S.J. (2003) Mechanisms of cytochrome c release by proapoptotic BCL-2 family members, *Biochem. Biophys. Res. Commun. 304(3),* 437-444.
19. Wei, M.C., Lindsten, T., Mootha, V.K., Weiler, S., Gross, A., Ashiya, M., Thompson, C.B., and Korsmeyer, S.J. (2000) tBID, a membrane-targeted death ligand, oligomerizes BAK to release cytochrome c, *Genes Dev. 14(16),* 2060-2071.
20. Tsujimoto, Y., Finger, L.R., Yunis, J., Nowell, P.C., and Croce, C.M. (1984) Cloning of the chromosome breakpoint of neoplastic B cells with the t(14;18) chromosome translocation, *Science 226(4678),* 1097-1099.
21. Tsujimoto, Y., Cossman, J., Jaffe, E., and Croce, C.M. (1985) Involvement of the bcl-2 gene in human follicular lymphoma, *Science 228(4706),* 1440-1443.

22. Reed, J.C., Miyashita, T., Takayama, S., Wang, H.G., Sato, T., Krajewski, S., Aimé-Sempé, C., Bodrug, S., Kitada, S., and Hanada, M. (1996) BCL-2 family proteins: regulators of cell death involved in the pathogenesis of cancer and resistance to therapy, *J. Cell. Biochem. 60(1),* 23-32.
23. Petros, A.M., Medek, A., Nettesheim, D.G., Kim, D.H., Yoon, H.S., Swift, K., Matayoshi, E.D., Oltersdorf, T., and Fesik, S.W. (2001) Solution structure of the antiapoptotic protein bcl-2, *Proc. Natl. Acad. Sci. U. S. A. 98(6),* 3012-3017. Epub 2001 Feb 27.
24. Petros, A.M., Olejniczak, E.T., and Fesik, S.W. (2004) Structural biology of the Bcl-2 family of proteins, *Biochim. Biophys. Acta. 1644(2-3),* 83-94.
25. Janiak, F., Leber, B., and Andrews, D.W. (1994) Assembly of Bcl-2 into microsomal and outer mitochondrial membranes, *J. Biol. Chem. 269(13),* 9842-9849.
26. Nguyen, M., Millar, D.G., Yong, V.W., Korsmeyer, S.J., and Shore, G.C. (1993) Targeting of Bcl-2 to the mitochondrial outer membrane by a COOH-terminal signal anchor sequence, *J. Biol. Chem. 268(34),* 25265-25268.
27. García-Sáez, A.J., Mingarro, I., Pérez-Payá, E., and Salgado, J. (2004) Membrane-insertion fragments of Bcl-xL, Bax, and Bid, *Biochemistry 43(34),* 10930-10943.
28. Hockenbery, D., Nuñez, G., Milliman, C., Schreiber, R.D., and Korsmeyer, S.J. (1990) Bcl-2 is an inner mitochondrial membrane protein that blocks programmed cell death, *Nature 348(6299),* 334-336.
29. Akao, Y., Otsuki, Y., Kataoka, S., Ito, Y., and Tsujimoto, Y. (1994) Multiple subcellular localization of bcl-2: detection in nuclear outer membrane, endoplasmic reticulum membrane, and mitochondrial membranes, *Cancer Res. 54(9),* 2468-2471.
30. Krajewski, S., Tanaka, S., Takayama, S., Schibler, MJ., Fenton, W., and Reed, J.C. (1993) Investigation of the subcellular distribution of the bcl-2 oncoprotein: residence in the nuclear envelope, endoplasmic reticulum, and outer mitochondrial membranes, *Cancer Res. 53(19),* 4701-4714.
31. Häcki, J., Egger, L., Monney, L., Conus, S., Rossé, T., Fellay, I., and Borner, C. (2000) Apoptotic crosstalk between the endoplasmic reticulum and mitochondria controlled by Bcl-2, *Oncogene 19(19),* 2286-2295.
32. Thomenius, M.J., and Distelhorst, C.W. (2003) Bcl-2 on the endoplasmic reticulum: protecting the mitochondria from a distance, *J. Cell Sci. 116(Pt 22),* 4493-4499.
33. Sheikh, M.S., and Huang, Y. (2004) TRAIL death receptors, Bcl-2 protein family, and endoplasmic reticulum calcium pool, *Vitam. Horm. 67,*169-188.
34. Oakes, S.A., Opferman, J.T., Pozzan, T., Korsmeyer, S.J., Scorrano, L., Oakes, S.A., Opferman, J.T., Pozzan, T., Korsmeyer, S.J., and Scorrano, L. (2003) Regulation of endoplasmic reticulum Ca2+ dynamics by proapoptotic BCL-2 family members, *Biochem. Pharmacol. 66(8),* 1335-1340.
35. Rong, Y., and Distelhorst, C.W. (2007) Bcl-2 Protein Family Members: Versatile Regulators of Calcium Signaling in Cell Survival and Apoptosis, *Annu. Rev. Physiol.* [Epub ahead of print].
36. Chami, M., Prandini, A., Campanella, M., Pinton, P., Szabadkai, G., Reed, J.C., and Rizzuto, R. (2004) Bcl-2 and Bax exert opposing effects on Ca2+ signaling, which do not depend on their putative pore-forming region, *J. Biol. Chem. 279(52),* 54581-54589.
37. Rudner, J., Jendrossek, V., and Belka, C. (2002) New insights in the role of Bcl-2 Bcl-2 and the endoplasmic reticulum, *Apoptosis 7(5),* 441-447.
38. Pinton, P., and Rizzuto, R. (2006) Bcl-2 and Ca2+ homeostasis in the endoplasmic reticulum, *Cell Death Differ. 13(8),* 1409-1418.

39. Jacobson, M.D., Burne, J.F., King, M.P., Miyashita, T., Reed, J.C., and Raff, M.C. (1993) Bcl-2 blocks apoptosis in cells lacking mitochondrial DNA. *Nature 361(6410),* 365-369.
40. Lam, M., Dubyak, G., Chen, L., Nuñez, G., Miesfeld, R.L., and Distelhorst, C.W. (1994) Evidence that BCL-2 represses apoptosis by regulating endoplasmic reticulum-associated Ca2+ fluxes, *Proc. Natl. Acad. Sci. U. S. A. 91(14),* 6569-6573.
41. He, H., Lam, M., McCormick, T.S., and Distelhorst, C.W. (1997) Maintenance of calcium homeostasis in the endoplasmic reticulum by Bcl-2, *J. Cell Biol. 138(6),* 1219-1228.
42. Pinton, P., Ferrari, D., Magalhães, P., Schulze-Osthoff, K., Di Virgilio, F., Pozzan, T., and Rizzuto, R. (2000) Reduced loading of intracellular Ca(2+) stores and downregulation of capacitative Ca(2+) influx in Bcl-2-overexpressing cells, *J. Cell Biol. 148(5),* 857-862.
43. Foyouzi-Youssefi, R., Arnaudeau, S., Borner, C., Kelley, W.L., Tschopp, J., Lew, D.P., Demaurex, N., and Krause, K.H. (2000) Bcl-2 decreases the free Ca2+ concentration within the endoplasmic reticulum, *Proc. Natl. Acad. Sci. U. S. A. 97(11),* 5723-5728.
44. Pinton, P., Ferrari, D., Rapizzi, E., Di Virgilio, F., Pozzan, T., and Rizzuto, R. (2001) The Ca2+ concentration of the endoplasmic reticulum is a key determinant of ceramide-induced apoptosis: significance for the molecular mechanism of Bcl-2 action, *EMBO J. 20(11),* 2690-2701.
45. Magnelli, L., Cinelli, M., Turchetti, A., and Chiarugi, V.P. (1994) Bcl-2 overexpression abolishes early calcium waving preceding apoptosis in NIH-3T3 murine fibroblasts, *Biochem. Biophys. Res. Commun. 204(1),* 84-90.
46. Wang, N.S., Unkila, M.T., Reineks, E.Z., and Distelhorst, C.W. (2001) Transient expression of wild-type or mitochondrially targeted Bcl-2 induces apoptosis, whereas transient expression of endoplasmic reticulum-targeted Bcl-2 is protective against Bax-induced cell death, *J. Biol. Chem. 276(47),* 44117-44128.
47. Baffy, G., Miyashita, T., Williamson, J.R., and Reed, J.C. (1993) Apoptosis induced by withdrawal of interleukin-3 (IL-3) from an IL-3-dependent hematopoietic cell line is associated with repartitioning of intracellular calcium and is blocked by enforced Bcl-2 oncoprotein production, *J. Biol. Chem. 268(9),* 6511-6519.
48. Distelhorst, C.W., Lam, M., and McCormick, T.S. (1996) Bcl-2 inhibits hydrogen peroxide-induced ER Ca2+ pool depletion, *Oncogene 12(10),* 2051-2055.
49. Kim PK, Annis MG, Dlugosz PJ, Leber B, Andrews DW. (2004) During apoptosis bcl-2 changes membrane topology at both the endoplasmic reticulum and mitochondria, *Mol. Cell 14(4),* 523-529.
50. Chen, R., Valencia, I., Zhong, F., McColl, K.S., Roderick, H.L., Bootman, M.D., Berridge, M.J., Conway, S.J., Holmes, A.B., Mignery, G.A., Velez, P., and Distelhorst, C.W. (2004) Bcl-2 functionally interacts with inositol 1,4,5-trisphosphate receptors to regulate calcium release from the ER in response to inositol 1,4,5-trisphosphate. *J. Cell Biol. 166(2),* 193-203.
51. Erin, N., Bronson, S.K., and Billingsley, M.L. (2003) Calcium-dependent interaction of calcineurin with Bcl-2 in neuronal tissue, *Neuroscience 117(3),* 541-555.
52. Shibasaki, F., Kondo, E., Akagi, T., and McKeon, F. (1997) Suppression of signalling through transcription factor NF-AT by interactions between calcineurin and Bcl-2, *Nature 386(6626),* 728-731.

53. Tagami, S., Eguchi, Y., Kinoshita, M., Takeda, M., and Tsujimoto, Y. (2000) A novel protein, RTN-XS, interacts with both Bcl-XL and Bcl-2 on endoplasmic reticulum and reduces their anti-apoptotic activity, *Oncogene 19(50),* 5736-5746.
54. Kuo, T.H., Kim, H.R., Zhu, L., Yu, Y., Lin, H.M., and Tsang, W. (1998) Modulation of endoplasmic reticulum calcium pump by Bcl-2, *Oncogene 17(15),* 1903-1910.
55. Dremina, E.S., Sharov, V.S., Kumar, K., Zaidi, A., Michaelis, E.K., and Schöneich, C. (2004) Anti-apoptotic protein Bcl-2 interacts with and destabilizes the sarcoplasmic/endoplasmic reticulum Ca2+-ATPase (SERCA), *Biochem. J. 383(Pt 2),* 361-370.
56. Dremina, E.S., Sharov, V.S., and Schöneich, C. (2006) Displacement of SERCA from SR lipid caveolae-related domains by Bcl-2: a possible mechanism for SERCA inactivation, *Biochemistry 45(1),* 175-184.
57. Dremina, E.S., Sharov, V.S., and Schöneich, C. (2006) HSP70 Protection Against the Inactivation of SERCA by Anti-Apoptotic Protein Bcl-2: a Possible Link Between Apoptosis, Oxidative Stress and Aging, *Free Radical Biol. Med. 41(1),* S80.
58. Ng, F.W., and Shore, G.C. (1998) Bcl-XL cooperatively associates with the Bap31 complex in the endoplasmic reticulum, dependent on procaspase-8 and Ced-4 adaptor, *J. Biol. Chem. 273(6),* 3140-3143.
59. Conus, S., Kaufmann, T., Fellay, I., Otter, I., Rossé, T., and Borner, C. (2000) Bcl-2 is a monomeric protein: prevention of homodimerization by structural constraints, *EMBO J. 19(7),* 1534-1544.
60. Hanada, M., Aimé-Sempé, C., Sato, T., and Reed, J.C. (1995) Structure-function analysis of Bcl-2 protein. Identification of conserved domains important for homodimerization with Bcl-2 and heterodimerization with Bax, *J. Biol. Chem. 270(20),* 11962-11969.
61. Sattler, M., Liang, H., Nettesheim, D., Meadows, R.P., Harlan, J.E., Eberstadt, M., Yoon, H.S., Shuker, S.B., Chang, B.S., Minn, A.J., Thompson, C.B., and Fesik, S.W. (1997) Structure of Bcl-xL-Bak peptide complex: recognition between regulators of apoptosis, *Science 275(5302),* 983-986.
62. Otter, I., Conus, S., Ravn, U., Rager, M., Olivier, R., Monney, L., Fabbro, D., amd Borner, C. (1998) The binding properties and biological activities of Bcl-2 and Bax in cells exposed to apoptotic stimuli, *J. Bio.l Chem. 273(11),* 6110-6120.
63. Zhang, Z., Lapolla, S.M., Annis, M.G., Truscott, M., Roberts, G.J., Miao, Y., Shao, Y., Tan, C., Peng, J., Johnson, A.E., Zhang, X.C., Andrews, D.W., and Lin, J. (2004) Bcl-2 homodimerization involves two distinct binding surfaces, a topographic arrangement that provides an effective mechanism for Bcl-2 to capture activated Bax, *J. Biol. Chem. 279(42),* 43920-43928.
64. Mikhailov, V., Mikhailova, M., Pulkrabek, D.J., Dong, Z., Venkatachalam, M.A., and Saikumar, P. (2001) Bcl-2 prevents Bax oligomerization in the mitochondrial outer membrane, *J. Biol. Chem. 276(21),* 18361-18374.
65. Martinou, J.C., and Green, D.R. (2001) Breaking the mitochondrial barrier, *Nat. Rev. Mo.l Cell Biol. 2(1),* 63-67.
66. Schendel, S.L., Xie, Z., Montal, M.O., Matsuyama, S., Montal, M., and Reed, J.C. (1997) Channel formation by antiapoptotic protein Bcl-2, *Proc. Natl. Acad. Sci. U. S. A. 94(10),* 5113-5118.
67. Schendel, S.L., Montal, M., and Reed, J.C. (1998) Bcl-2 family proteins as ion-channels, *Cell Death Differ. 5(5),* 372-380.
68. Reed, J.C. (1997) Double identity for proteins of the Bcl-2 family, *Nature 387(6635),* 773-776.

69. Muchmore, S.W., Sattler, M., Liang, H., Meadows, R.P., Harlan, J.E., Yoon, H.S., Nettesheim, D., Chang, B.S., Thompson, C.B., Wong, S.L., Ng, S.L., and Fesik, S.W. (1996) X-ray and NMR structure of human Bcl-xL, an inhibitor of programmed cell death, *Nature 381(6580),* 335-341.
70. Minn, A.J., Vélez, P., Schendel, S.L., Liang, H., Muchmore, S.W., Fesik, S.W., Fill, M., and Thompson, C.B. (1997) Bcl-x(L) forms an ion channel in synthetic lipid membranes, *Nature 385(6614),* 353-357.
71. Ito, T., Deng, X., Carr, B., and May, W.S. (1997) Bcl-2 phosphorylation required for anti-apoptosis function, *J. Biol. Chem. 272(18),* 11671-11673.
72. Ruvolo, P.P., Deng, X., May, W.S. (2001) Phosphorylation of Bcl2 and regulation of apoptosis, *Leukemia 15(4),* 515-522.
73. Agostinis, P. (2003) Bcl2 phosphorylation: a tie between cell survival, growth, and ROS, *Blood 102(9),* 3079.
74. Deng, X., Gao, F., Flagg, T., and May, W.S. Jr. (2004) Mono- and multisite phosphorylation enhances Bcl2's antiapoptotic function and inhibition of cell cycle entry functions, *Proc. Natl. Acad. Sci. U. S. A. 101(1),* 153-158.
75. Basu, A., DuBois, G., and Haldar, S. (2006) Posttranslational modifications of Bcl2 family members--a potential therapeutic target for human malignancy, *Front. Biosci. 11,* 1508-1521.
76. Deng, X., Gao, F., Flagg, T., Anderson, J., and May, W.S. (2006) Bcl2's flexible loop domain regulates p53 binding and survival, *Mol. Cell. Biol. 26(12),* 4421-4434.
77. Tamura, Y., Simizu, S., Osada, H. (2004) The phosphorylation status and anti-apoptotic activity of Bcl-2 are regulated by ERK and protein phosphatase 2A on the mitochondria, *FEBS Lett. 569(1-3),* 249-255.
78. Du, L., Lyle, C.S., and Chambers, T.C. (2004) Characterization of vinblastine-induced Bcl-xL and Bcl-2 phosphorylation: evidence for a novel protein kinase and a coordinated phosphorylation/dephosphorylation cycle associated with apoptosis induction, *Oncogene 24(1),* 107-117.
79. Jiffar, T., Kurinna, S., Suck, G., Carlson-Bremer, D., Ricciardi, M.R., Konopleva, M., Andreeff, M., and Ruvolo, P.P. (2004) PKC alpha mediates chemoresistance in acute lymphoblastic leukemia through effects on Bcl2 phosphorylation, *Leukemia, 18(3),* 505-512.
80. Ishikawa, Y., Kusaka, E., Enokido, Y., Ikeuchi, T., and Hatanaka, H. (2003) Regulation of Bax translocation through phosphorylation at Ser-70 of Bcl-2 by MAP kinase in NO-induced neuronal apoptosis, *Mol. Cell. Neurosci. 24(2),* 451-459.
81. Lin, S.S., Bassik, M.C., Suh, H., Nishino, M., Arroyo, J.D., Hahn, W.C., Korsmeyer, S.J., and Roberts, T.M (2006) PP2A regulates BCL-2 phosphorylation and proteasome-mediated degradation at the endoplasmic reticulum, *J. Biol. Chem. 281(32),* 23003-23012.
82. Bassik, M.C., Scorrano, L., Oakes, S.A., Pozzan, T., and Korsmeyer, S.J. (2004) Phosphorylation of BCL-2 regulates ER Ca2+ homeostasis and apoptosis, *EMBO J. 23(5),* 1207-1216.
83. Voehringer, D.W., and Meyn, R.E. (2000) Redox aspects of Bcl-2 function, *Antioxid. Redox Signal. 2(3),* 537-550.
84. Jang, J.H., and Surh, Y.J. (2003) Potentiation of cellular antioxidant capacity by Bcl-2: implications for its antiapoptotic function. *Biochem. Pharmacol. 66(8),* 1371-1379.
85. Nicholson, D.W. (2000) From bench to clinic with apoptosis-based therapeutic agents, *Nature 407(6805),* 810-816.

86. Wang, J.L., Liu, D., Zhang, Z.J., Shan, S., Han, X., Srinivasula, S.M., Croce, C.M., Alnemri, E.S., and Huang, Z. (2000) Structure-based discovery of an organic compound that binds Bcl-2 protein and induces apoptosis of tumor cells, *Proc. Natl. Acad. Sci. U. S. A. 97(13),* 7124-7129.
87. Kim, K.M., Giedt, C.D., Basañez, G., O'Neill, J.W., Hill, J.J., Han, Y.H., Tzung, S.P., Zimmerberg, J., Hockenbery, D.M., and Zhang, K.Y. (2001) Biophysical characterization of recombinant human Bcl-2 and its interactions with an inhibitory ligand, antimycin A, *Biochemistry 40(16),* 4911-4922.
88. Tzung, S.P., Kim, K.M., Basañez, G., Giedt, C.D., Simon, J., Zimmerberg, J., Zhang, K.Y., and Hockenbery, D.M. (2001) Antimycin A mimics a cell-death-inducing Bcl-2 homology domain 3, *Nat. Cell Biol. 3(2),* 183-191.
89. Degterev, A., Lugovskoy, A., Cardone, M., Mulley, B., Wagner, G., Mitchison, T., and Yuan, J. (2001) Identification of small-molecule inhibitors of interaction between the BH3 domain and Bcl-xL, *Nat. Cell Biol. 3(2),* 173-182.
90. Dharap, S.S., Chandna, P., Wang, Y., Khandare, J.J., Qiu, B., Stein, S., and Minko, T. (2006) Molecular targeting of BCL2 and BCLXL proteins by synthetic BCL2 homology 3 domain peptide enhances the efficacy of chemotherapy, *J. Pharmacol. Exp. Ther. 316(3),* 992-998.
91. Berridge, M.J., Lipp, P., and Bootman, M.D. (2000) The versatility and universality of calcium signaling, *Nat. Rev. Mol. Cell. Biol. 1(1),* 11-21.
92. Carafoli, E. (2002) Calcium signaling: a tale for all seasons, *Proc. Natl. Acad. Sci. U. S. A. 99(3),* 1115-1122.
93. Clapham, D.E. (1995) Calcium signaling, *Cell 80(2),* 259-268.
94. Hajnóczky, G., Davies, E., and Madesh, M. (2003) Calcium Signaling and apoptosis, *Biochem. Biophys. Res. Commun. 304(3),* 445-454.
95. Divet, A., Paesante, S., Bleunven, C., Anderson, A., Treves, S., and Zorzato, F. (2005) Novel sarco(endo)plasmic reticulum proteins and calcium homeostasis in striated muscles, *Muscle Re. Cell Motil. 26(1),* 7-12.
96. Rossi, A.E., and Dirksen, R.T. (2006) Sarcoplasmic reticulum: the dynamic calcium governor of muscle, *Muscle Nerve. 33(6),* 715-731.
97. Periasamy, M., and Kalyanasundaram, A. (2007) SERCA pump isoforms: their role in calcium transport and disease, *Muscle Nerve. 35(4),* 430-442.
98. East, J.M. (2000) Sarco(endo)plasmic reticulum calcium pumps: recent advances in our understanding of structure/function and biology (review), *Mol. Membr. Biol. 17(4),* 189-200.
99. Lytton, J., Westlin, M., Burk, S.E., Shull, G.E., and MacLennan, D.H. (1992) Functional comparisons between isoforms of the sarcoplasmic or endoplasmic reticulum family of calcium pumps, *J. Biol. Chem. 267(20),* 14483-14489.
100. Dode, L., Andersen, J.P., Leslie, N., Dhitavat, J., Vilsen, B., and Hovnanian, A. (2003) Dissection of the functional differences between sarco(endo)plasmic reticulum Ca2+-ATPase (SERCA) 1 and 2 isoforms and characterization of Darier disease (SERCA2) mutants by steady-state and transient kinetic analyses, *J. Biol. Chem. 278(48),* 47877-47889.
101. Dode, L., Vilsen, B., Van Baelen, K., Wuytack, F., Clausen, J.D., and Andersen, J.P. (2002) Dissection of the functional differences between sarco(endo)plasmic reticulum Ca2+-ATPase (SERCA) 1 and 3 isoforms by steady-state and transient kinetic analyses, *J. Biol. Chem. 277(47),* 45579-45591.

102. Toyofuku, T., Kurzydlowski, K., Lytton, J., and MacLennan, D.H. (1992) The nucleotide binding/hinge domain plays a crucial role in determining isoform-specific Ca2+ dependence of organellar Ca(2+)-ATPases, *J. Biol. Chem. 267(20),* 14490-14496.
103. Martonosi, A.N., and Pikula, S. (2003) The structure of the Ca2+-ATPase of sarcoplasmic reticulum, *Acta. Biochim. Pol. 50(2),* 337-365.
104. Toyoshima, C., Nakasako, M., Nomura, H., and Ogawa, H. (2000) Crystal structure of the calcium pump of sarcoplasmic reticulum at 2.6 A resolution, *Nature 405(6787),* 647-655.
Toyoshima, C., and Mizutani, T. (2004) Crystal structure of the calcium pump with a bound ATP analogue, *Nature 430(6999),* 529-535.
105. Lancaster, C.R. (2002) A P-type ion pump at work, *Nat. Struct. Biol. 9(9),* 643-645.
106. Toyoshima, C., Nomura, H., and Sugita, Y. (2003) Structural basis of ion pumping by Ca(2+)-ATPase of sarcoplasmic reticulum, *FEBS Lett. 555(1),* 106-110.
107. Andersen, J.P., and Vilsen, B. (1998) Structure-function relationships of the calcium binding sites of the sarcoplasmic reticulum Ca(2+)-ATPase, *Acta. Physiol. Scand. Suppl. 643,* 45-54.
108. MacLennan, D.H., Rice, W.J., and Green, N.M. (1997) The mechanism of Ca2+ transport by sarco(endo)plasmic reticulum Ca2+-ATPases, *J. Biol. Chem. 272(46),* 28815-28818.
109. Ma, H., Lewis, D., Xu, C., Inesi, G., and Toyoshima, C. (2005) Functional and structural roles of critical amino acids within the"N", "P", and "A" domains of the Ca2+ ATPase (SERCA) headpiece, *Biochemistry 44(22),* 8090-8100.
110. McIntosh, D.B., Clausen, J.D., Woolley, D.G., MacLennan, D.H., Vilsen, B., and Andersen, J.P. (2003) ATP binding residues of sarcoplasmic reticulum Ca2+-ATPase, *Ann. N. Y. Acad. Sci. 986,*101-105.
111. Clausen, J.D., McIntosh, D.B., Vilsen, B., Woolley, D.G., and Andersen, J.P. (2003) Importance of conserved N-domain residues Thr441, Glu442, Lys515, Arg560, and Leu562 of sarcoplasmic reticulum Ca2+-ATPase for MgATP binding and subsequent catalytic steps. Plasticity of the nucleotide-binding site, *J. Biol. Chem. 278(22),* 20245-20258.
112. Hua, S., Ma, H., Lewis, D., Inesi, G., and Toyoshima, C. (2002) Functional role of "N" (nucleotide) and "P" (phosphorylation) domain interactions in the sarcoplasmic reticulum (SERCA) ATPase, *Biochemistry 41(7),* 2264-2272.
113. Abu-Abed, M., Mal, T.K., Kainosho, M., MacLennan, D.H., and Ikura, M. (2002) Characterization of the ATP-binding domain of the sarco(endo)plasmic reticulum Ca(2+)-ATPase: probing nucleotide binding by multidimensional NMR, *Biochemistry 41(4),* 1156-1164.
114. Webb, R.J., Khan, Y.M., East, J.M., and Lee, A.G. (2000) The importance of carboxyl groups on the lumenal side of the membrane for the function of the Ca(2+)-ATPase of sarcoplasmic reticulum, *J. Biol. Chem. 275(2),* 977-982.
115. Kimura, Y., Kurzydlowski, K., Tada, M., and MacLennan, D.H. (1997) Phospholamban inhibitory function is activated by depolymerization, *J. Biol. Chem. 272(24),* 15061-15064.
116. Asahi, M., Kimura, Y., Kurzydlowski, K., Tada, M., and MacLennan, D.H. (1999) Transmembrane helix M6 in sarco(endo)plasmic reticulum Ca(2+)-ATPase forms a functional interaction site with phospholamban. Evidence for physical interactions at other sites, *J. Biol. Chem. 274(46),* 32855-32862.

117. Chen, Z., Stokes, D.L., Rice, W.J., and Jones, L.R. (2003) Spatial and dynamic interactions between phospholamban and the canine cardiac Ca2+ pump revealed with use of heterobifunctional cross-linking agents, *J. Biol. Chem. 278(48),* 48348-48356.
118. Toyoshima, C., Asahi, M., Sugita, Y., Khanna, R., Tsuda, T., and MacLennan, D.H. Modeling of the inhibitory interaction of phospholamban with the Ca2+ ATPase, *Proc. Natl. Acad. Sci. U. S. A. 100(2),* 467-472.
119. Asahi, M., McKenna, E., Kurzydlowski, K., Tada, M., and MacLennan, D.H. (2000) Physical interactions between phospholamban and sarco(endo)plasmic reticulum Ca2+-ATPases are dissociated by elevated Ca2+, but not by phospholamban phosphorylation, vanadate, or thapsigargin, and are enhanced by ATP, *J. Biol. Chem. 275(20),* 15034-15038.
120. Tatulian, S.A., Chen, B., Li, J., Negash, S., Middaugh, C.R., Bigelow, D.J., and Squier, T.C. (2002) The inhibitory action of phospholamban involves stabilization of alpha-helices within the Ca-ATPase, *Biochemistry 41(3),* 741-751.
121. Odermatt, A., Becker, S., Khanna, V.K., Kurzydlowski, K., Leisner, E., Pette, D., and MacLennan, D.H. (1998) Sarcolipin regulates the activity of SERCA1, the fast-twitch skeletal muscle sarcoplasmic reticulum Ca2+-ATPase, *J. Biol. Chem. 273(20),* 12360-12369.
122. Asahi, M., Sugita, Y., Kurzydlowski, K., De Leon, S., Tada, M., Toyoshima, C., and MacLennan, D.H. (2003) Sarcolipin regulates sarco(endo)plasmic reticulum Ca2+-ATPase (SERCA) by binding to transmembrane helices alone or in association with phospholamban, *Proc. Natl. Acad. Sci. U. S. A. 100(9),* 5040-5045.
123. Asahi, M., Kurzydlowski, K., Tada, M., and MacLennan, D.H. (2002) Sarcolipin inhibits polymerization of phospholamban to induce superinhibition of sarco(endo)plasmic reticulum Ca2+-ATPases (SERCAs), *J. Biol. Chem. 277(30),* 26725-26728.
124. Algenstaedt, P., Antonetti, D.A., Yaffe, M.B., and Kahn, C.R. (1997) Insulin receptor substrate proteins create a link between the tyrosine phosphorylation cascade and the Ca2+-ATPases in muscle and heart, *J. Biol. Chem. 272(38),* 23696-23702.
125. Tupling, A.R., Gramolini, A.O., Duhamel, T.A., Kondo, H., Asahi, M., Tsuchiya, S.C., Borrelli, M.J., Lepock, J.R., Otsu, K., Hori, M., MacLennan, D.H., and Green, H.J. (2004) HSP70 binds to the fast-twitch skeletal muscle sarco(endo)plasmic reticulum Ca2+ -ATPase (SERCA1a) and prevents thermal inactivation, *J. Biol. Chem. 279(50),* 52382-52389.
126. Fischer, L., Gukovskaya, A.S., Young, S.H., Gukovsky, I., Lugea, A., Buechler, P., Penninger, J.M., Friess, H., and Pandol, S.J. (2004) Phosphatidylinositol 3-kinase regulates Ca2+ signaling in pancreatic acinar cells through inhibition of sarco(endo)plasmic reticulum Ca2+-ATPase, *Am. J. Physiol. Gastrointest. Liver Physiol. 287(6),* G1200-G1212.
127. Viner, R.I., Williams, T.D., and Schöneich, C. (1999) Peroxynitrite modification of protein thiols: oxidation, nitrosylation, and S-glutathiolation of functionally important cysteine residue(s) in the sarcoplasmic reticulum Ca-ATPase, *Biochemistry 38(38),* 12408-12415.
128. Kanski, J., Alterman, M.A., and Schöneich, C. (2003) Proteomic identification of age-dependent protein nitration in rat skeletal muscle, *Free Radic. Biol. Med. 35(10),* 1229-1239.

129. Adachi, T., Matsui, R., Xu, S., Kirber, M., Lazar, H.L., Sharov, V.S., Schöneich, C., and Cohen, R.A. (2002) Antioxidant improves smooth muscle sarco/endoplasmic reticulum Ca(2+)-ATPase function and lowers tyrosine nitration in hypercholesterolemia and improves nitric oxide-induced relaxation, *Circ. Res. 90(10),* 1114-1121.
130. Lee, A.G. (1998) How lipids interact with an intrinsic membrane protein: the case of the calcium pump, *Biochim. Biophys. Acta. 1376(3),* 381-390.
131. Starling, A.P., East, J.M., and Lee, A.G. (1993) Effects of phosphatidylcholine fatty acyl chain length on calcium binding and other functions of the (Ca(2+)-Mg2+)-ATPase, *Biochemistry 32(6),* 1593-1600.
132. Wang, Y., Tsui, Z., and Yang, F. (1999) Antagonistic effect of ganglioside GM1 and GM3 on the activity and conformation of sarcoplasmic reticulum Ca(2+)-ATPase, *FEBS Lett. 457(1),* 144-148.
133. Landolfi, B., Curci, S., Debellis, L., Pozzan, T., and Hofer, A.M. (1998) Ca2+ homeostasis in the agonist-sensitive internal store: functional interactions between mitochondria and the ER measured In situ in intact cells, *J. Cell Biol. 142(5),* 1235-1243.
134. Rizzuto, R., Pinton, P., Carrington, W., Fay, F.S., Fogarty, K.E., Lifshitz, L.M., Tuft, R.A., and Pozzan, T. (1998) Close contacts with the endoplasmic reticulum as determinants of mitochondrial Ca2+ responses, *Science 280(5370),* 1763-1766.
135. Pizzo, P., and Pozzan, T. (2007) Mitochondria-endoplasmic reticulum choreography: structure and signaling dynamics, *Trends Cell Biol. 17(10),* 511-517.
136. Rutter, G.A. (2006) Moving Ca2+ from the endoplasmic reticulum to mitochondria: is spatial intimacy enough? *Biochem. Soc. Trans. 34(Pt 3),* 351-355.
137. Demaurex, N., and Distelhorst, C. (2003) Cell biology. Apoptosis--the calcium connection, *Science 300(5616),* 65-67.
138. Romagnoli, A., Aguiari, P., De Stefani, D., Leo, S., Marchi, S., Rimessi, A., Zecchini, E., Pinton, P., and Rizzuto, R. (2007) Endoplasmic reticulum/mitochondria calcium cross-talk, *Novartis. Found. Symp. 287,* 122-131.
139. Szabadkai, G., and Rizzuto, R. (2004) Participation of endoplasmic reticulum and mitochondrial calcium handling in apoptosis: more than just neighborhood? *FEBS Lett. 567(1),* 111-115.
140. Szegezdi, E., Logue, S.E., Gorman, A.M., and Samali, A. (2006) Mediators of endoplasmic reticulum stress-induced apoptosis, *EMBO Rep. 7(9),* 880-885.
141. Oakes, S.A., Lin, S.S., and Bassik, M.C. (2006) The control of endoplasmic reticulum-initiated apoptosis by the BCL-2 family of proteins, *Curr. Mol. Med. 6(1),* 99-109.
142. Nutt, L.K., Pataer, A., Pahler, J., Fang, B., Roth, J., McConkey, D.J., and Swisher, S.G. (2002) Bax and Bak promote apoptosis by modulating endoplasmic reticular and mitochondrial Ca2+ stores, *J. Biol. Chem. 277(11),* 9219-9225.
143. Oakes, S.A., Scorrano, L., Opferman, J.T., Bassik, M.C., Nishino, M., Pozzan, T., and Korsmeyer, S.J. (2005) Proapoptotic BAX and BAK regulate the type 1 inositol trisphosphate receptor and calcium leak from the endoplasmic reticulum, *Proc. Natl. Acad. Sci. U. S. A. 102(1),* 105-110.
144. Scorrano, L., Oakes, S.A., Opferman, J.T., Cheng, E.H., Sorcinelli, M.D., Pozzan, T., and Korsmeyer, S.J. (2003) BAX and BAK regulation of endoplasmic reticulum Ca2+: a control point for apoptosis, *Science 300(5616),* 135-139.

Chapter 2:
Interactions of Bcl-2 with SERCA; Using wild type Bcl-2.

2.1: Introduction to the analytical strategies.

2.1.1: Cross-linking in protein-protein interaction studies.

Cross-linking is an important method which has been used in studies of protein interactions for decades. In this method, interaction partners are covalently bound to each other using a suitable cross-linking reagent. In general, the reaction involves two steps. First, one of the interaction partners is labeled with the selected cross-linking reagent. Next the second interaction partner is added in the form of purified protein or a mixture of proteins such as a cell lysate and the proteins are allowed to associate with each other. Then cross-linking is initiated after the proteins are assumed to be associated. Cross-linking results in a covalent bond connecting the interfaces involved in the interaction. The covalent bond keeps the proteins/interfaces connected during the course of analysis.

The analysis of the cross-linked products reveals information at three levels; (1) Identification of the interacting proteins, (2) Identification of the domains/interfaces and (3) Identification of the exact residues involved in the interactions. This information gives insight into the architecture of protein complexes, which is important in understanding the specific function of a protein complex. Cross-linking is used successfully to study transient or low affinity interactions which are otherwise difficult to detect and define. The cross-linking reagents contain different functionalities that specifically react with amines, thiols or acidic groups in

amino acid residues. Usually a reagent contains two functional groups connected by a spacer arm. These reagents are categorized based on their functionalities. Homobifunctional cross-linking reagents have the same terminal activated groups while the two groups are different in heterobifunctional reagents, making possible reaction with different functional groups in the proteins. In addition, these reagents are developed with a wide range of spacer arm lengths. Selection of the proper cross-linking reagent is critical for a successful analysis. The selected reagent should efficiently cross-link the interfaces without significant alterations in the interaction (*1-7*).

(a) Photo cross-linking:

Photo cross-linking reagents are a group of heterobifunctional reagents in which one functional group is photoactivatable whereas the other functional group is a chemically reactive group with a thiol (sulfhydryl), amine or acidic group specificity. The photophore moiety of an effective photo cross-linker must be chemically inert prior to the photoactivation. Also it should be activatable under mild conditions not damaging the protein complex. The lifetime of the excited state of the photophore should be shorter than the off-rate of the protein complex. Further the excited photophore should nonspecifically react with any amino acid residue in close proximity to form a covalent bond. Due to these properties, unlike the other bifunctional cross-linkers, the photo cross-linkers provide a measure of control over the reaction (*1, 2, 5*).

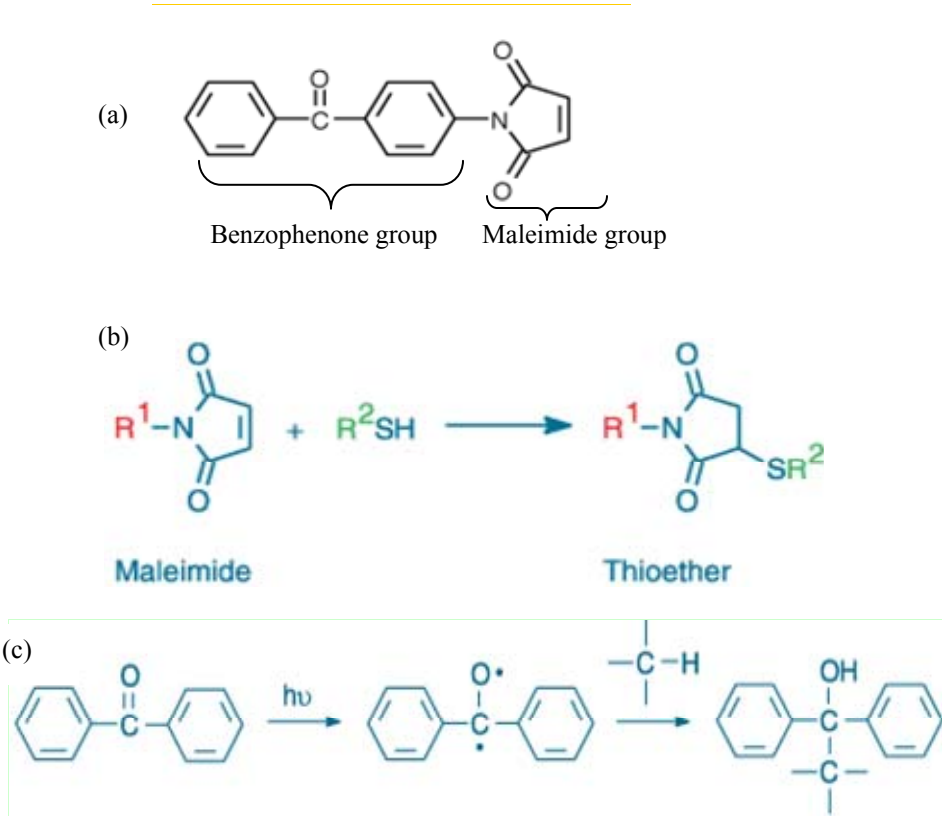

SCHEME 2.1: Benzophenone-4-maleimide (BPM): (a) Structure of BPM, (b) Reaction of a Maleimide group with a thiol (sulfhydryl) group; R^1-benzophenone group, R^2-protein with a thiol group, (c) Reaction of a Benzophenone group upon photo activation. (Adapted from www.probes.com)

Benzophenone-4-maleimide (BPM) was the photo cross-linking reagent used in this study for characterization of SERCA/Bcl-2 interactions. This is a commercially available reagent and has all the favorable properties explained above. Scheme 2.1-a shows the structure of BPM and the chemistries associated with cross-linking reactions. It has a thiol reactive maleimide group and a photoactivatable benzophenone group. The maleimide group reacts with a thiol group producing a thioether bond (Scheme 2.1-b). Benzophenone group can be photo activated at ~350

nm of UV light and once excited it reacts with any neighboring CH-bond (Scheme 2.1-c). Since this biradical formation upon photoactivation is a reversible reaction, cross-linking is more efficient (*2, 8*).

Photo cross-linking of interacting proteins is achieved in two steps. First, one of the interacting proteins is labeled with the cross-linking reagent, BPM in this study. Next the second protein is added and the two proteins are allowed to interact with each other followed by irradiation with UV light, triggering the covalent bond formation. Finally the cross-linked products are analyzed using a suitable analytical method. These steps are shown in Figure 2.1, using BPM as the cross-linking reagent.

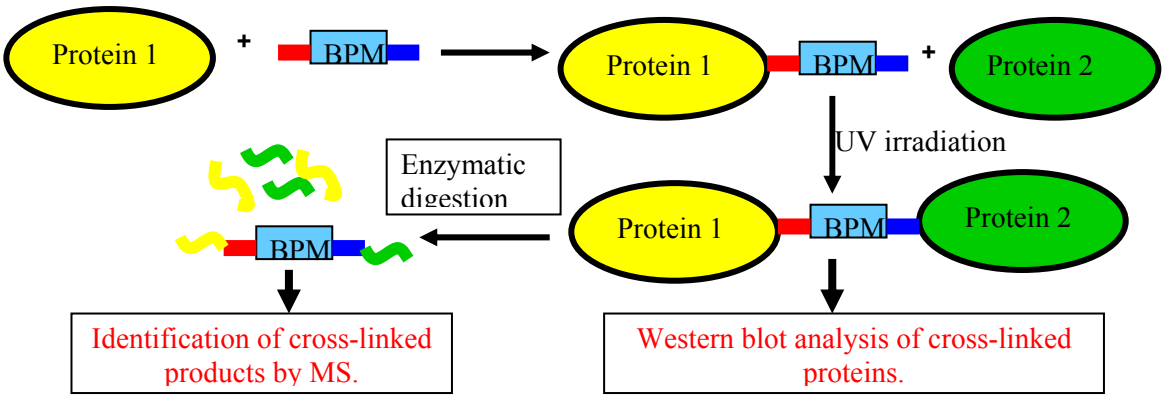

FIGURE 2.1: Photo cross-linking of interacting proteins using BPM: First, protein-1 is labeled with BPM. Next protein-2 is added and the two proteins are allowed to interact with each other followed by irradiation with UV light, triggering the covalent bond formation. Cross-linked products can be analyzed using a suitable analytical method such as western blotting and/or mass spectrometry.

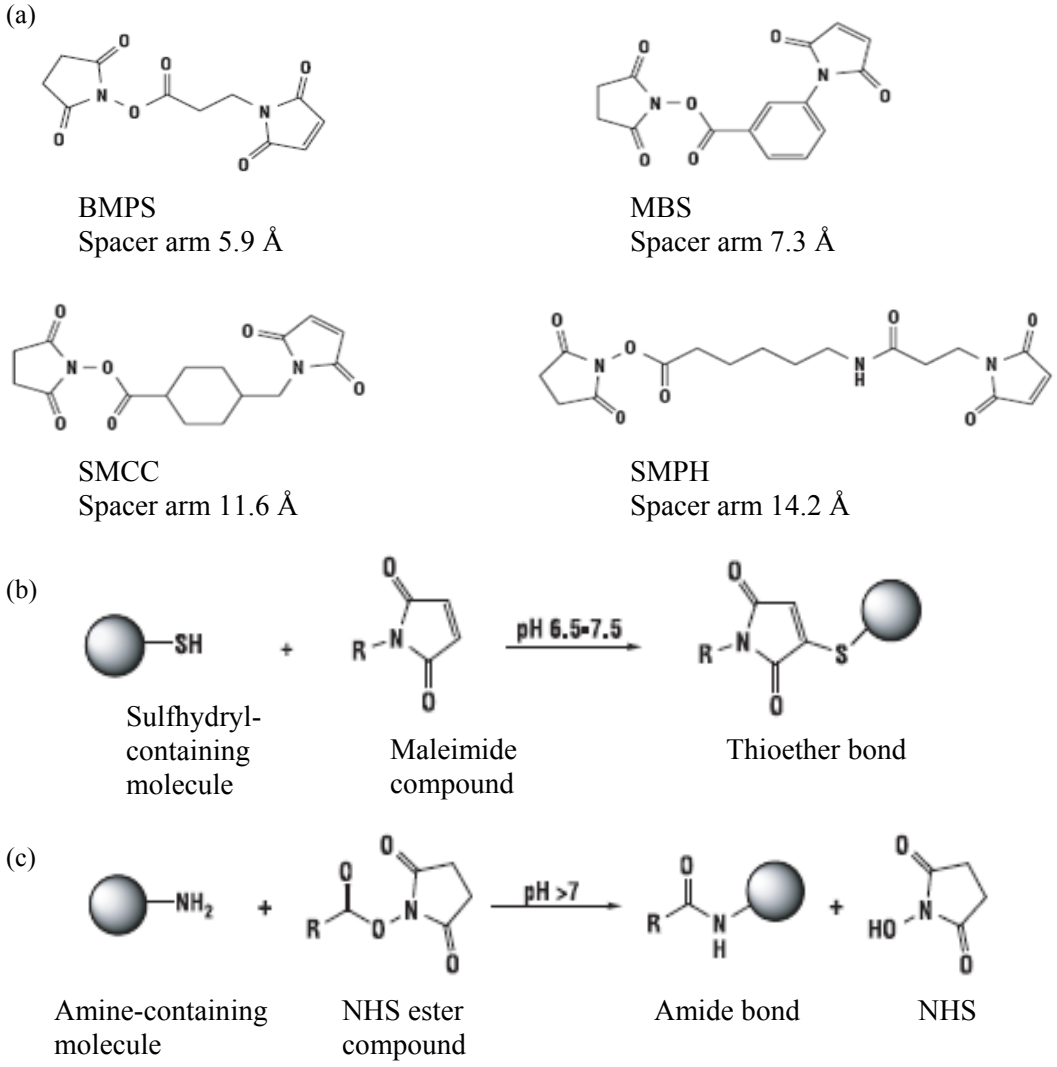

SCHEME 2.2: Chemical cross-linking reagents: (a) Structures of heterobifunctional cross-linking reagents, N-[β-maleimidopropyloxy]succinimide ester (BMPS), m-maleimidobenzoyl-N-hydroxysuccinimide ester (MBS), Succinimidyl 4-(N-maleimidomethyl)cyclohexane-1-carboxylate (SMCC) and Succinimidyl-6-[(β-maleimidopropionamido)hexanoate (SMPH). (b) Reaction of the Maleimide group with a thiol (sulfhydryl) group. (c) Reaction of the NHS ester group with an amine group. (Adapted from Cross-linking Reagents-Technical Handbook, www.piercenet.com)

(b) Chemical cross-linking:

Chemical cross-linking was also used to characterize SERCA/Bcl-2 interactions. The four heterobifunctional cross-linking reagents, N-[β-maleimidopropyloxy]succinimide ester (BMPS), m-maleimidobenzoyl-N-hydroxysuccinimide ester (MBS), Succinimidyl 4-(N-maleimidomethyl)cyclohexane-1-carboxylate (SMCC), and Succinimidyl-6-[(β-maleimidopropionamido)hexanoate (SMPH) used in the study are shown in Scheme 2.2-a. All these four reagents have a thiol (sulfhydryl) reactive maleimide group and an amine reactive N-hydroxysuccinimide (NHS) ester group and spacer arm lengths ranging from 5.9 Å - 14.2 Å. The chemistries of the two functionalities are also shown in the Scheme 2.2-b, c (*9*).

2.1.2: Bcl-2Δ21 and His_6-Bcl-2Δ17.

A truncated form of Bcl-2, Bcl-2Δ21, purified from GST-Bcl-2Δ21 fusion protein and also the commercially available truncated and hexahistidine tagged Bcl-2, His_6-Bcl-2Δ17, were used in photo cross-linking studies. Both these proteins contain only one thiol (sulfhydryl) group at Cys158 and the photo cross-linking reagent, BPM was attached to this site. The advantage of the His_6-Bcl-2Δ17 is the ability to purify cross-linked products using affinity chromatography. Ni^{2+} or Co^{2+} chelated affinity resins can be used to trap His_6-Bcl-2Δ17 and the trapped proteins can be eluted with high concentrations of imidazole. This makes the reaction mixture less complex and the identification of cross-linked proteins easier.

2.1.3: Monitoring cysteine derivatization efficiency of Bcl-2Δ21.

For an effective cross-linking reaction, thiol reactive cross-linking reagents should efficiently react with the cysteine group of Bcl-2Δ21, Cys158. To monitor the efficiency of Cys158 derivatization, a maleimide-based fluorescent reagent, ThioGlo1 was utilized. Free cysteines react with this reagent producing fluorescent ThioGlo1-cysteine adducts. The intensity of the fluorescence indicates the amount of free cysteine in the sample.

2.1.4: Analysis of cross-linked products.

After covalently connecting the pairs of functional groups of interacting proteins, the products are subjected to suitable analytical procedures. Mass spectrometry and western blotting were the methods of choice in this study.

(a) Mass spectrometry in cross-linking studies:

Mass spectrometry is a state-of-the-art analytical method which has been used successfully in combination with cross-linking, to study protein interactions in recent years. After the cross-linking reaction the products are isolated and enzymaticaly digested. The resulting mixture of peptides is subjected to MS analysis (*10-18*). This is called "Bottom-up strategy" for the analysis of cross-links and all the associated steps are schematically shown in Figure 2.2 (*19*). The assignment of the cross-linked peptides is done manually or using software programs (*20, 21*). Using tandem mass

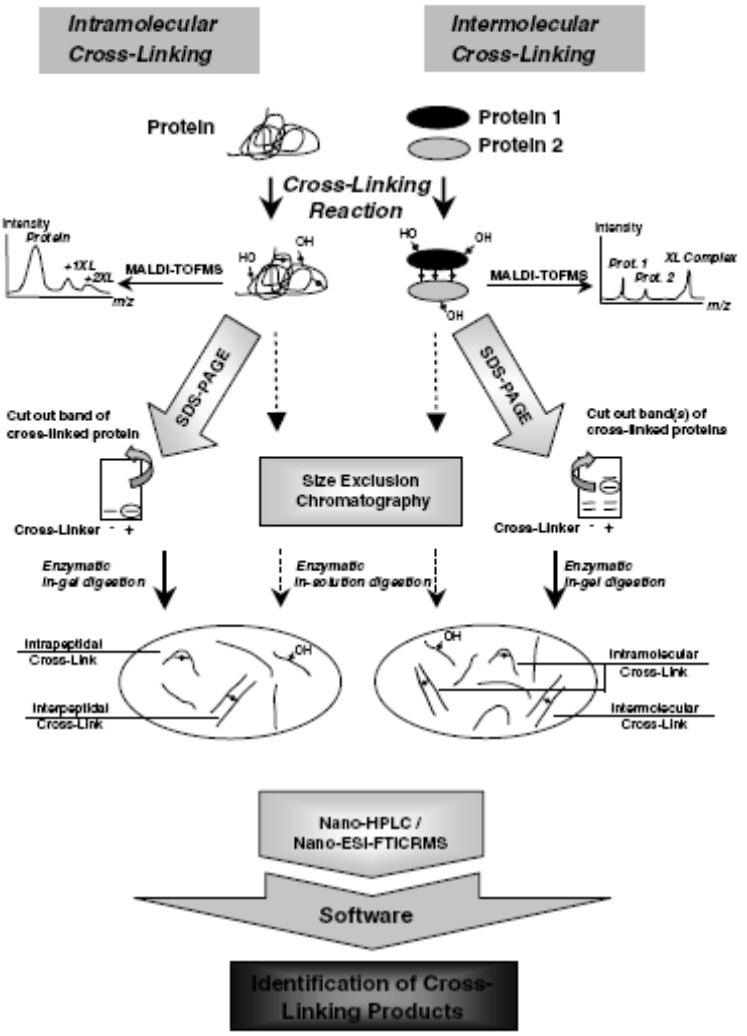

FIGURE 2.2: Bottom-up strategy for the analysis of protein cross-links: Both inter- or intra-molecularly cross-linked proteins can be analyzed. SDS-PAGE or size exclusion chromatography is used to isolate cross-linked products. LC/MS is used to analyze cross-linked products after enzymatic in-gel or in-solution digestion. MALDI-MS can be used to monitor the extent of cross-linking prior to the digestion of products. (Figure adapted from Sinz, A. (2005) *Anal. Bioanal. Chem. 381,* 44-47.)

spectrometry (MS/MS) the exact cross-linking site/sites can be determined. The masses of the proteins involved in the interaction do not affect the MS analysis, since proteolytic peptides are analyzed. Another associated advantage is, even a femtomole amount of cross-linked product is enough for analysis due to the higher sensitivity of the modern MS instruments. In this study, ESI-FTICR-MS was used to analyze cross-linked products after 1D-SDS-PAGE and in-gel tryptic digestion. FTICR-MS allows unambiguous assignment of cross-linked peptides and exact cross-linking sites/residues as well, due to the higher accuracy and resolution and also the MS/MS ability of the instrument (*15-18*).

(b) Western blotting in cross-linking studies:

Western blotting is a classical, yet very useful method for analysis of cross-linked proteins. After the cross-linking reaction, the mixture is fractionated using SDS-PAGE and transferred onto a nitrocellulose membrane. Then the cross-linked proteins are probed using antibodies raised against the protein/proteins of interest. Comparing the cross-linking reaction sample with appropriate control samples in the western blot, cross-linked products can be identified (*22*). The expected SERCA/Bcl-2 cross-linked products are shown in the simulated western blots in Figure 2.3.

2.1.5: GST-Bcl-2Δ21 binding assay.

Detailed introduction of this assay is presented in the Chapter 3 since most of the binding assay experiments are related to that chapter.

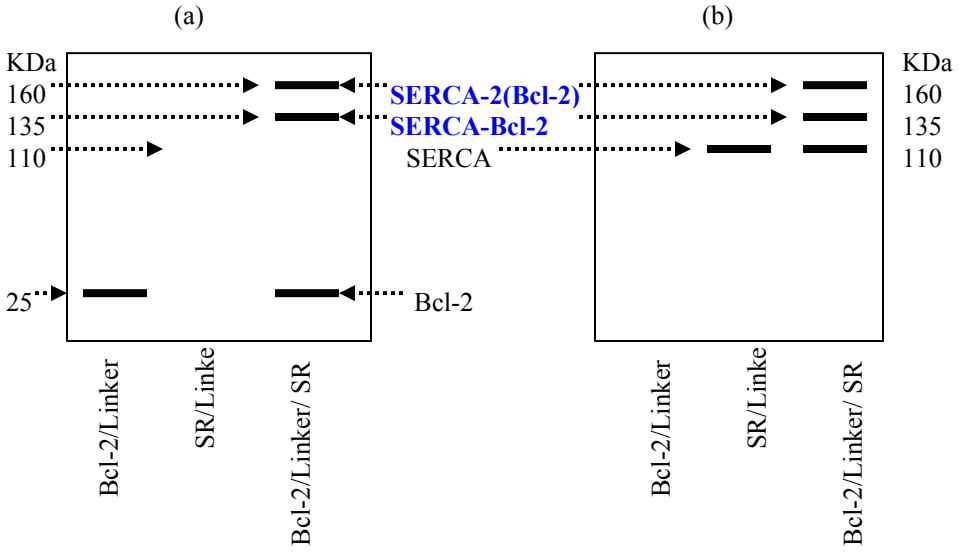

FIGURE 2.3: Simulated western blots of SERCA/Bcl-2 cross-linking reaction samples: (a) With Bcl-2 antibody. (b) With SERCA antibody. If the molecular ratio between SERCA (~110 kDa) and Bcl-2 (25 kDa) is 1:1 and/or 1:2, bands at ~135 kDa and/or ~160 kDa are seen only with the cross-linking reaction sample, Bcl-2/Linker/SR but not with the two control samples, Bcl-2/Linker and SR/Linker.

2.2: Materials and methods.

2.2.1: Bcl-2Δ21 expression and purification.

(a) Expression of Bcl-2Δ21:

The *E.coli* host strain containing the pGEX3T vector of GST-Bcl-2Δ21 fusion protein was available in the lab (Clone of human Bcl-2Δ21 needed for GST-Bcl-2Δ21 plasmid construction has been kindly provided by Prof. S. J. Korsmeyer, Harvard Medical School, Boston, MA, U.S.A.). The protein expression and purification protocol was adapted from Dremina et al. (*23*). A 1 liter of Luria-Bertani

(LB) medium was inoculated with a 10 ml of overnight culture and further incubated at 37°C with vigorous shaking at 220 rpm until the optical density, A_{600}, reached 0.4. Isopropyl β-D-thiogalactoside (0.1 mM) (IPTG) (American Bioanalytical, Natick, MA, U.S.A.) was added to induce the expression of GST-Bcl-2Δ21 and further incubated at 32°C with vigorous shaking at 220 rpm for another 6 hours. The cells were harvested by centrifugation and stored at -20°C until used.

(b) Purification of Bcl-2Δ21:

For the purification of GST-Bcl-2Δ21, the cell pellet was re-suspended in ice-cold STE buffer (Tris-buffered saline) containing 7.5 mM Tris (pH 8.0), 150 mM NaCl and 3 mM EDTA. The cell suspension was incubated with Lysozyme (0.1 mg/ml) on ice for 20 min. It was sonicated in the presence of 1.5% (w/v) Sarkosyl (Fisher BioReagents, U.S.A.), 5 mM DTT, 100 μM Phenylmethylsulfonyl fluoride (PMSF) (Sigma, St. Louis, MO) and 1 mM Benzamidine. Resulting cell lysate was centrifuged at 15000g for 40 min at 4°C to pellet the cell debris. The supernatant was incubated with 500 μl (250 μl of bed volume) of slurried Glutathione-agarose beads (Sigma, St. Louis, MO, U.S.A.) in the presence of 2% Triton X-100 for 3 h at 4°C with gentle rotation. The beads were spun down and washed six times with 1 ml portions of STE buffer containing 1% Triton X-100, then two additional times with 1 ml portions of STE buffer without Triton X-100. The beads were resuspended in 250 μl of STE, incubated with 5 units of Thrombin for 1 h at room temperature to cleave GST-Bcl-2Δ21, then spun down. The supernatant was incubated with 10 μl of pre-

washed thrombin-binding beads (Sigma, St. Louis, MO, U.S.A.) for 15 min at 4°C. The mixture was centrifuged to separate the supernatant of 250 µl of STE containing purified Bcl-2Δ21. This procedure yielded ca. 75 µg of Bcl-2Δ21 (250 µl of 0.3 mg/ml) per liter of LB medium as measured by the Coomassie Plus protein assay (Pierce, Rockford, IL, U.S.A.). Purified proteins were subjected to SDS-PAGE and analyzed by western blotting with mouse monoclonal anti-Bcl-2 antibody (sc-7382, Santa Cruz Biotechnology, Santa Cruz, CA, U.S.A.). The SDS-PAGE and western blotting procedure is explained in the section 2.2.12.

(c)Bcl-2Δ21 Storage Conditions:

In order to find the best storage conditions for the purified protein, a set of six samples of Bcl-2Δ21 were prepared as follows by mixing freshly purified protein with two protease inhibitors; 1 mM (1), 0.5 mM (2) and 0.1 mM (3) of PMSF and 1 X (4) and 0.5 X (5) of protease inhibitors cocktail (Roche Diagnostics, Indianapolis, IN, U.S.A.), respectively and control sample (6), without any protease inhibitors added. The samples were stored at -20°C. Another set of samples prepared in the same way were stored at 4°C. A fraction of each sample was subjected to SDS-PAGE and Coomassie Blue staining after 18 h, 1 week, and 2 weeks of storage.

2.2.2: Isolation of SR Vesicles.

Native SR vesicles, isolated from hind limb skeletal muscles of Fisher 344 rats according to the procedure by Fernandez et al. (*24*), were kindly provided by Dr.

E. Dremina (Department of Pharmaceutical Chemistry, University of Kansas, KS, U.S.A.). According to Dremina et al. (*25*) these purified SR vesicles contain ca. 40% of SERCA1 as determined by densitometry of Coomassie Blue-stained gels.

2.2.3: Optimization of BPM labeling reaction conditions.

(a) Optimum reaction time:

Samples of Bcl-2Δ2 were prepared with the final concentration of 5 μM in STE (pH 7.5) buffer and incubated with 50 μM BPM (Sigma, St. Louis, MO), at room temperature with stirring, for 30 min and for 1 h separately. The samples were incubated with 20 μM ThioGlo1 (Covalent Associates, Woburn, MA, U.S.A.), for 1 h at 37°C in 200 mM phosphate buffer (pH 7.4). The control sample was prepared in the same way but without incubation with BPM. 1 ml of each of these samples was used to measure the fluorescence of ThioGlo1-cysteine adducts, at excitation and emission wavelengths of 379 nm and 513 nm, respectively. Shimadzu RF5000U fluorescence spectrophotometer was used for measurements.

(b) Effect of the redox status of Bcl-2Δ2 cysteine:

Samples of Bcl-2Δ2 (7.5 μM) were incubated both with and without 15 μM DTT for 30 min at room temperature with stirring followed by dialysis with STE (pH 7.5) buffer over night using 3500 MWCO Slide-A-Lyzer MINI dialysis units (Pierce, Rockford, IL). Then the samples were incubated with 20 μM ThioGlo1 for 1 h at

37°C in 200 mM phosphate buffer (pH 7.4) and the fluorescence was measured in the same way as above.

(c) Effect of native and denatured Bcl-2Δ21:

Two samples of Bcl-2Δ2 (0.5 μM) in STE (pH 7.5) buffer were incubated with 5 μM of BPM, at room temperature with stirring, for 30 min in the presence and absence of 2% SDS (w/v). The control samples, with Bcl-2Δ2/without BPM and without Bcl-2Δ2/with BPM were prepared in the same way. All the samples were incubated with 20 μM ThioGlo1 for 1 h at 37°C in 200 mM phosphate buffer (pH 7.4). Fluorescence was measured in the same way as above.

(d) Effect of mild denaturing agents:

Samples of Bcl-2Δ2 (0.5 μM) in STE (pH 7.5) buffer containing 1, 5, 10, 15% Nonidet P40 (NP-40) (w/v) and also 0.2% CHAPS (w/v) were incubated first, for 30 min in the presence or absence of 5 μM of BPM at room temperature with stirring, next for another 1 h at 37°C with 20 μM ThioGlo1 (Covalent Associates, Woburn, MA, U.S.A.), in 200 mM phosphate buffer (pH 7.4). Fluorescence was measured in the same way as above.

(e) Lowest effective concentration of SDS:

Samples of Bcl-2Δ2 (1 μM) were incubated with 20 μM ThioGlo1 for 1 h at 37°C in 200 mM phosphate buffer (pH 7.4) containing 0, 0.05, 0.1, 0.2, 0.5, 0.75 and 1% SDS (w/v), respectively and the fluorescence was measured in the same way as above.

(f) Comparison of Bcl-2Δ2 and His_6-Bcl-2Δ17 in cysteine derivatization:

Bcl-2Δ2 and His_6-Bcl-2Δ17 with the final concentrations of 0.3 μM were incubated with 20 μM ThioGlo1 for 1 h at 37°C in 200 mM inorganic phosphate buffer (pH 7.4) in the presence and absence of 0.2% SDS (w/v) and the fluorescence was measured in the same way as above.

2.2.4: Labeling Cys158 of Bcl-2Δ21/ His_6-Bcl-2Δ17 using optimized conditions.

Bcl-2Δ21/His_6-Bcl-2Δ17 (4 μM) was incubated with 40 μM BPM for 30 min at room temperature with stirring, in the presence of 0.05% of SDS in STE buffer (pH 7.5). DMF (Dimethylformamide) was added to the mixture so that the contribution of organic solvent to the final reaction mixture was only 8%. Then 400 μM of DTT was added to react with excess BPM and incubated at room temperature with stirring for another 10 min. Sample was dialyzed with 2 L of STE (pH 7.5) for 4 h using 3500 MWCO Slide-A-Lyzer MINI dialysis units (Pierce, Rockford, IL). The buffer was changed after first two hours. Alternatively, Zeba™ Desalt Spin Columns (Pierce, Rockford, IL, U.S.A.) or 10k MWCO Microcon Centrifugal Filter Devices (Millipore Corporation, Bedford, MA, U.S.A.) were used. After dialysis/spin columns/micro

filtration, the protein concentration was determined using Coomassie Plus protein assay (Pierce, Rockford, IL). In all above steps precautions were taken to prevent exposure of samples to light. In the case of His_6-Bcl-2Δ17 (EMD Biosciences, San Diego, CA), 8 μM His_6-Bcl-2Δ17 and 80 μM BPM was used and all the reaction steps were the same. BPM labeling reaction sample was characterized as explained below in section 2.2.5.

2.2.5: Characterization of BPM labeling reaction samples.

(a) RP-HPLC separation of BPM labeling reaction mixture:

100 μL of BPM labeling reaction mixture was loaded into a Vydac C4 column (250×4.6mm i.d.), pre-equilibrated with 10% ethanol (v/v) in 0.1% aqueous TFA. Products on the column were eluted at a flow rate of 0.5 mL/min using a linear gradient, increasing ethanol percentage by 1.5%/min. Chromatograms were recorded at 280 nm (for protein detection) and 260 nm (λ_{max} of thiol conjugated BPM).

(b) Mass spectrometric analysis of BPM labeling reaction mixture:

BPM labeling reaction samples were subjected to SDS-PAGE and analyzed by ESI-FTICR-MS after in-gel tryptic digestion. In-gel tryptic digestion procedure is explained in section 2.2.14.

(c) Effect of BPM treated Bcl-2Δ21 on Ca^{2+}-ATPase activity of SERCA:

Concentrated SR vesicle suspension (ca. 20 mg of SR protein/ml) was diluted in STE buffer (pH 7.5), the buffer used for BPM labeling of Bcl-2Δ21, so that the contribution from the SR storage buffer is <5%. The final concentration of SR proteins in this sample was 0.35 mg/mL. BPM treated or none treated Bcl-2Δ21 was added into the diluted SR sample with the final concentration of 0.17 mg/ml. The control samples of SR without Bcl-2Δ21 were also prepared in the same way. All the samples were incubated in 1.5 mL Eppendorf tubes at 37^{o}C for 3 h using a dry thermostat without agitation. Protease inhibitor, PMSF (1 mM) was added to each sample to prevent proteolytic degradation.

The Ca^{2+} dependent ATPase activity assay procedure was adapted from Dremina et al. (*23*). Briefly, total and basal ATPase activities of SERCA in the sample were measured at 25^{o}C using a colorimetric assay for inorganic phosphate (P_i) (*26*). Basal activity was subtracted from the total activity to obtain Ca^{2+} dependent ATPase activity. This measured activity is the Ca^{2+} dependent ATPase activity of SERCA in the sample since it has been shown before that this activity can be completely inhibited by the addition of thapsigargin, well known inhibitor of SERCA (*23*). The Ca^{2+} dependent ATPase activity of SERCA of the three samples was measured both before and after the incubation at 37^{o}C for 3 h.

2.2.6: Optimization of photo cross-linking reaction conditions.

(a) Molar ratio between SERCA and Bcl-2Δ21:

The photo cross-linking reaction samples of Bcl-2Δ21/BPM/SR were prepared by mixing BPM treated Bcl-2Δ21 with purified SR vesicles in STE (pH 7.5) buffer so that the molar ratios between Bcl-2Δ21 and SERCA were 10:1, 5:1, 2:1, 1:1, 1:2 and 1:5, respectively. The control sample of Bcl-2Δ21/BPM was prepared using the same amount of BPM treated Bcl-2Δ21 without SR. For the control sample of SR/BPM, 40 μM BPM in the buffer (pH 7.5 STE buffer, 0.05% SDS, 8% DMF) without Bcl-2Δ21 was subjected to the same BPM labeling reaction steps followed by the addition of the same amount of SR. Protease inhibitor PMSF (1 mM) was used in each sample to prevent proteolytic degradation. All the samples were incubated in 1.5 mL Eppendorf tubes at 37^{o}C for 1 h using a dry thermostat without agitation. After incubation, the samples were transferred into quartz tubes and irradiated with 350 nm UV light for 30 min using a Rayonet photochemical reactor (The Southern New England Ultraviolet Company). Finally the samples were boiled for 5 min with sample buffer (2% SDS, 10% glycerol, and 125 mM Tris pH 6.8) and analyzed by western blotting after SDS-PAGE.

(b) Incubation time for SERCA and Bcl-2Δ21:

The photo cross-linking reaction samples of Bcl-2Δ21/BPM/SR were prepared by mixing BPM treated Bcl-2Δ21 with purified SR vesicles in STE (pH 7.5) buffer so that the molar ratio between Bcl-2Δ21 and SERCA was 2:1. The control

sample of Bcl-2Δ21/BPM was prepared using the same amount of BPM treated Bcl-2Δ21 without SR. For the control sample of SR/BPM, 40 μM BPM in the buffer (pH 7.5 STE buffer, 0.05% SDS, 8% DMF) without Bcl-2Δ21 was subjected to the same BPM labeling reaction steps followed by the addition of the same amount of SR. Protease inhibitor PMSF (1 mM) was used in each sample to prevent proteolytic degradation. Samples were incubated in 1.5 mL Eppendorf tubes at 37^{o}C using a dry thermostat without agitation for 2 h, 1 ½ h, 1 h, 45 min, 30 min, 15 min and 5 min. After incubation, samples were transferred into quartz tubes and irradiated with 350 nm UV light for 30 min using a Rayonet photochemical reactor (The Southern New England Ultraviolet Company). Finally the samples were boiled for 5 min with sample buffer (2% SDS, 10% glycerol, and 125 mM Tris pH 6.8) and analyzed by western blotting after SDS-PAGE.

2.2.7: Photo cross-linking of BPM treated Bcl-2Δ21/His_6-Bcl-2Δ17 with SERCA using optimized reaction conditions.

Bcl-2Δ21/BPM/SR sample was prepared by mixing BPM treated Bcl-2Δ21 with purified SR vesicles in STE (pH 7.5) buffer so that the final concentrations were 1.4 μM and 0.7 μM, respectively, and the molar ratio between Bcl-2Δ21 and SERCA was 2:1. BPM treated Bcl-2Δ21 (1.4 μM) was diluted in STE (pH 7.5) buffer without SR for the control sample of Bcl-2Δ21/BPM. For the control sample of SR/BPM, 40 μM BPM in buffer (pH 7.5 STE buffer, 0.05% SDS, 8% DMF) without Bcl-2Δ21 was subjected to the same BPM labeling reaction steps followed by addition of SR

with the same 0.7 μM final concentration of SERCA. Protease inhibitor PMSF (1 mM) was used in each sample to prevent proteolytic degradation. All three samples were incubated in 1.5 mL Eppendorf tubes at 37^{o}C for 15 min using a dry thermostat without agitation. After incubation, samples were transferred into quartz tubes and irradiated with 350 nm UV light for 30 min using a Rayonet photochemical reactor (The Southern New England Ultraviolet Company). Finally the samples were boiled for 5 min with sample buffer (2% SDS, 10% glycerol, and 125 mM Tris pH 6.8). Samples were analyzed by Coomassie Blue staining and western blotting after SDS-PAGE. In addition mass spectrometry was also used after SDS-PAGE and in-gel tryptic digestion. Photo cross-linking reaction samples using His_6-Bcl-2Δ17, were subjected to Ni^{2+} affinity purification as explained below and fractions collected were boiled for 5 min with sample buffer before SDS-PAGE and western blot analysis.

2.2.8: Ni^{2+} affinity purification of photo cross-linked products of His_6-Bcl-2Δ17.

A HisTrapHP (1 ml) Ni^{2+} affinity column (GE Healthcare, UK) was used to affinity purify cross-linked products. First the column was washed with 6 ml of distilled water to remove the storage solution. Then the column was equilibrated with six column volumes (6 ml) of the binding buffer, 2 mM imidazole. Cross-linking reaction samples, diluted in 1 ml of binding buffer, were injected to the column and the column was washed with binding buffer. Proteins bound to the column were eluted with increasing concentrations of imidazole, 50 mM (2 ml), 100 mM (2 ml) and 500 mM (3 ml) and fractions were collected. Cross-linking reaction samples

were run through the column in the order of SR/BPM, His_6-Bcl-2Δ17/BPM and His_6-Bcl-2Δ17/BPM/SR and the column was washed with water, re-equilibrated with the binding buffer between each run.

2.2.9: Chemical cross-linking of Bcl-2Δ21 with SERCA.

(a) Starting with Bcl-2Δ21:

STE buffer in purified Bcl-2Δ21 was exchanged with PBS buffer (pH 7.2, 0.1 M Sodium phosphate, 0.15 M NaCl and 5 mM EDTA) using 10k MWCO Microcon Centrifugal Filter Devices (Millipore Corporation, Bedford, MA, U.S.A.) and the concentration was determined using Coomassie Plus protein assay (Pierce, Rockford, IL). Reaction samples were prepared by mixing Bcl-2Δ21 (7.5 μM) with 0.75 mM of chemical cross-linking reagent, BMPS, MBS, SMCC or SMPH (Pierce, Rockford, IL, U.S.A.) separately, so that the Bcl-2Δ21:linker ratio is 1:100 (mol/mol). Organic solvent, DMSO, was 4% (v/v) in each sample. All samples were incubated for 30 min at room temperature with stirring. Samples were run through Zeba^{TM} Desalt Spin Columns (Pierce, Rockford, IL, U.S.A.) and the protein concentration was determined. Each sample was split into two fractions and Bcl-2Δ21/Linker/SR samples were prepared by diluting SR vesicles in one fraction so that the molar ratio between SERCA and Bcl-2Δ21 was 1:2. The other fraction was Bcl-2Δ21/Linker without added SR. For SR/Linker samples, 0.75 mM of chemical cross-linking reagent (BMPS, MBS, SMCC or SMPH) in the buffer (PBS pH 7.2, 0.1 M sodium phosphate, 0.15 M NaCl and 5 mM EDTA, 4% DMSO) without Bcl-2Δ21 was

subjected to the same reaction steps followed by the addition of the same amount of SR. Samples were incubated in 1.5 mL Eppendorf tubes at 37^{o}C for 30 min using a dry thermostat without agitation. Finally the samples were boiled for 5 min with sample buffer (2% SDS, 10% glycerol, and 125 mM Tris pH 6.8) and analyzed by western blotting after SDS-PAGE. In a separate experiment 1:20 (mol/mol) of Bcl-2Δ21: linker ratio was used and all other steps were the same.

(b) Starting with SERCA:

SR was diluted in PBS buffer to a final SERCA concentration of 2.5 μM and mixed with chemical cross-linking reagent (0.25 mM) (BMPS, MBS, SMCC or SMPH) separately, so that the SERCA:linker ratio is 1:100 (mol/mol). Organic solvent, DMSO, was 4% (v/v) in each sample. All samples were incubated for 30 min at room temperature with stirring. Samples were run through Zeba^{TM} Desalt Spin Columns (Pierce, Rockford, IL, U.S.A.) and protein concentration was determined. Each sample was split into two fractions and SR/Linker/Bcl-2Δ21 sample was prepared by adding Bcl-2Δ21 (in PBS buffer) into one fraction so that the molar ratio between SERCA and Bcl-2Δ21 was 1:2. The other fraction was the control sample of SR/Linker without added Bcl-2Δ21. For Bcl-2Δ21/Linker samples, 0.25 mM of chemical cross-linking reagent (BMPS, MBS, SMCC or SMPH) in the buffer (PBS pH 7.2, 0.1 M sodium phosphate, 0.15 M NaCl and 5 mM EDTA, 4% DMSO) without SR was subjected to the same reaction steps followed by the addition of the same amount of Bcl-2Δ21 as in the experimental samples. Samples were incubated in

1.5 mL Eppendorf tubes at 37^{o}C for 30 min using a dry thermostat without agitation. Finally the samples were boiled for 5 min with sample buffer (2% SDS, 10% glycerol, and 125 mM Tris pH 6.8) and analyzed by western blotting after SDS-PAGE.

2.2.10: Analysis of other possible SR proteins associated with Bcl-2 or SERCA.

(a)Using western blotting:

Ni^{2+} affinity chromatographic fractions of photo cross-linking samples of His_6-Bcl-2Δ17 were subjected to western blot analysis with antibodies raised against Glycogen Phosphorylase, Sarcalumenin, Mitsugumin-29 and Calcium Channel (α2/δ-1 subunit), after SDS-PAGE.

(b)Using GST- Bcl-2Δ21 binding assay:

For the GST-Bcl-2Δ21 binding assay, 100 µg of SR were solubilised in 150 µL of lysis buffer (10 mM Tris (pH 7.4), 10 mM EDTA, 1% Nonidet P40 (NP40), 1mM PMSF and protease inhibitors (Roche Diagnostics)). This mixture was incubated with 10 µg of GST-Bcl-2Δ21 for 2 h at 4^{o}C. For a control, another 100 µg of SR in 150 µL of lysis buffer were incubated without GST-Bcl-2Δ21. Then all the samples were incubated with 30 µL of (packed volume) pre-washed glutathione–agarose beads, for another 2 h at 4^{o}C. The beads were spun down at 10000g and washed three times with lysis buffer and three times with STE. Addition of 30 µL of

STE was followed by boiling for 5 min with sample buffer (2% SDS, 10% glycerol, 125 mM Tris pH 6.8) and by SDS-PAGE and western blot analysis.

2.2.11: Comparison of young and old SERCA in photo cross-linking with Bcl-2Δ21.

SR vesicles purified from tissues of both young (5-6 months) and old (34 months) rats were used to prepare samples. Bcl-2Δ21/BPM/SR sample was prepared by mixing BPM treated Bcl-2Δ21 with purified SR vesicles in STE (pH 7.5) buffer so that the final concentrations were 1.4 μM and 0.7 μM, respectively, and the molar ratio between Bcl-2Δ21 and SERCA was 2:1. BPM treated Bcl-2Δ21 (1.4 μM) was diluted in STE (pH 7.5) buffer without SR for the sample of Bcl-2Δ21/BPM. For the SR/BPM sample, 40 μM BPM in the buffer (pH 7.5 STE buffer, 0.05% SDS, 8% DMF) without Bcl-2Δ21 was subjected to the same BPM labeling reaction steps followed by SR addition with the same 0.7 μM final concentration of SERCA. Protease inhibitor PMSF (1 mM) was used in each sample to prevent proteolytic degradation. All three samples were incubated in 1.5 mL Eppendorf tubes at 37^{o}C for 1 h using a dry thermostat without agitation. After incubation, samples were transferred into quartz tubes and irradiated with 350 nm UV light for 30 min using a Rayonet photochemical reactor (The Southern New England Ultraviolet Company). Finally the samples were boiled for 5 min with sample buffer (2% SDS, 10% glycerol, and 125 mM Tris pH 6.8) and analyzed by western blotting after SDS-PAGE.

2.2.12: Details of SDS-PAGE and western blotting.

Samples boiled with the sample buffer were separated on precast 4-20% gradient gels from Bio-Rad Laboratories (Hercules, CA) or Invitrogen (Carlsbad, CA) using tris-glycine running buffer. For MS analysis, the gels were stained with Coomassie Blue protein staining reagent. For western blot analysis, the gels were electroblotted onto 0.45 μm polyvinyldifluoride (PVDF) membrane (Millipore, Bedford, MA) and ECL detection kit (GE Healthcare, UK) was used to visualize the spots according to the manufacturer's procedure.

2.2.13: Antibodies.

Mouse monoclonal anti-Bcl-2 antibody (sc-7382), Goat polyclonal Anti-Glycogen Phosphorylase antibody (sc-46347), Mouse monoclonal Sarcalumenin antibody (sc-58845) and Goat polyclonal Anti-Mg29 antibody (sc-23441) were purchased from Santa Cruz Biotechnology (Santa Cruz, CA). Anti-SERCA1 mouse monoclonal antibody (MA3-912) was from Affinity Bioreagents (Golden, CO). Rabbit Anti-Calcium Channel (α2/δ-1 subunit) antibody (C5105), Secondary horseradish peroxidase (HRP)-conjugated anti-rabbit antibodies (A0545) and anti-goat antibodies (A5420) were from Sigma (St. Louis, MO). Secondary (HRP)-conjugated anti-mouse antibodies (31437) were from Pierce Biotechnology (Rockford, IL).

2.2.14: In-gel tryptic digestion procedure.

The bands of interest were excised from Coomassie Blue stained gels, cut into smaller pieces and washed twice with 0.2 M NH_4HCO_3/50% (v/v) acetonitrile for 45 min at 37^oC. Protein reduction and alkylation was performed by incubating the gel pieces first with 10 mM DTT in 0.2 M NH_4HCO_3 for 30 min at 60^oC, followed by reaction with 20 mM iodoacetamide for 30 min at room temperature in the dark. Discarded the solution, gel pieces were washed with 200 µl of 0.2 M NH_4HCO_3/50% (v/v) acetonitrile and 250 µl of 100% acetonitrile was added to shrink the gel pieces. After 15 min, acetonitrile was removed and dried the gel pieces. Then the gel pieces were re-swollen in 20 µl of 0.2 M NH_4HCO_3 containing 5 mM $CaCl_2$ and sequencing grade modified trypsin (Promega, Madison, WI) at an approximate 5:1 molar ratio of protein to trypsin. 40-50 µl of 0.2 M NH_4HCO_3/10% (v/v) acetonitrile were added to cover the gel pieces and incubated over night (16-18 h) at 37^oC. After spinning down the gel pieces, the supernatant was submitted to the ESI-FTICR-MS facility of the Analytical Proteomics Laboratory, The University of Kansas, for analysis.

2.3: Results and Discussion.

2.3.1: Expression and purification of Bcl-2Δ21.

Bcl-2Δ21, a truncated form of human Bcl-2, was expressed in *E. coli* as a GST (Glutathione-S-Transferase) fusion protein. Affinity of GST for GSH (glutathione) helps the purification of the fusion protein from the bacterial cell lysate

using affinity chromatography. GST-Bcl-2Δ21 has an approximate apparent molecular weight of 47 kDa (Figure 2.4-a, lane 2). A thrombin cleavage site is located in the fusion protein and the incubation of GST-Bcl-2Δ21, bound to GSH-agarose beads, with thrombin yields Bcl-2Δ21. Thrombin binding beads help the removal of thrombin resulting in purified Bcl-2Δ21. Both GST and Bcl-2Δ21 have approximate apparent molecular weights of 25 kDa (Figure 2.4-a, lanes 3 and 4, respectively). The purified protein is Bcl-2Δ21 as confirmed by western blotting with monoclonal anti-Bcl-2 antibody (Figure 2.4-b).

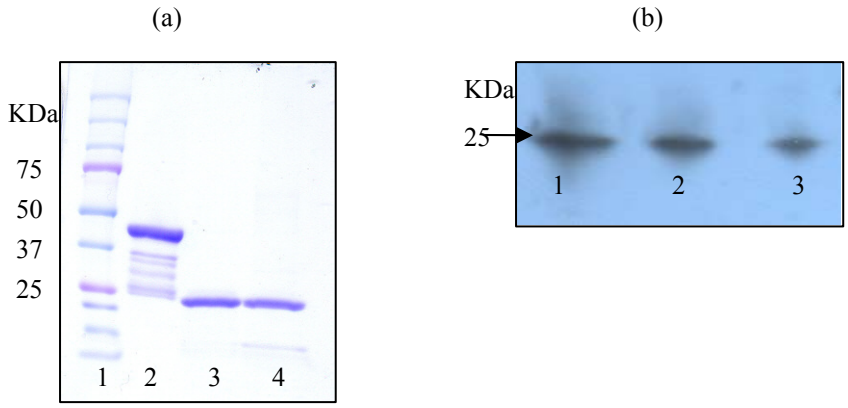

FIGURE 2.4: Expression and purification of Bcl-2Δ21: (a) Coomassie Blue staining of proteins after SDS-PAGE: lane 1, molecular weight standard; lane 2, GST-Bcl-2Δ21 bound to GSH-agarose beads; lane 3, purified Bcl-2Δ21; and lane 4, GST bound to GSH-agarose beads after thrombin cleavage of GST-Bcl-2Δ21. (b) Analysis of purified Bcl-2Δ21 by western blotting with anti-Bcl-2 monoclonal antibody: lanes 1, 2 and 3 are 0.1, 0.05 and 0.025 μg of Bcl-2Δ21, respectively.

If not used immediately, purified Bcl-2Δ21 was stored with 0.1 mM PMSF at -20°C, the best storage conditions to prevent proteolytic degradation of Bcl-2Δ21 as identified from the results (data not shown) of the experiment explained in section 2.2.1-c.

2.3.2: Optimization of BPM labeling reaction conditions.

(a) Optimum reaction time:

The Bcl-2Δ21 sample which was not incubated with BPM prior to the reaction with ThiGlo1 has more free cysteines and yields more ThioGlo1-cysteine adducts and hence more fluorescence (Figure 2.5, sample 1). The two samples incubated with BPM have fewer free cysteines to react with ThiGlo1 and produce fewer adducts and less fluorescence (Figure 2.5, samples 2 and 3). Even though less fluorescence was expected for the sample reacted with BPM for 1 h (Figure 2.5, sample 3) compared to the sample incubated with BPM only for 30 min (Figure 2.5, sample 2), both showed the same fluorescence intensity. This reveals that the 30 min incubation with BPM is sufficient to produce the maximum amount of BPM labeled Bcl-2Δ21.

(b) Effect of the redox status of Bcl-2Δ2 cysteine:

Since BPM is a thiol reactive cross-linking reagent, the redox status of the cysteine affects the efficiency of the BPM labeling reaction. If the only cysteine residue of Bcl-2Δ2, Cys158, is oxidized during protein purification steps it would result in a lower yield of BPM-Bcl-2Δ2. Fluorescence measurement of ThioGlo1-

cysteine adducts of samples without and with DTT (dithiothreitol) treatment does not show a significant difference (Figure 2.6, samples 1 and 2, respectively). This reveals that the purified Bcl-2Δ2 contains no/very little oxidized cysteines and almost all the cysteines in the sample are available for the reaction with BPM. On the other hand, the slightly higher fluorescence of DTT-treated sample could be due to the reaction of ThioGlo1 with excess DTT even after overnight dialysis (Figure 2.6, sample 2).

FIGURE 2.5: Optimum reaction time for BPM labeling of Bcl-2Δ21 as determined by ThioGlo1 labeling of free cysteine residues: (1), sample which was not reacted with BPM prior to the addition of ThioGlo1; (2) and (3), samples which reacted with BPM for 30 min and 1 h, respectively, prior to the addition of ThioGlo1.

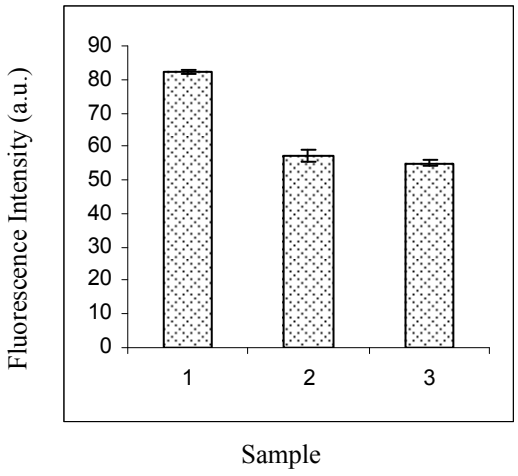

FIGURE 2.6: Redox status of cysteine of Bcl-2Δ21 as determined by ThioGlo1 labeling of free cysteine residues: (1), sample was not treated with DTT; (2), sample was treated with DTT prior to the addition of ThioGlo1.

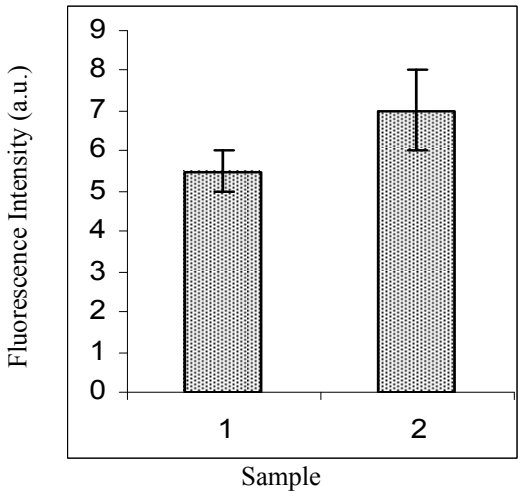

(c) Effect of native and denatured Bcl-2Δ21:

As described in section 2.3.2-a, when ThioGlo1 is added to Bcl-2Δ21 which has been reacted with BPM, there should be no free cysteines available for adduct formation with ThioGlo1. Therefore the comparison of fluorescence intensity of this sample ("Bcl-2Δ21→BPM→ThioGlo1"), with that of Bcl-2Δ21 which is directly reacted with ThioGlo1 ("Bcl-2Δ21→ ThioGlo1") should reveal the amount of BPM-Bcl-2Δ2 produced. As indicated by these two samples prepared using native Bcl-2Δ21, less than 10% of the BPM-Bcl-2Δ2 appears to have formed (compare the difference between 1 and 2 in Figure 2.7).

Based on the NMR structure of Bcl-2 (*27*), the only cysteine, Cys158, of Bcl-2Δ21 is buried in the interior of the molecule. Therefore the BPM labeling reaction was performed under denaturing conditions. The same two samples ("Bcl-2Δ21→ThioGlo1" and "Bcl-2Δ21→BPM→ThioGlo1") were prepared in the presence of 2% SDS, a strong protein denaturing agent and measured florescence (Figure 2.7, samples 3 and 4 respectively). Comparison of these two samples shows a BPM-Bcl-2Δ2 yield of about 65% under denaturing conditions. Samples 5 and 6 in Figure 2.7 are the two controls indicating the background fluorescence. The control sample 5 contains both BPM and ThioGlo1 but lacks Bcl-2Δ21 whereas sample 6 contains only ThioGlo1.

Above results confirm that the cysteine residue in Bcl-2Δ2 is not well exposed in the native molecule. Upon denaturation the residue becomes exposed yielding more BPM-Bcl-2Δ2. However, since SDS is a very strong denaturing agent it could

drastically change the native conformation of Bcl-2Δ2, necessary for the interaction with SERCA. Attempts to use mild denaturing agents such as NP-40 and CHAPS did not increase the BPM labeling efficiency (data not shown). Therefore the lowest effective SDS concentration which yields a reasonable amount of BPM-Bcl-2Δ2 was determined. Approximately 50% of BPM-Bcl-2Δ2 could be achieved in the presence of 0.05% SDS (data not shown) and BPM-Bcl-2Δ2 for photo cross-linking experiments was prepared in the presence of 0.05% SDS. This SDS concentration is enough for facilitating the reaction between BPM and Cys158 of Bcl-2Δ2 and can be dialyzed out before the cross-linking reaction.

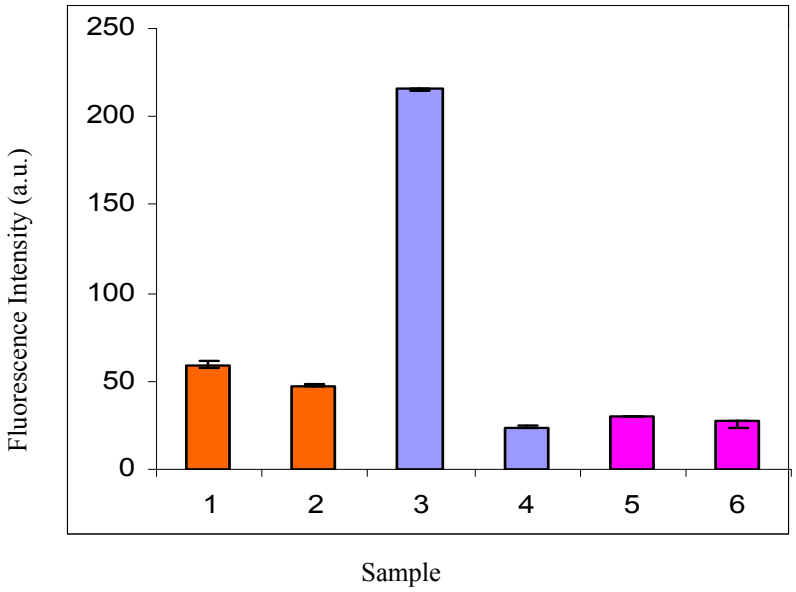

FIGURE 2.7: Comparison of native and denatured Bcl-2Δ21 in BPM labeling, as determined by ThioGlo1 labeling of free cysteine residues: (1) and (3), Bcl-2Δ21→ThioGlo1; (2) and (4), Bcl-2Δ21→BPM→ThioGlo1; (5), BPM/ThioGlo1 alone; (6), ThioGlo1 alone; (●), samples without 2% SDS; (●), samples with 2% SDS.

(d) Comparison of Bcl-2Δ2 and His_6-Bcl-2Δ17 in cysteine derivatization:

His_6-Bcl-2Δ17 in the native form (Figure 2.8, 2-●) is slightly more efficient compared to native Bcl-2Δ2 (Figure 2.8, 1-●) in cysteine derivatization as revealed by fluorescence measurement of ThioGlo1-cysteine adducts. The hexahistidine tag of His_6-Bcl-2Δ17 might be affecting the conformation of the molecule thus making Cys158 more exposed and available for derivatization. The two proteins under denaturing conditions also show the same pattern in cysteine derivatization (Figure 2.8, 1and 2-●). However the differences in fluorescence measurements of the two proteins might be within experimental error. The measurements were not replicated in this experiment due to lack of sufficient proteins and therefore no error bars are available. Over all, the two proteins are comparable in cysteine derivatization ability.

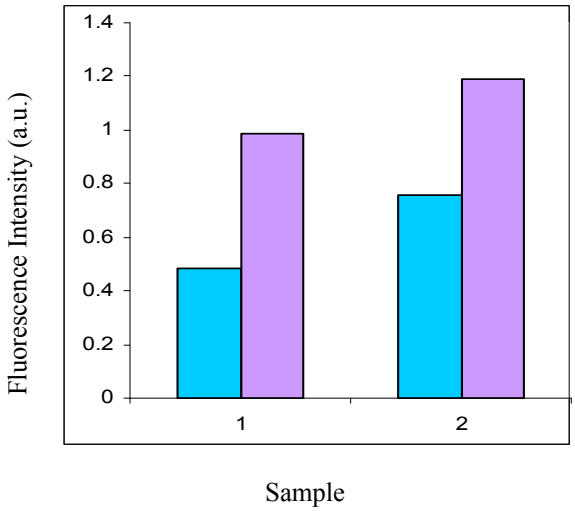

FIGURE 2.8: Comparison of Bcl-2Δ2 and His_6-Bcl-2Δ17 in cysteine derivatization, as determined by ThioGlo1 labeling of free cysteine residues: (1), samples of Bcl-2Δ21; (2), samples of His_6-Bcl-2Δ17; (●) samples without 0. 2% SDS; (●) samples with 0.2% SDS.

2.3.3: Characterization of BPM labeling reaction sample.

(a) RP-HPLC separation of BPM labeling reaction mixture:

Figure 2.9 shows the chromatograms of BPM labeling reaction samples recorded at 280 nm for protein detection. When a sample of Bcl-2Δ21 which was not subjected to BPM labeling, was run through the RP-HPLC column, Bcl-2Δ21 eluted at 58 min (blue line). The peak at 62 min might be due to proteolytic and/or hydrolytic degradation product of Bcl-2Δ21. When the BPM labeling reaction mixture is subjected to RP-HPLC, in addition to the Bcl-2Δ21 peak, additional peaks should appear for BPM-Bcl-2Δ21 and also for left over BPM, if any after dialysis. As expected, additional peaks were seen eluting at 43 min and at 50 min (red line).

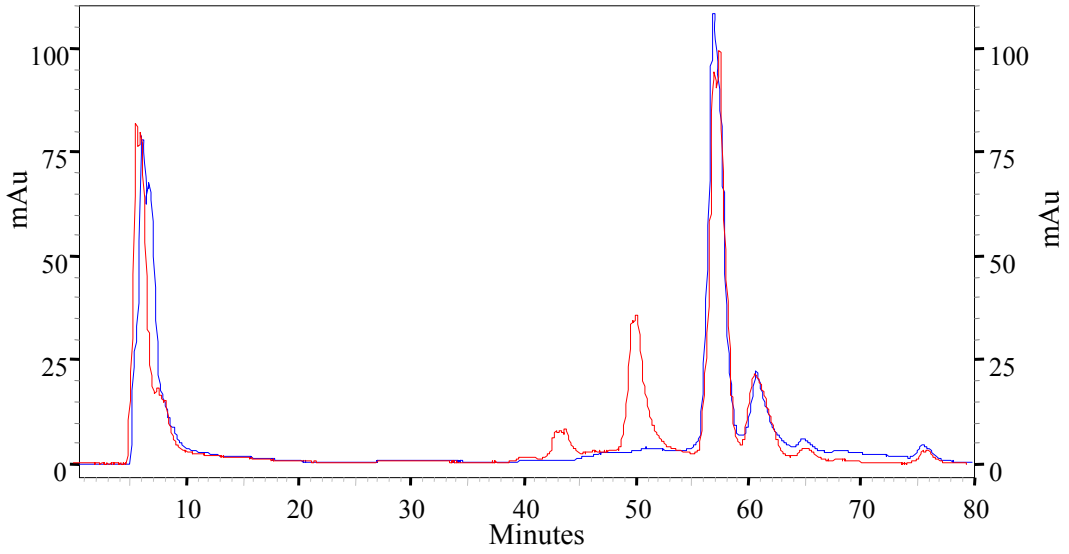

FIGURE 2.9: Determination of BPM-Bcl-2Δ21 using RP-HPLC separation of the reaction mixture; Chromatograms recorded at 280 nm: (—), Bcl-2Δ21 sample before BPM labeling; (—), Bcl-2Δ21 sample after BPM labeling.

According to the chromatograms in Figure 2.10 which were recorded at 260 nm, the maximum absorbance of BPM-thiol adducts, the peak eluting at 50 min showed an increase in absorbance and hence it could be the peak of BPM-Bcl-2Δ21. The peak at 43 min could be postulated as unreacted BPM. Absorbance of unlabeled Bcl-2Δ21 at 260 nm (Figure 2.10, peak at 58 min) is probably due to the tryptophan residues in the molecule.

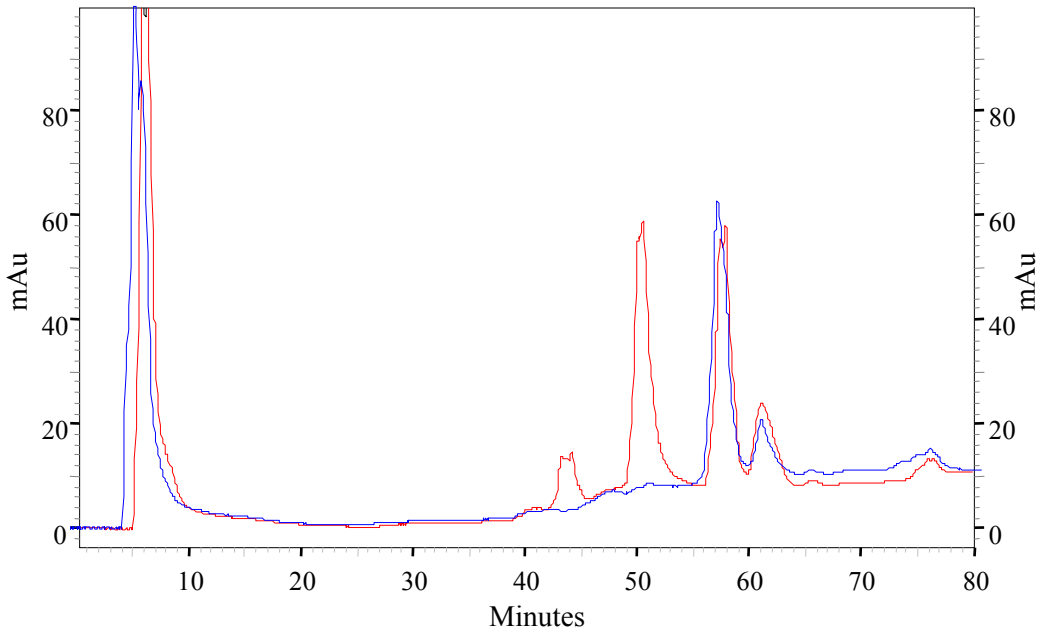

FIGURE 2.10: Determination of BPM-Bcl-2Δ21 using RP-HPLC separation of the reaction mixture; Chromatograms recorded at 260 nm: (—), Bcl-2Δ21 sample before BPM labeling; (—), Bcl-2Δ21 sample after BPM labeling.

In order to further verify the identity of these two peaks at 43 min and 50 min, the BPM labeling reaction sample was spiked with increasing concentrations of BPM separately, prior to the RP-HPLC separation. Chromatograms recorded at 260 nm are

shown in Figure 2.11. The chromatogram in black is for Bcl-2Δ21 which was not subjected to BPM labeling. Materials eluted in between 25-32 min could probably be some impurities trapped in the column. BPM labeling reaction samples spiked with 25 μM and 40 μM BPM are indicated in blue and red, respectively. The absorbance intensity of the peak at 43 min was clearly increased with 40 μM BPM verifying that the material eluting at 43 min is BPM and hence the peak at 50 min is BPM-Bcl-2Δ21. Over all these RP-HPLC data indicate the success of the BPM labeling of Bcl-2Δ21, yet do not confirm the presence of BPM-Bcl-2Δ21 in the reaction mixture. Mass spectrometry was utilized to confirm the presence of BPM-Bcl-2Δ21 in the mixture (see below).

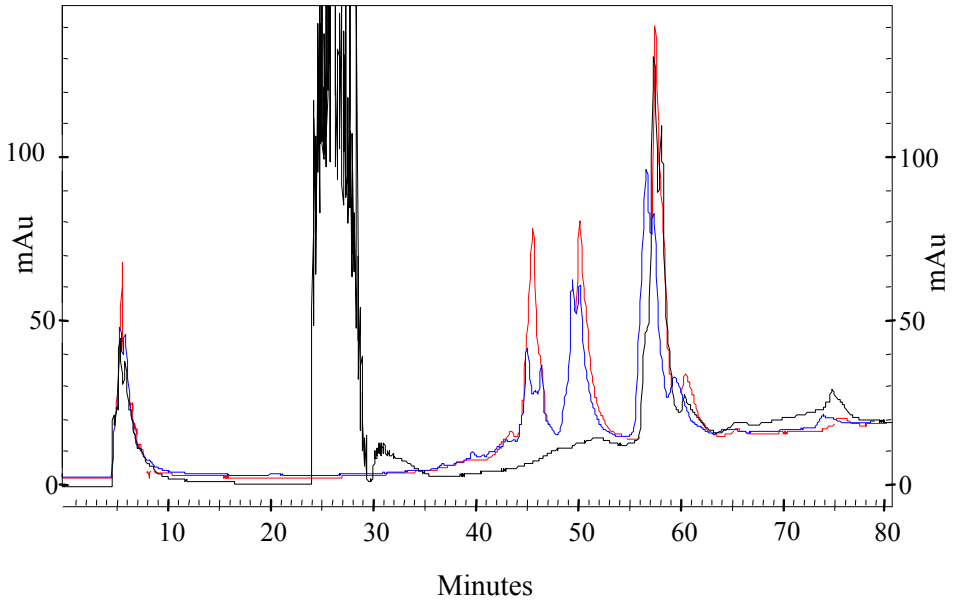

FIGURE 2.11: RP-HPLC separation of BPM labeling reaction mixture after BPM spiking; Chromatograms recorded at 260 nm: Bcl-2Δ21sample before BPM labeling (—), BPM labeling reaction samples spiked with 25μM (—) and 40μM (—) BPM are shown.

(b) Mass spectrometric analysis of BPM labeling reaction mixture:

Analysis of the BPM labeling reaction mixture by ESI-FTICR-MS, after in-gel tryptic digestion, reveals the presence of +3-ly charged Bcl-2Δ21 peptide (m/z 767.0187) labeled with the hydrolyzed form of BPM. The associated mass error of this peptide ion, 8.2 ppm, is below the accepted maximum error (10 ppm) of FTICR-MS. The MS/MS spectrum of this peptide is shown in Figure 2.12. Both singly and doubly charged y_7 and b_{12} ions were found, confirming the presence of derivatized Cys158 and these ions are circled in the spectrum.

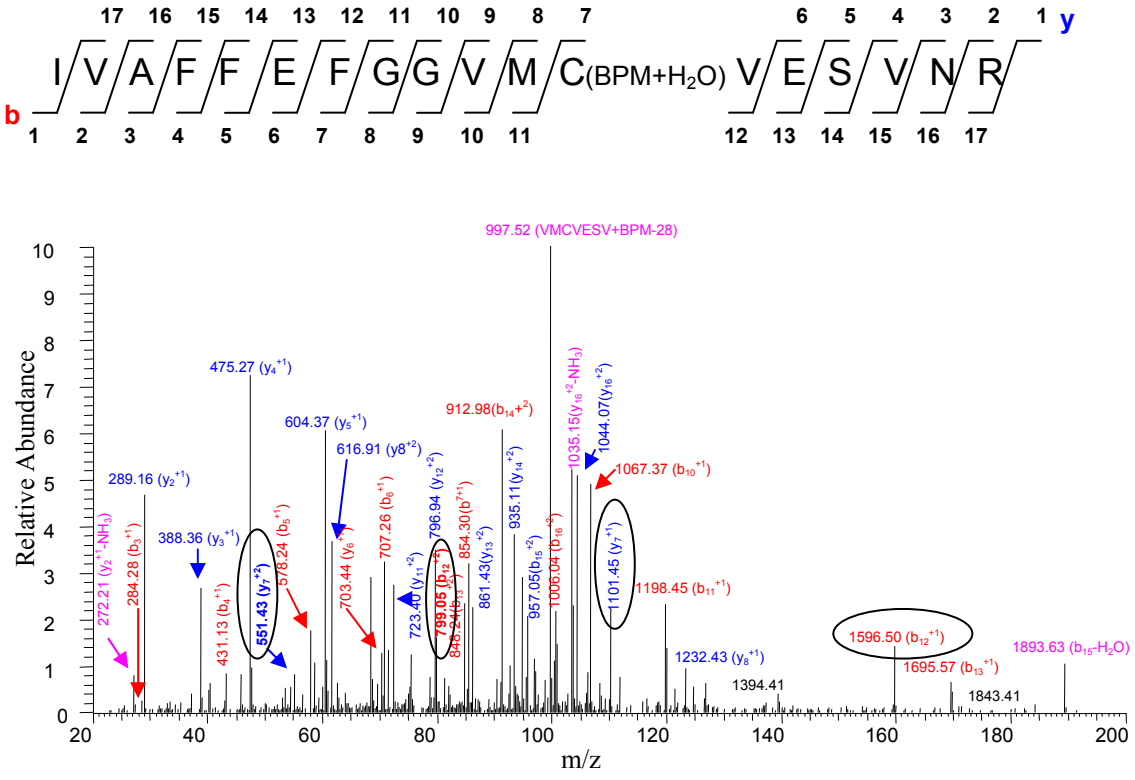

FIGURE 2.12: MS/MS spectrum of BPM labeled peptide of Bcl-2Δ21: Sequence of the peptide is shown above the spectrum; y and b ions are labeled in blue and red respectively; Internal fragment ions and neutral losses are indicated in pink; y_7 and b_{12} ions which include the cysteine labeled with hydrolyzed BPM are circled.

(c) Effect of BPM-Bcl-2Δ21 on Ca^{2+}-ATPase activity of SERCA:

When the interface of interacting proteins is identified through cross-linking, the site of the cross-linking reagent is a key factor. If it is too close to the interface or at a site directly involved in the interaction, it might block the proteins interacting with each other. In the case of Bcl-2Δ21 and SERCA interactions, the photo cross-linking reagent, BPM is attached to Cys158 of Bcl-2Δ21. This BPM labeled Bcl-2Δ21 might fail to interact with and inactivate SERCA. Dremina et al. (*23*) have previously shown that the modification of Cys158 of Bcl-2Δ21 does not have any effect on the inhibition of SERCA activity, as determined using carboxymethylated and also peroxynitrite-treated Bcl-2Δ21. In order to confirm that the labeling of Cys158 with BPM is also not affecting the inhibition of SERCA, the Ca^{2+}-ATPase activity assay was utilized.

Sample 1 of Figure 2.13 shows the Ca^{2+}-ATPase activity of the SR in STE buffer. The two activity values of this sample before and after 3 h of incubation are almost the same. The SR sample incubated with BPM treated Bcl-2Δ21 shows a significant reduction of activity compared to the activity before the incubation (Figure 2.13, Sample 2), confirming that BPM treatment does not affect the inhibition of SERCA by Bcl-2Δ21. The activity of this SR sample, measured right after mixing with BPM treated Bcl-2Δ21 and before the incubation shows reduced activity. Therefore the few minutes taken for the first measurement of activity should be long enough to inactivate some of the SERCA in the sample. The third sample (Sample 3 in Figure 2.13) shows activity values comparable to those of Sample 1. This proves

that the reduced activity in Sample 2 after 3 h of incubation is not due to the effect of left over SDS in the buffer but is due to the BPM-Bcl-2Δ21. However, the BPM labeling reaction conditions used yield only about 50% of BPM-Bcl-2Δ21 and hence the reduction in activity could result from unlabeled Bcl-2Δ21 in the sample. In a separate experiment, two Bcl-2Δ21 samples with and without BPM treatment were compared for their ability to reduce the Ca^{2+}-ATPase activity of the SR. Both samples could successfully reduce the activity (data not shown) further confirming that the BPM treatment does not affect the inhibition of SERCA by Bcl-2Δ21.

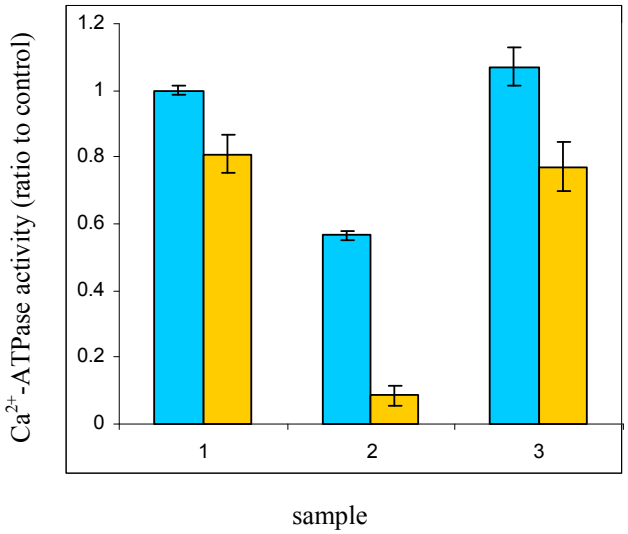

FIGURE 2.13: Effect of BPM treated Bcl-2Δ21 on Ca^{2+}-ATPase activity of SERCA: (1), SR in STE buffer; (2), SR mixed with BPM-Bcl-2Δ21 in STE buffer; (3), SR in the STE buffer which was subjected to BPM labeling reaction conditions; (●) before incubation at 37 °C; (●) after incubation at 37 °C.

2.3.4: Photo cross-linking of Bcl-2Δ21 with SERCA.

In photo cross-linking of Bcl-2Δ21with SERCA, the molar ratio of the two proteins and the incubation time of Bcl-2Δ21/SR mixture prior to UV irradiation, were critical parameters for the formation of cross-linked products. Out of the different molar ratios examined, cross-linked products were clearly seen, in the western blot with Bcl-2Δ21 antibody, when 2:1 (Bcl-2Δ21: SERCA) ratio was used. Complete inactivation of SERCA has been reported previously, after 2 hours of co-incubation of the two proteins with this ratio (*23, 25*). With only 15 min of co-incubation of Bcl-2Δ21 and SR, clear cross-linked bands appeared in the western blot. The prolonged incubation times did not increase the intensity of the cross-linked bands but smeared lanes in the western blots (data not shown). The results of the photo cross-linking experiment completed with 2:1 (Bcl-2Δ21: SERCA) molar ratio and 15 min of co-incubation are explained below.

The Figure 2.14 shows the western blots of photo cross-linked samples. The apparent molecular weights of SERCA and Bcl-2Δ21 are ~110 kDa and 25 kDa, respectively. Therefore the cross-linked products should appear at 135 kDa and/or 160 kDa if the molar ratio is 1:1 and 2:1 (Bcl-2Δ21: SERCA), respectively. As predicted, two bands appear at 135 kDa and 160 kDa, with the sample containing both BPM treated Bcl-2Δ21and SR (Bcl-2Δ21/BPM/SR) in the western blot of the Bcl-2 antibody (Figure 2.14-a, lane 3). The intensities of these cross-linked bands are significantly lower compared to the bands of monomer and the dimer of Bcl-2Δ21. This is acceptable if the interaction is transient as reported previously by Dremina et

al. (*23, 25*). As revealed by the relatively lower intensity of the band at 160 kDa compared to that of the 135 kDa band, the 1:1 ratio (Bcl-2Δ21: SERCA) is more favorable.

Importantly, the control sample of Bcl-2Δ21/BPM without SR shows only the monomer and the dimer of Bcl-2Δ21, but no higher oligomers (compare lanes 2 and 3 of Figure 2.14-a). Therefore the two bands seen above 100 kDa with the Bcl-2Δ21/BPM/SR sample are probably due to cross-linking of Bcl-2Δ21 with SERCA. However, it is possible that some other protein/proteins in the SR, which can interact with Bcl-2Δ21, produce bands with identical molecular weights. This is discussed in a later section.

A significant amount of homodimer of Bcl-2Δ21 is seen in the western blot. It is already known that the homodimerization of Bcl-2 involves two distinct surfaces of Bcl-2, the acceptor and donor surfaces. The Cys158 of Bcl-2Δ21 is located in BH1, one of the domains in the acceptor surface (*28*). Therefore, the cross-linking reagent attached at Cys158 in Bcl-2Δ21 can easily form a covalent bond with the other Bcl-2Δ21 molecule in the dimer. It is interesting to see more homodimers of Bcl-2Δ21 in the presence of SR (compare 50 kDa band in lanes 2 and 3 of Figure 2.14-a). The SR vesicle membrane might be facilitating the homodimerization of Bcl-2Δ21. The band at 160 kDa could probably be due to the interaction of the homodimer of Bcl-2Δ21 with a SERCA molecule and the Cys158, hence the BH1 domain of the second molecule of Bcl-2Δ21 in the dimer should be involved in the interactions with

SERCA. The bands seen between 25 kDa and 50 kDa should be the degradation products of the dimer of Bcl-2Δ21.

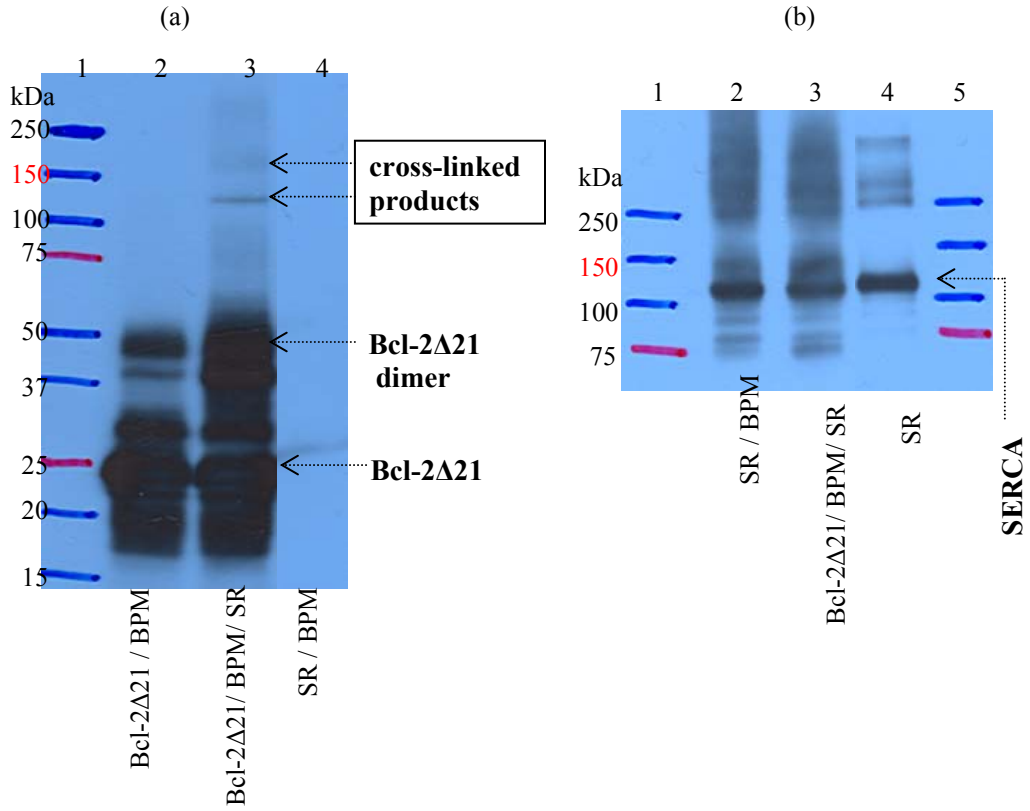

FIGURE 2.14: Photo cross-linking of Bcl-2Δ21 with SERCA: (a) Bcl-2 antibody WB of cross-linked samples; (b) SERCA antibody WB of cross-linked samples; (Bcl-2Δ21/BPM), sample containing BPM treated Bcl-2Δ21 alone; (Bcl-2Δ21/BPM/SR), sample containing both BPM treated Bcl-2Δ21 and SR; (SR/BPM), sample containing SR in the STE buffer which was subjected to BPM labeling reaction conditions; (SR), a fraction of purified SR loaded in the gel as the control for the WB.

The SERCA antibody WB of the cross-linking experimental samples is shown in the Figure 2.14-b. Unexpectedly, the result of this WB is not consistent with that of the Bcl-2 antibody WB. The photo cross-linked reaction sample, Bcl-2Δ21/BPM/SR, (Figure 2.14-b, lane 3) and also the control sample without Bcl-2Δ21, SR/BPM, (Figure 2.14-b, lane 2) show identical results in the WB.

A fraction of purified SR vesicles was loaded on the gel (Figure 2.14-b, lane 4) as a control for the WB. Compared to this lane 4, not only the photo cross-linking reaction sample, Bcl-2Δ21/BPM/SR, but also the control sample, SR/BPM, show a band corresponding to the dimer of SERCA-Bcl-2Δ21 at 135 kDa, where the cross-linked bands are seen in the WB with the Bcl-2 antibody. It should be mentioned here that the purified SR vesicles contain a very small fraction of co-purified Bcl-2 and it can cause the band in the SR/BPM control sample. If that is the case, the intensity of the band of Bcl-2Δ21/BPM/SR sample should be higher than that of the SR/BPM control sample because the Bcl-2Δ21/BPM/SR sample contains a relatively huge amount of Bcl-2Δ21 and therefore more cross-linked SERCA-Bcl-2Δ21. However the intensities of the bands of the two samples are the same. On the other hand the same SR/BPM control sample in the WB of Bcl-2 antibody does not show any band in the same region (Figure 2.14-a, lane 4). For these reasons the bands in the two samples are probably not the cross-linked SERCA and Bcl-2Δ21/Bcl-2.

The control sample was prepared by dissolving SR in the STE buffer, which was subjected to all the BPM labeling reaction steps but without Bcl-2Δ21 and therefore it should indicate the effect of BPM left in the buffer, if any, after dialysis.

Therefore the bands seen above the SERCA band (110 kDa), with both samples, are probably caused by the BPM left in the sample, even after 4 hours of dialysis. There are 24 cysteine residues in SERCA and any left over BPM can label some of these cysteines. The BPM labeled SERCA should appear above 110 kDa in the WB.

Furthermore, only a pale smear is seen corresponding to the trimer of SERCA-2Bcl-2Δ21 (160 kDa) and the intensity of this smear is also the same in both samples. These results suggest that WB with SERCA antibody does not indicate the presence of SERCA/Bcl-2Δ21 cross-linked products. The monoclonal SERCA antibody used in our studies recognizes an epitope located between Ala506 and the C-terminal of the molecule. If the SERCA interface for Bcl-2Δ21 is located within this region of the molecule, antibody recognition might be affected and the results seen in the WB of SERCA antibody can be accepted. In fact which is the case as revealed by mass spectrometric data (see 2.3.6).

Also if there are some other proteins in the SR which are comparable with Bcl-2Δ21 in size and can interact with SERCA , the BPM labeled SERCA can cross-link with those proteins causing bands in the same region as the cross-linked products of SERCA and Bcl-2Δ21. This is addressed under "Other possible SR proteins associated with Bcl-2 or SERCA".

2.3.5: Photo cross-linking of His_6-Bcl-2Δ17 with SERCA.

In photo cross-linking reactions with His_6-Bcl-2Δ17 samples were subjected to Ni^{2+} affinity purification. This procedure helps to purify cross-linked products of His_6-Bcl-2Δ17 from the reaction mixture thereby making the sample less complex and also enriched with cross-linked products.

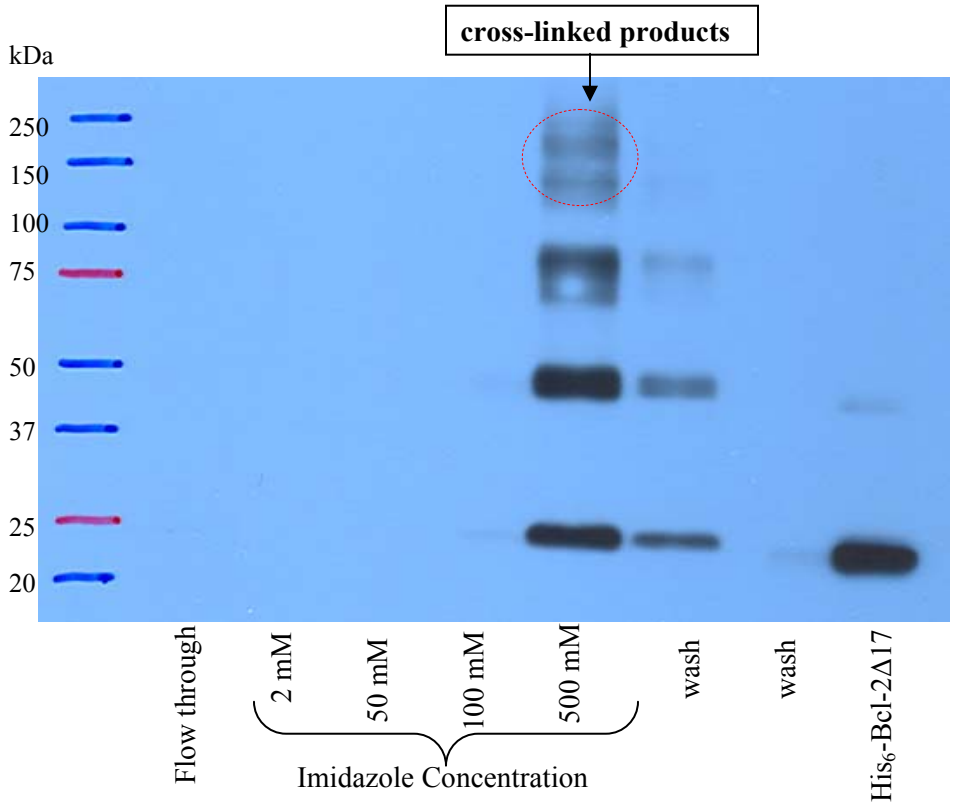

FIGURE 2.15: Photo cross-linking of His_6-Bcl-2Δ17 with SERCA: Bcl-2 antibody western blot of the fractions of His_6-Bcl-2Δ17/BPM/SR cross-linking reaction sample eluted from the Ni^{2+} column with different concentrations of imidazole (Im). The last lane is 0.1µg of His_6-Bcl-2Δ17 as a control for the western blot.

The fractions of His_6-Bcl-2Δ17/BPM/SR sample in the WB of Bcl-2 antibody show His_6-Bcl-2Δ17 in the 500 mM Im fraction (Figure 2.15). The same 500 mM fraction shows monomer, dimer and also probably a trimer of His_6-Bcl-2Δ17. Consistent with the results seen for the cross-linking reaction of Bcl-2Δ21, two bands (marked with a circle) are seen corresponding to the cross-linked products of His_6-Bcl-2Δ17 with SERCA with the sizes of 135 kDa and 160 kDa. His_6-Bcl-2Δ17/BPM control sample fractions did not show any band above 100 kDa (data not shown), confirming that these two bands are not due to oligomerization of BPM-His_6-Bcl-2Δ17.

Figures 2.16-a and b are SERCA antibody western blots of the BPM-His_6-Bcl-2Δ17/SR sample and the SR/BPM control sample, respectively. The comparison of the fractions of His_6-Bcl-2Δ17/BPM/SR cross-linking reaction sample (Figure 2.16-a) reveals that SERCA is also trapped in the column and is eluted with high concentrations of Im. This could be due to the association of SERCA with His_6-Bcl-2Δ17. However, since SERCA is seen in the higher Im fractions of the SR/BPM control sample, SERCA itself has some affinity for the Ni^{2+} ions.

The 100 mM Im fraction of the Bcl-2Δ17/BPM/SR sample shows a band at ~135 kDa which is not detected in the western blot with Bcl-2 antibody (compare the 100 mM Imidazole fraction in Figure 2.15 with that of Figure 2.16-a). This confirms the presence of some other product/products of SERCA of the same size as the cross-linked SERCA-His_6-Bcl-2Δ17 dimer. Since this band is seen only with Bcl-

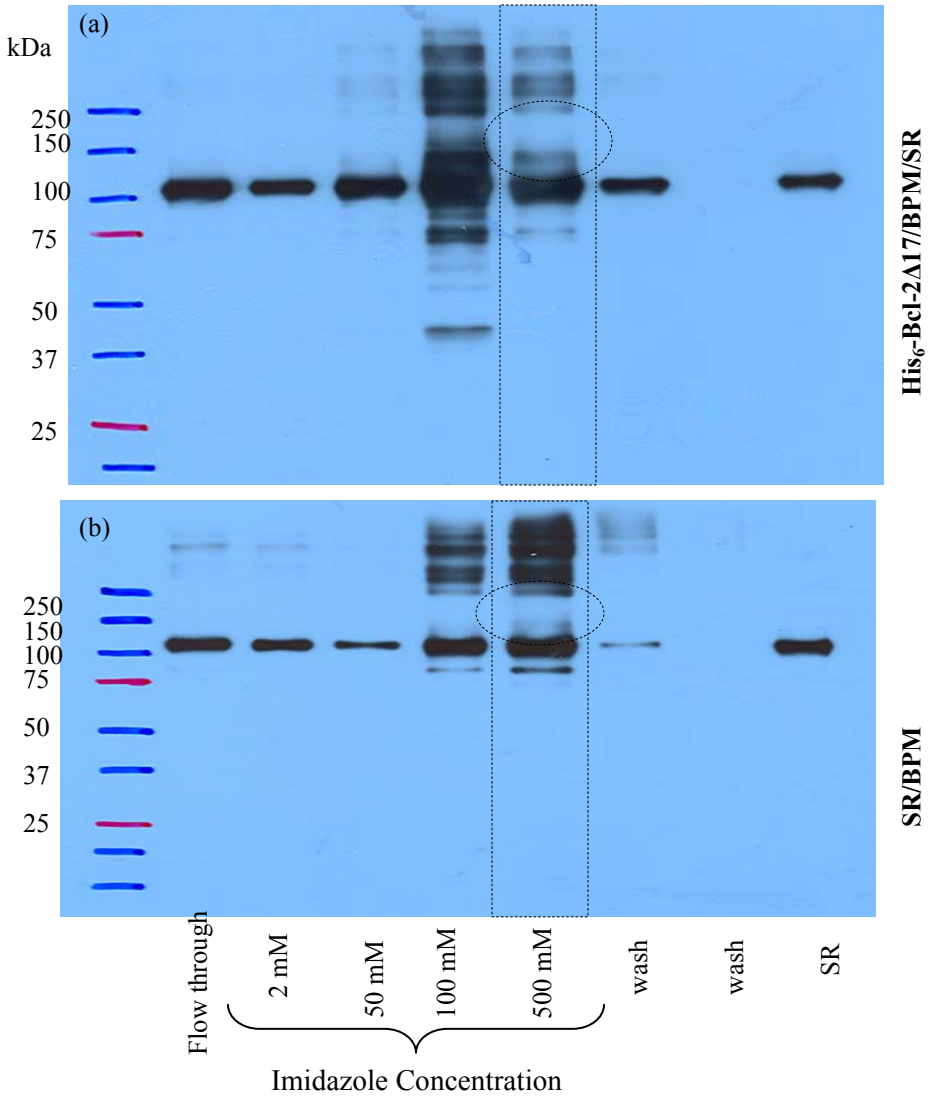

FIGURE 2.16: Photo cross-linking of His_6-Bcl-2Δ17 with SERCA: SERCA antibody western blots of the fractions of the His_6-Bcl-2Δ17/BPM/SR cross-linking reaction sample (a) and the SR/BPM control sample (b) eluted from the Ni^{2+} column with different concentrations of imidazole (Im). The last lane is a fraction of purified SR vesicles as a control for the western blot. The lanes and the regions of the two western blots that should be compared with the western blot in Figure 2.15 are marked with dashed lines.

2Δ17/BPM/SR sample and not with the SR/BPM control, formation of these other product/products of SERCA should be facilitated by the presence of His_6-Bcl-2Δ17.

Two bands that can be considered as cross-linked products of His_6-Bcl-2Δ17 were seen in the fraction of 500 mM Im with the western blot of Bcl-2 antibody (Figure 2.15). When the same fraction is considered in the western blots of SERCA antibody, the His_6-Bcl-2Δ17/BPM/SR sample indicates a band at ~135 kDa with a higher intensity compared to the SR/BPM control sample (compare the circled regions of the western blots in Figure 2.16). This band could rather be product/products of SERCA carrying over to the fraction of 500 mM Im other than the cross-linked dimer of SERCA-His_6-Bcl-2Δ17. In addition the western blots of SERCA antibody do not reveal a band at 160 kDa corresponding to the trimer of SERCA-2His_6-Bcl-2Δ17. These observations with the western blots of SERCA antibody further supports the assumption that after binding with Bcl-2, SERCA is not recognized by the antibody.

2.3.6: Chemical cross-linking of Bcl-2 Δ21 with SERCA.

In addition to the photo cross-linking using BPM, four heterobifunctional chemical cross-linkers, BMPS, MBS, SMCC and SMPH, with different spacer lengths were used to cross-link Bcl-2Δ21 with SERCA. The two functionalities of the cross-linkers are the amine reactive NHS-ester and the sulfhydryl reactive maleimide group. Since the Bcl-2Δ21 purification buffer, STE, consists of Tris which contains primary amines, it was exchanged with the PBS buffer before the cross-linking

reaction, to prevent the reaction of the cross-linker with the Tris. The cross-linking experiments were completed using the same two-step procedure used in photo cross-linking. In the first step the cross-linker is attached to one of the proteins and the excess reagent is removed. The addition of the second protein during the second step results in cross-linked products. Experiments were completed starting with either Bcl-2Δ21 (Bcl-2Δ21-Linker → SR) or SR (SR-Linker → Bcl-2Δ21). The reaction started with Bcl-2Δ21 (Bcl-2Δ21-Linker → SR) did not show any cross-linked products (data not shown). The modification of Bcl-2Δ21 by the cross-linker at multiple sites might have drastically changed the conformation of Bcl-2Δ21 necessary for the association with SERCA. On the other hand, the reaction started with SR (SR-Linker → Bcl-2Δ21) generated clear western blots and are explained below.

When the linker is added to SR, all the SR proteins including SERCA are labeled with the linker. Upon mixing with Bcl-2Δ21, linker-attached SERCA and also the other proteins capable of interacting with Bcl-2Δ21, make cross-linked products. The western blot with Bcl-2 antibody clearly shows the products of Bcl-2Δ21 above 100 kDa (Figure 2.17, lanes 3-6). The possible SERCA/Bcl-2Δ21 products should also be among these bands. The absence of bands above 100 kDa with the control samples of cross-linker/Bcl-2Δ21 (Figure 2.17, lanes 7-10) and also of Bcl-2Δ21/SR (lane 2) confirms that the bands seen with the samples of SR/cross-linker/Bcl-2Δ21 are not oligomers but cross-linked products of Bcl-2Δ21 with the proteins of SR.

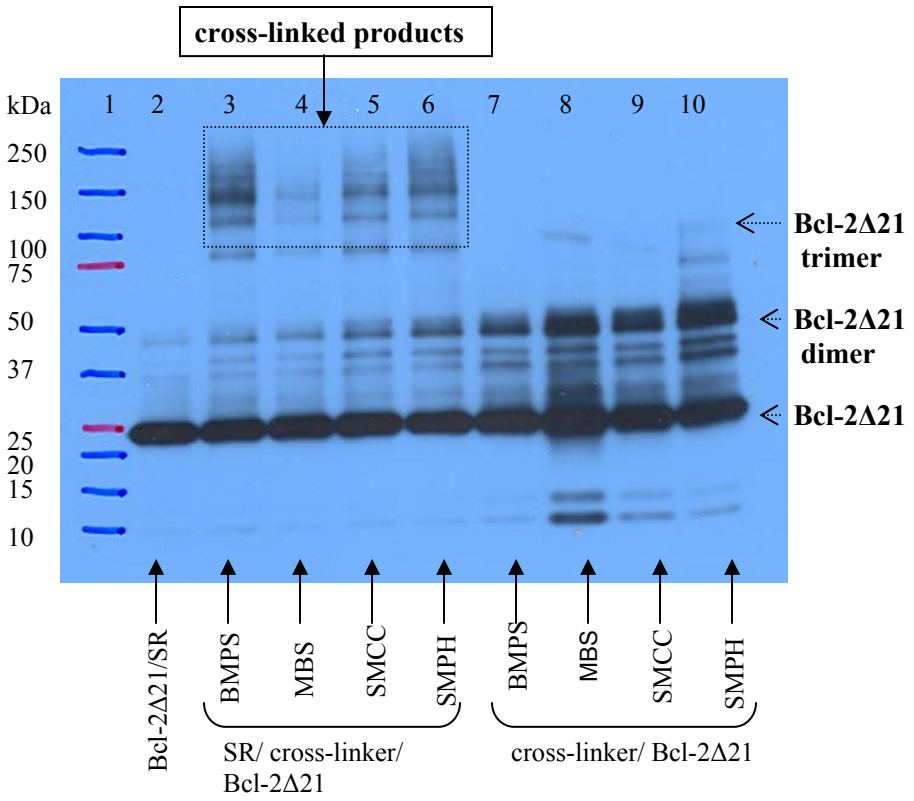

FIGURE 2.17: Chemical cross-linking of Bcl-2Δ21 with SERCA: Bcl-2 antibody western blot of the chemical cross-linking reaction samples of SR/cross-linker/Bcl-2Δ21 and cross-linker/ Bcl-2Δ21. The cross-linked products of Bcl-2Δ21 seen with the samples of SR/cross-linker/Bcl-2Δ21 are boxed. Bcl-2Δ21/SR is the control sample without any cross-linker.

Out of the four cross-linkers used, one with the optimum spacer length should efficiently cross-link the interfaces of the SERCA/Bcl-2Δ21 complex, thereby producing the most intense band in the western blot. The western blot of Bcl-2 antibody reveals less cross-linked products with MBS while the other three cross-

linkers, BMPS, SMCC and SMPH, show the same yields (compare lanes 3-6 in Figure 2.17). However since all the bands above 75kDa of SR/MBS/Bcl-2Δ21 (lane 4) are less intense, this could probably be the result of some structural constraints associated with MBS in cross-linking. Since BMPS, SMCC and SMPH show the same efficiency, the distance between the interface/interfaces of Bcl-2Δ21/SERCA complex can range from ~6-14Å.

In order to identify the cross-linked products of SERCA, the chemical cross-linking reaction samples were probed with SERCA antibody (Figure 2.18). As seen in the western blot, almost all SERCA in the two sets of samples of SR/cross-linker/Bcl-2Δ21 and SR/cross-linker is present as higher oligomers of >250 kDa. Two cross-linked products of SERCA are seen with the samples of SR/cross-linker/Bcl-2Δ21 (Figure 2.18, lanes 3-6) specifically with SMCC and BMPS. However the same bands are seen even in the absence of Bcl-2Δ21 as seen with the control samples of SR/cross-linker (Figure 2.18, lanes 7-10), which did not show any band with Bcl-2 antibody (data not shown). Nevertheless the pattern of the intensities of these bands is not comparable to those with Bcl-2 antibody. Therefore these products cannot be of SERCA/Bcl-2Δ21 and the previously made assumption, after binding with Bcl-2, SERCA is not recognized by the antibody, should be emphasized here too. Since the intensities of the bands are higher in the samples of SR/cross-linker/Bcl-2Δ21, cross-linking of SERCA with other SR proteins is somehow facilitated by the presence of Bcl-2Δ21.

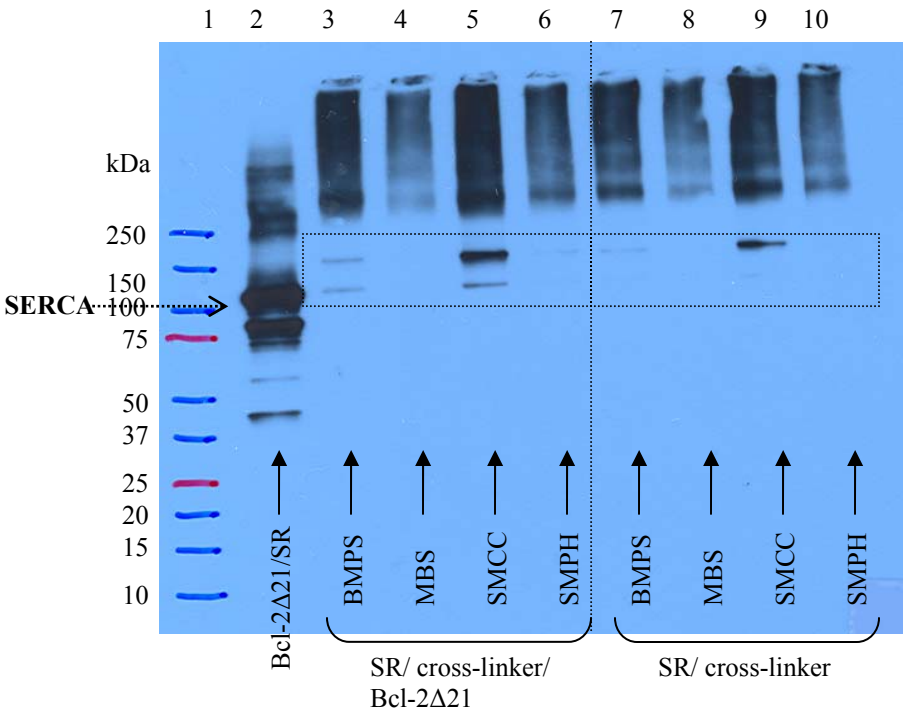

FIGURE 2.18: Chemical cross-linking of Bcl-2Δ21 with SERCA: SERCA antibody western blot of the chemical cross-linking reaction samples of SR/cross-linker/Bcl-2Δ21 and the control samples of SR/cross-linker and Bcl-2Δ21/SR. The region of the blot indicating cross-linked products is boxed.

2.3.7: Mass spectrometric analysis of photo cross-linked SERCA/Bcl-2Δ21.

After the cross-linking reaction, the sample was subjected to SDS-PAGE. In the first mass spectrometric trial, the gel band corresponding to the 160 kDa band identified with Bcl-2 antibody, was cut out from the lanes of the Bcl-2Δ21/BPM/SR sample and also from the SR/BPM and Bcl-2Δ21/SR control samples, in-gel digested with Trypsin and subjected to ESI-FTICR-MS analysis. The digests of the control

samples in the order of SR/BPM and Bcl-2Δ21/SR, were run in the instrument first followed by the digests of Bcl-2Δ21/BPM/SR sample, in order to prevent any carry over effect. The amino acid coverages of SERCA were 45%, 45% and 39% for the Bcl-2Δ21/BPM/SR, Bcl-2Δ21/SR and SR/BPM, respectively. The appearance of SERCA in the gel bands of SR/BPM and Bcl-2Δ21/SR control samples is acceptable since SERCA was seen at 160 kDa of the control samples in the western blots of SERCA antibody. Importantly, Bcl-2Δ21 peptides showed up in the digests of the Bcl-2Δ21/BPM/SR sample and also of the Bcl-2Δ21/SR control sample with the amino acid coverages of 50% and 55%, respectively. When this Bcl-2Δ21/SR control sample was subjected to western blot analysis with Bcl-2 antibody, Bcl-2Δ21 was seen at 160 kDa with relatively lower intensity compared to the band of Bcl-2Δ21/BPM/SR sample (see Figure 2.25). Therefore the appearance of Bcl-2Δ21 peptides in this Bcl-2Δ21/SR control sample is acceptable.

In another trial the gel bands corresponding to both 160 kDa and 135 kDa bands, identified with Bcl-2 antibody, were cut out from Bcl-2Δ21/BPM/SR and the SR/BPM control sample and analyzed by MS after in-gel tryptic digestion. As in the first trial, SERCA showed up in the SR/BPM control sample with the amino acid coverages of 51% and 48% in 135 kDa and 160 kDa gel bands, respectively. The coverages of SERCA of Bcl-2Δ21/BPM/SR sample were 42% and 49% in 135 kDa and 160 kDa gel bands, respectively. However Bcl-2Δ21, with amino acid coverage of 13%, was seen only in the 135 kDa band but not in the 160 kDa band probably due to the suppression of relatively lower abundant Bcl-2Δ21 peptides by the highly

abundant peptides generated from the proteins of SR including SERCA present in the gel band. The results of the two mass spectrometric trials explained above are summarized in the following table.

TABLE 2.1: Summary of mass spectrometric results: The amino acid coverages of Bcl-2Δ21 and SERCA in 135 kDa and 160 kDa gel bands of Bcl-2Δ21/BPM/SR, Bcl-2Δ21/SR and SR/BPM samples are shown. † Cross-linked SERCA-Bcl-2Δ21 dipeptide was identified in this sample.

		SR/BPM		Bcl-2Δ21/BPM/SR		Bcl-2Δ21/SR	
		Bcl-2Δ21	SERCA	Bcl-2Δ21	SERCA	Bcl-2Δ21	SERCA
Trial 1	160 kDa	–	37%	50% †	45%	55%	45%
Trial 2	135 kDa	–	51%	13%	49%		
	160 kDa	–	48%	–	42%		

The successful identification of the cross-linked peptides using mass spectrometry depends on the concentration of the cross-linked material in the sample to be analyzed. In the case of SERCA and Bcl-2Δ21, the yield of cross-linked SERCA-Bcl-2Δ21 is much lower as revealed by western blotting with Bcl-2 antibody. Therefore some separation techniques should be involved in order to enrich the sample with the low-abundance cross-linked products. Using 1D SDS-PAGE, the complex mixture of Bcl-2Δ21/BPM/SR cross-linking reaction sample can be separated based on the apparent molecular weights. Even though the gel bands of interest are now enriched with the cross-linked products, the in-gel digest is a

complex mixture of peptides of SERCA and Bcl-2Δ21itself and also of some other SR proteins of the same molecular weight as the cross-linked products. Therefore the concentration of low-abundance cross-linked peptide/peptides would still be outside the dynamic range of the mass spectrometer. Also the signal for the cross-linked product can be easily suppressed by highly abundant peptides. On-line RP-HPLC separation, associated with LC/MS methodologies is extremely helpful in analyzing such low abundant cross-linked peptides.

The MS data mentioned above were further analyzed for the possible cross-linked SERCA-Bcl-2Δ21 dipeptides. This was done manually by comparing the theoretical masses of SERCA-Bcl-2Δ21 dipeptides with the experimentally found masses. The SERCA-Bcl-2Δ21 dipeptide formed by cross-linking of the Bcl-2Δ21 peptide, ^{147}IVAFFEFGGVMC(BPM)VESVNR^{164} with the SERCA peptide, ^{568}DTPPKR^{573} was identified in the 160 kDa band of the Bcl-2Δ21/BPM/SR sample in the first MS trial (see Table 2.1).

Figures 2.19 and 2.20 show MS1 of $[M+4H]^{+4}$ and $[M+3H]^{+3}$ ions, respectively, of the identified dipeptide. The spacing between the isotopic peaks of $[M+4H]^{+4}$ and $[M+3H]^{+3}$ ions are 1/4 and 1/3 respectively, confirming the charge states. The excellent peak resolution that can be achieved with FTICR-MS is helpful in identifying the isotopic peak envelopes of the two ions. The calculated m/z values of the two ions are 749.1099 ($[M+4H]^{+4}$) and 998.4798 ($[M+3H]^{+3}$), with associated errors of 24.2 ppm and 33.3 ppm, respectively. Even though these error values are

higher than the maximum error level of masses detected by FTICR-MS, still those are acceptable for a low abundant cross-linked dipeptide.

These two ions were found only in the sample of Bcl-2Δ21/BPM/SR and when the two control samples were searched, no peaks were found with the same m/z and isotopic distribution. Figure 2.21 shows the intensities of the five isotopic peaks of $[M+4H]^{+4}$ ion of Bcl-2Δ21/BPM/SR sample, relative to the intensities of the same m/z values found in the same chromatographic time window of the two control samples. This clearly indicates that $[M+4H]^{+4}$ ion is present only in the Bcl-2Δ21/BPM/SR sample but not in the two control samples.

Furthermore, the theoretical masses of +3ly and +4ly charged peptide ions generated from SERCA and Bcl-2Δ21 itself and also from the intramolecularly cross-linked peptides of Bcl-2Δ21, were searched and no m/z was found with the same masses reported here. Since purified SR vesicles were used in the experiments as the source of SERCA, all the samples contain the other proteins found in the SR and hence the digests contain the peptides of these other SR proteins. The theoretical masses of these other SR proteins, showed up only in the Bcl-2Δ21/BPM/SR sample but not in the two control samples, were also searched and no matching ions were found. Therefore the identified ions can be confirmed as of the cross-linked SERCA-Bcl-2Δ21 dipeptide.

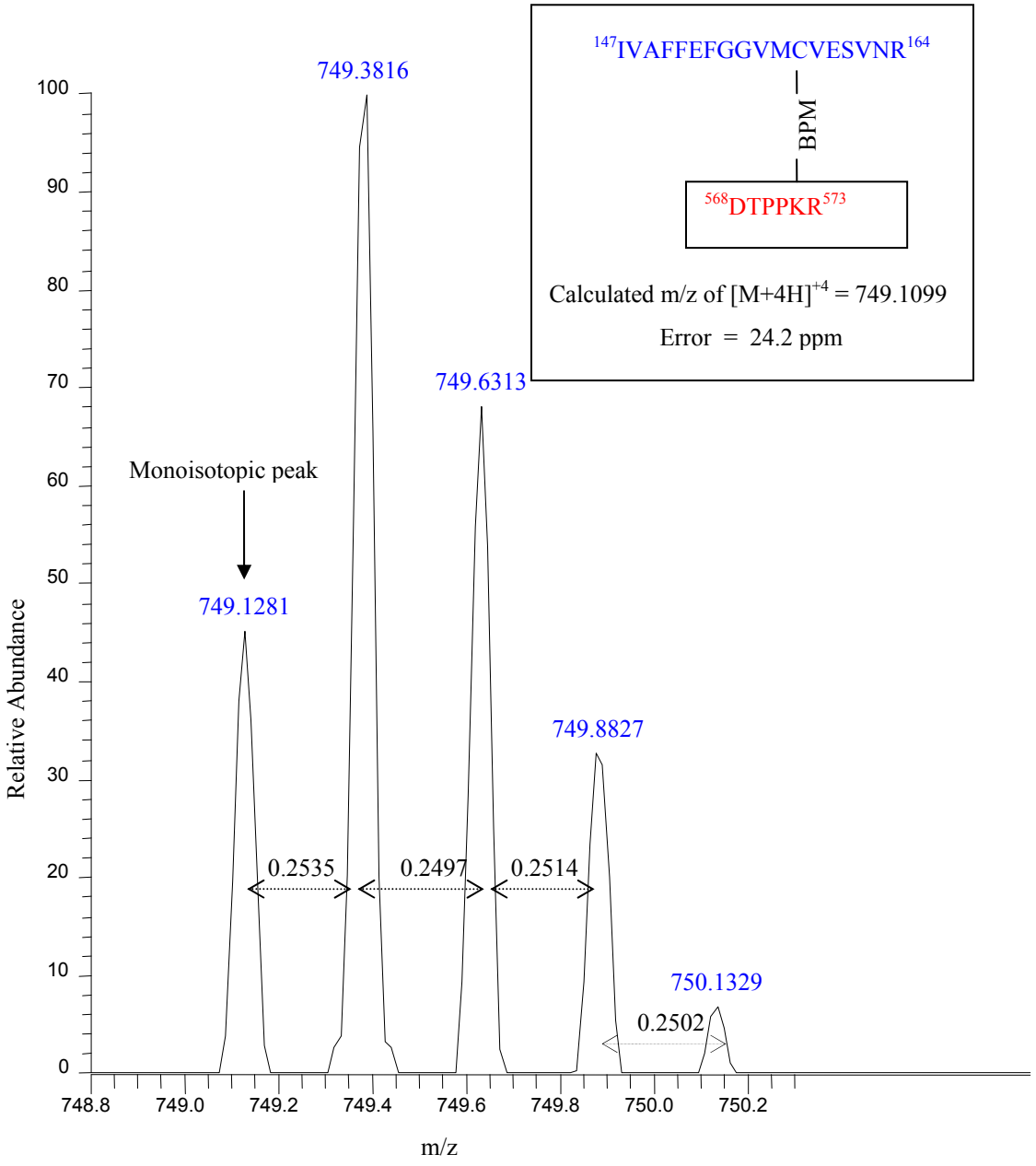

FIGURE 2.19: Mass Spectrum of $[M+4H]^{+4}$ of the cross-linked SERCA-Bcl-2Δ21 dipeptide: The isotopic peak distribution of MS1 of quadruply charged ion is shown. The spacing between peaks are shown confirming the +4 charge state. In-set shows the cross-linked dipeptide, peptide of SERCA in red and peptide of Bcl-2Δ21 in blue.

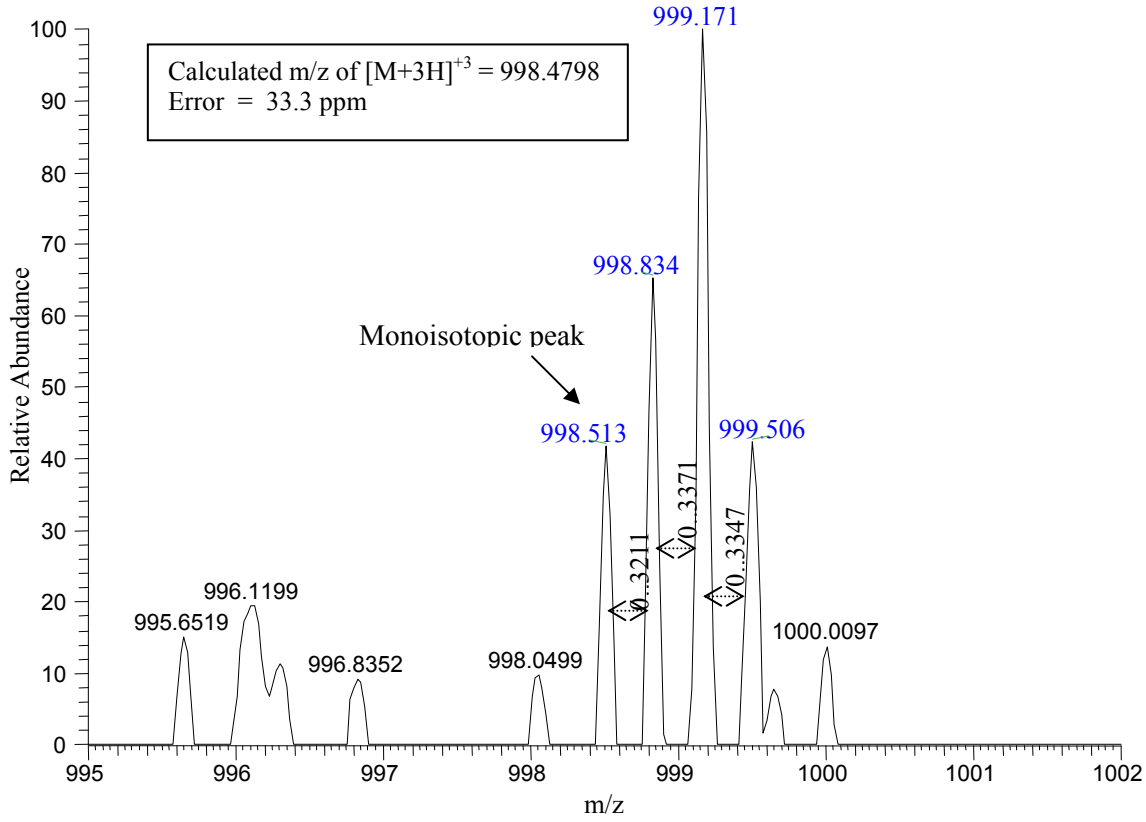

FIGURE 2.20: Mass Spectrum of $[M+3H]^{+3}$ of the cross-linked SERCA-Bcl-2Δ21 dipeptide: The isotopic peak distribution of MS1 of triply charged ion is shown. Four peaks belonging to the isotopic envelope are labeled in blue. Spacing between peaks are shown confirming the +3 charge state.

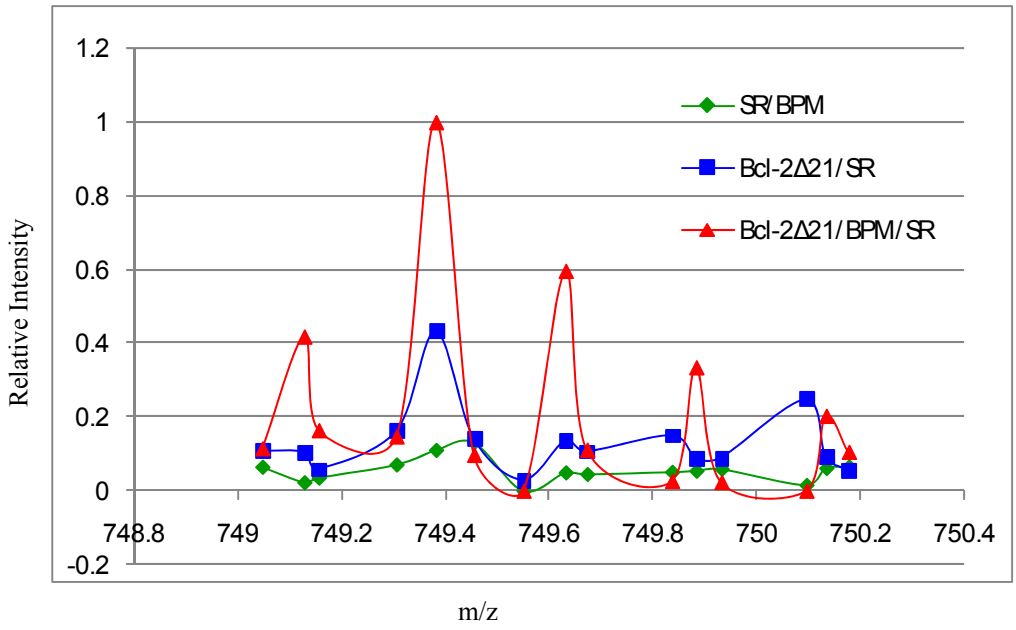

FIGURE 2.21: Intensities of the isotopic peaks of $[M+4H]^{+4}$ relative to the control samples: (—) Bcl-2Δ21/BPM/SR; (—) Bcl-2Δ21/SR; (—) SR/BPM.

Figure 2.22 shows the 3-D structure of SERCA showing the position of this cross-linked SERCA peptide. The identified SERCA peptide, ^{568}DTPPKR^{573}, cross-linked to Bcl-2Δ21, is located at cytoplasmic ATP binding domain (residues 505-680). More importantly it is located right next to ^{560}RCLALA^{565}, one of the conserved motifs in SERCA (*29*). Furthermore, in a previous study using a fragment of SERCA (residues 357-600) containing the ATP binding domain, it was found that Thr569 was among the residues whose backbone conformation was changed upon nucleotide

binding, as measured using NMR spectroscopy (*30*). Therefore the residue Thr569 and hence ^{568}DTPPKR^{573} could be directly involved in ATP binding during the catalytic cycle of SERCA. However, there are no mutational studies available to date, confirming the importance of this residue in ATP binding of SERCA.

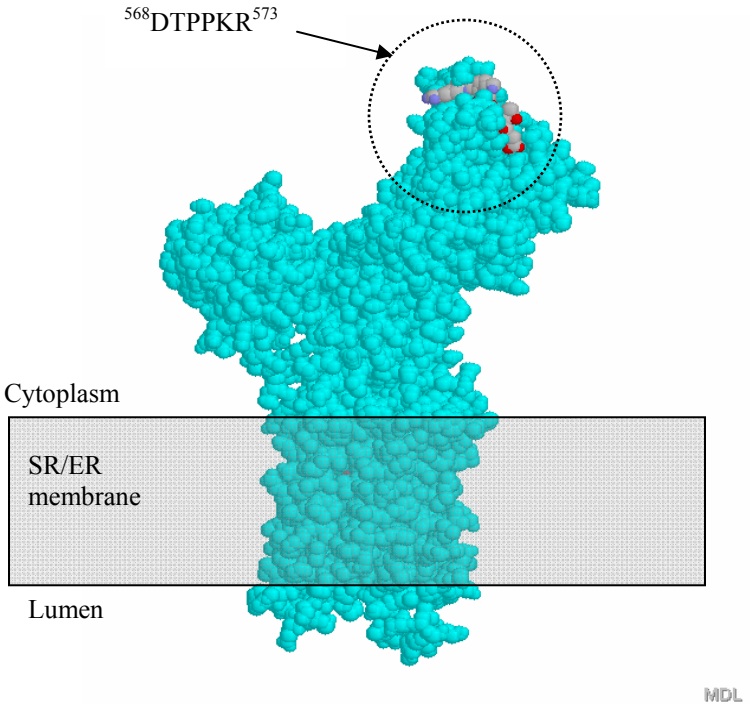

FIGURE 2.22: The 3-D structure of SERCA showing the peptide cross-linked to Bcl-2Δ21: ^{568}DTPPKR^{573} peptide of SERCA located in the ATP binding domain is circled. The structure of SERCA is from protein data bank (PDB code 1SU4).

The Bcl-2Δ21 peptide, ^{147}IVAFFEFGGVMC(BPM)VESVNR^{164}, belongs to the BH1 domain which is one of the three domains in the hydrophobic surface groove of Bcl-2Δ21 explained in the chapter 1. Therefore this hydrophobic surface groove of Bcl-2Δ21 might directly but transiently interact with the ATP binding domain of

SERCA thus blocking the cross-talk between ATP binding and phosphorylation domains which is required for SERCA activity. As reported previously, SERCA-Bcl-2Δ21 interaction does not change the ATP binding affinity of the domain (*23*). Interaction of Bcl-2Δ21 with the ATP binding domain would not necessarily change the affinity of the domain for ATP. Apart from this ATP binding domain, Bcl-2Δ21 might interact with other domains of SERCA which are not identified under this study.

In order to identify the exact cross-linking residue within this SERCA peptide, MS/MS data of the identified ions are needed. However, MS/MS of the $[M+4H]^{+4}$ and $[M+3H]^{+3}$ ions could not be found probably because, the ion currents of the two ions, m/z 749.1281 and m/z 998.5131, are considerably lower (5.03E2 and 5.06E2, respectively) than the defined threshold (10E6) for MS/MS during the MS run. The benzophenone group of the cross-linking reagent, BPM, abstracts a proton from an adjacent, geometrically accessible C-H bond upon UV irradiation. When a hetero atom such as N or S is next to the alkyl group, this H abstraction by benzophenone is more favorable (*8*). The identified cross-linked SERCA peptide, ^{568}DTPPKR^{573}, contains two Prolines (P), a Lysine (K) and an Arginine (R), and all contain alkyl groups adjacent to N atoms. Therefore, the exact cross-linking site could be one of these residues. The spacer arm length of BPM is within 8-11Å, therefore the distance between Cys158 of Bcl-2Δ21and the cross-linked residue in SERCA should be within this range.

2.3.8: Other possible SR proteins associated with Bcl-2Δ21 or SERCA.

Purified SR vesicles were used as the source of SERCA in all the cross-linking experiments. It is possible that Bcl-2Δ21 and also SERCA can interact with some other proteins in SR and produce cross-linked products comparable in size to the products of SERCA/Bcl-2Δ21. Therefore the digests of 135 kDa and 160 kDa gel bands might contain these other products. Searching the mass spectrometric data against the mouse/rat data base for the identification of the proteins in the digests revealed some SR proteins which are reasonable in size to be considered as cross-linked to Bcl-2Δ21 or SERCA. Suspected Bcl-2Δ21 cross-linked proteins are Dihydropyridine-sensitive L-type calcium channel subunits α-2/ δ precursor (125 kDa, P54290), Sarcalumenin precursor (99 kDa, Q7TQ48) and Glycogen phosphorylase, muscle form (97 kDa, P00489). A suspected SERCA cross-linked protein found was Mitsugumin-29 (Mg29) (29 kDa, O89104). Mg29 has recently been found in the triad-junction of skeletal muscle (*31*).

Affinity purified fractions of the photo cross-linking reaction sample of His_6-Bcl-2Δ17/BPM/SR and also the GST-Bcl-2Δ21 binding assay samples were subjected to western blot analysis using the antibodies for the suspected Bcl-2Δ21 cross-linked proteins, Dihydropyridine-sensitive L-type calcium channel subunits α-2/ δ precursor, Sarcalumenin precursor and Glycogen phosphorylase, muscle form. The three western blots of the photo cross-linked samples did not show any band that can be considered as a cross-linked product (data not shown). Also the western blots of the GST-Bcl-2Δ21 binding assay samples show that these three proteins do not

directly associate with Bcl-2Δ21 (data not shown). Therefore the presence of these three proteins in the digests is probably due to the contamination during manual isolation of the gel bands of interest.

The affinity purified fractions of photo cross-linking reaction sample, His_6-Bcl-2Δ17/BPM/SR, and of the control sample, BPM/SR, were subjected to western blot analysis with the antibody for Mg29, the suspected SERCA cross-linked protein. No band was seen at 29 kDa for the monomer of Mg29, a band slightly above 100 kDa was seen instead with the fractions of both His_6-Bcl-2Δ17/BPM/SR and BPM/SR (Figure 2.23-a,b). This band of Mg29 could be due to associated SERCA/Mg29 or an oligomer, probably a tetramer (116 kDa), of Mg29. The western blots of SERCA antibody of the same sample fractions reveal the highest amount of SERCA in the fraction of 100 mM Im (lane 5 in Figure 2.23-c,d) and the band of Mg29 shows the same pattern of intensity as SERCA (compare a, b with c, d), indicating direct or indirect association of this product of Mg29 with SERCA. Interestingly the intensities of the band are significantly higher with the fractions of His_6-Bcl-2Δ17/BPM/SR (compare a and b in Figure 2.23). Therefore the association of SERCA with the product of Mg29 might be facilitated by the presence of His_6-Bcl-2Δ17.

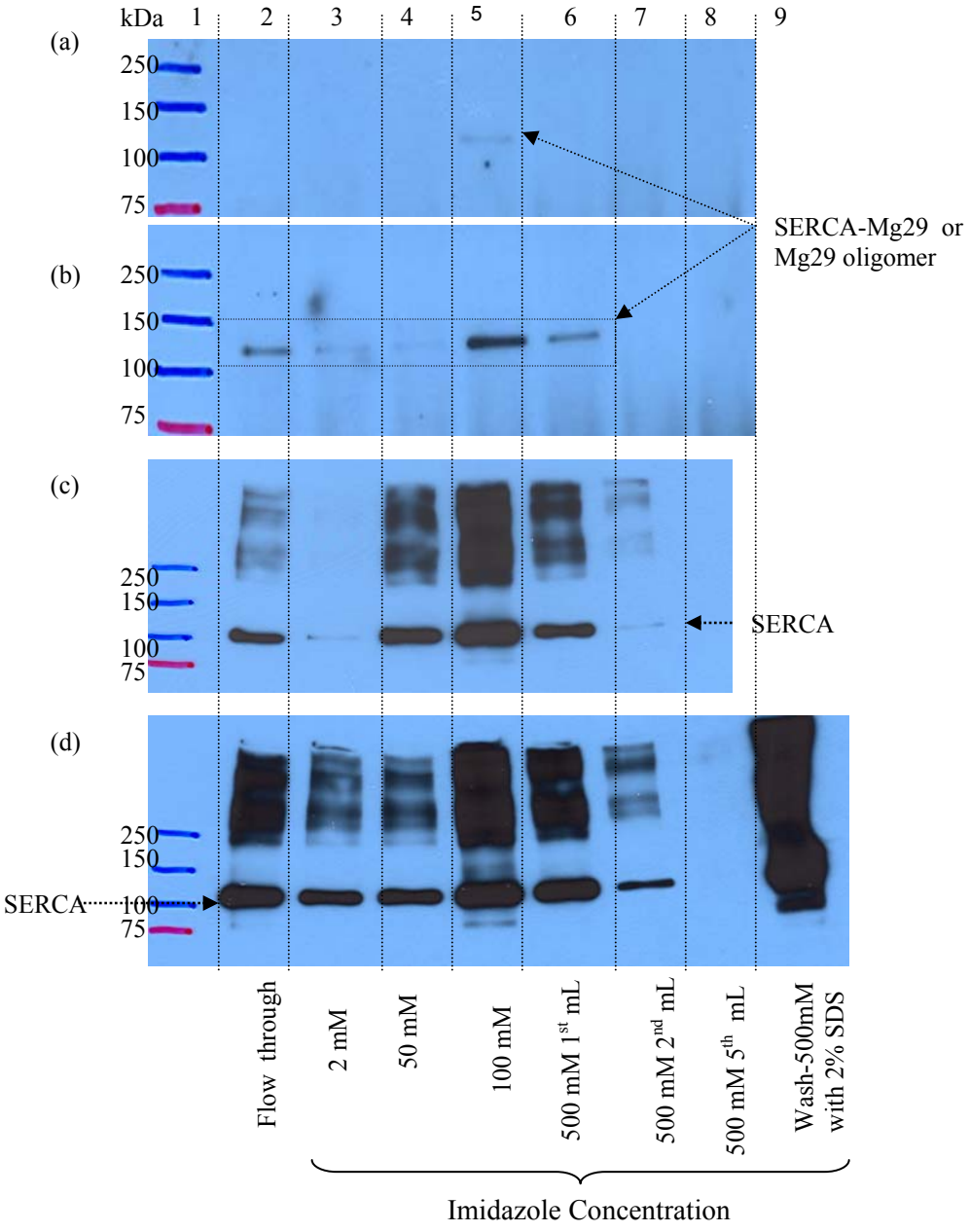

FIGURE 2.23: Affinity purified fractions of photo cross-linking reaction samples: (a),(b), western blots of Mg29 antibody; (c),(d), western blots of SERCA antibody; (a),(c), fractions of the SR/BPM control sample; (b),(d), fractions of the His_6-Bcl-2Δ17/BPM/SR sample.

GST-Bcl-2Δ21 binding assay was also utilized to further verify Bcl-2Δ21-facilitated association of Mg29 with SERCA. As reported before, SERCA is seen with the sample of GST-Bcl-2Δ21/SR (Figure 2.24-a). Interestingly the western blot of Mg29 antibody shows the same band (Figure 2.24-b) previously detected with affinity purified fractions of photo cross-linking samples (Figure 2.23-a). As mentioned before, this could be postulated as a tetramer of Mg29 or a complex of SERCA/Mg29. These results further confirm the association of Mg29 with SERCA supported by Bcl-2Δ21. The three proteins might be candidates of a protein complex which is involved in controlling SERCA activity. However, more experiments are needed to confirm this.

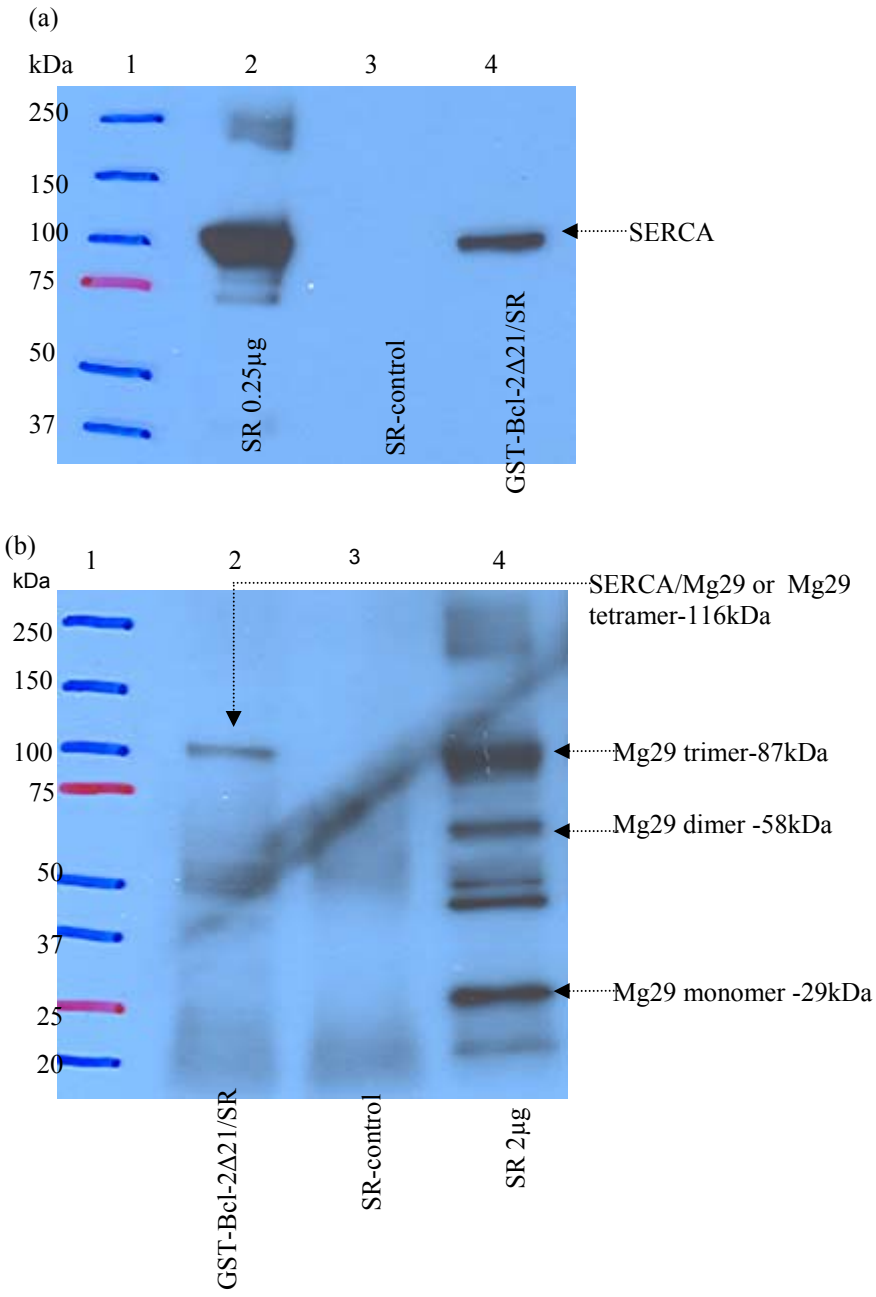

FIGURE 2.24: GST-Bcl-2Δ21 binding assay samples: (a) western blot of SERCA antibody; (b) western blot of Mg29 antibody; GST-Bcl-2Δ21/SR sample shows the proteins of SR associated with GST-Bcl-2Δ21; SR-control sample shows the proteins of SR non-specifically bound to glutathione-agarose beads.

2.3.9: Comparison of young and old SERCA in photo cross-linking with Bcl-2Δ21.

Young and old SERCA was compared for the efficiency of cross-linking with Bcl-2Δ21, using the SR vesicles purified from tissues of young (5-6 months) and old (34 months) rats. Since BPM treated Bcl-2Δ21 in this experiment was allowed to interact with SERCA for 45 min (optimum incubation time is 15 min as determined in a later experiment), the cross-linking reaction samples, Bcl-2Δ21/BPM/SR(Y) and Bcl-2Δ21/ BPM/SR(O), show many non-specific products resulting in rather smeared lanes with Bcl-2 antibody (Figure 2.25-a). Yet the western blot clearly indicates the difference between young and old SERCA in cross-linking with Bcl-2Δ21. The cross-linked products of Bcl-2Δ21/SERCA with 1:1 and 1:2 (mol/mol) (SERCA: Bcl-2Δ21) ratio are seen with both young and old SERCA (Figure 2.25-a). However, relatively less products were seen with old SERCA (compare lanes 2 and 8 in Figure 2.25-a). As seen with previous experiments, the western blot with SERCA antibody does not show results compatible to Bcl-2 antibody (Figure 2.25-b).

As revealed by this cross-linking experiment, association of Bcl-2Δ21 with old SERCA is relatively less efficient. Post translational modifications such as phosphorylation, nitration, cause alterations in structure and function of a protein. SERCA is reported to accumulate oxidational modifications with aging, resulting in reduced activity and conformational changes in the molecule. These structural and functional alterations in SERCA, due to aging, could make the interaction with Bcl-2Δ21 less efficient. Therefore anti-apoptotic action of Bcl-2Δ21 at the level of ER might become less effective with aging.

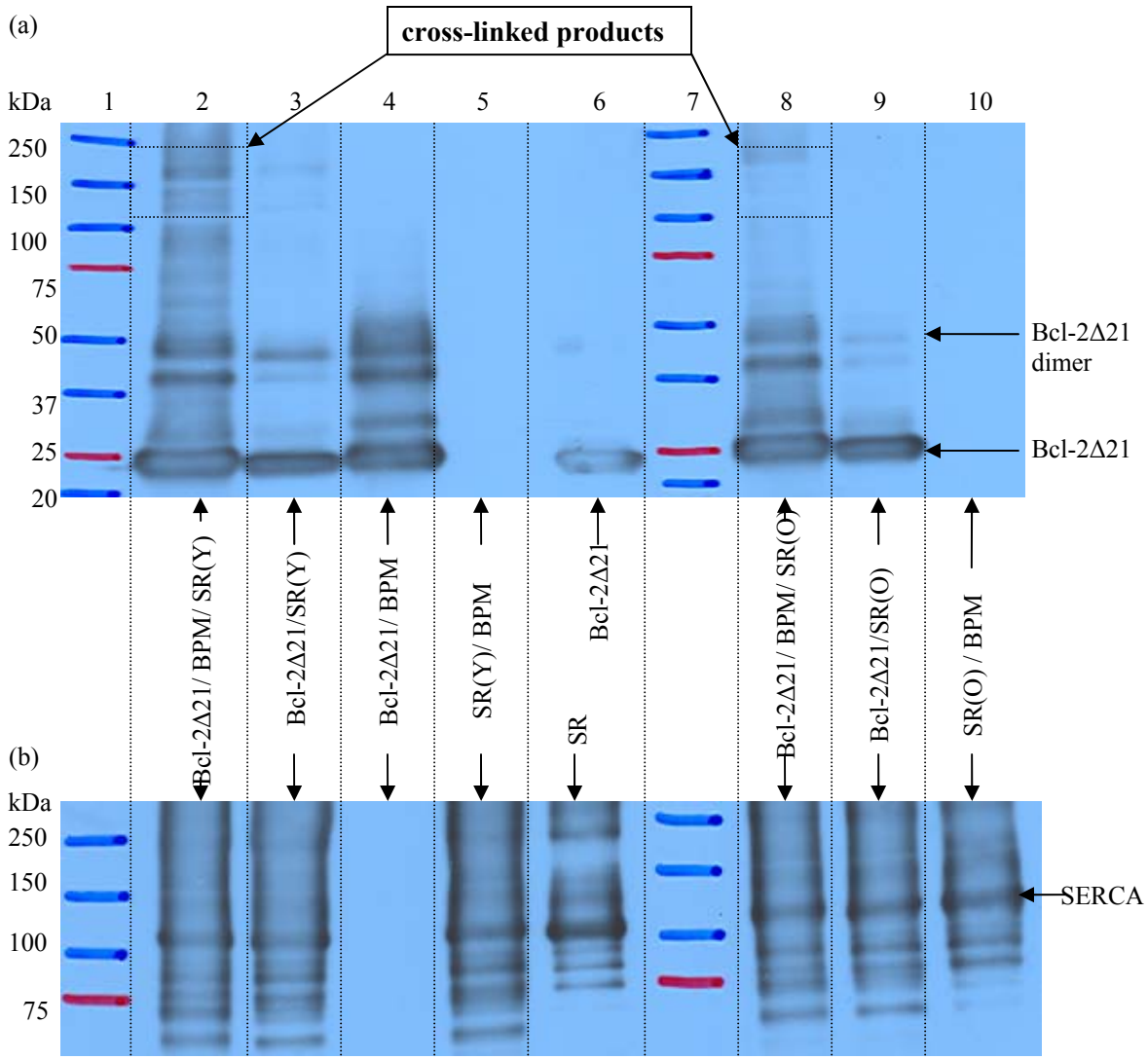

FIGURE 2.25: Young and old SERCA in photo cross-linking with Bcl-2Δ21: (a) western blot with Bcl-2 antibody, the regions of the Bcl-2Δ21/SERCA cross-linked products with young and old SERCA are boxed; (b) western blot with SERCA antibody; Photo cross-linking reaction samples of young and old SERCA are labeled as Bcl-2Δ21/BPM/SR(Y) and Bcl-2Δ21/ BPM/SR(O) respectively (lanes 2 and 8).

2.4: Conclusions.

In conclusion, the experiments described in this chapter suggest a direct interaction of Bcl-2Δ21 with SERCA. The two proteins can interact with both 1:1 and 2:1 (Bcl-2Δ21: SERCA) molar ratio. The BH1 domain, therefore the hydrophobic surface groove of Bcl-2Δ21 is involved in the interaction. Fulfilling one of the major objectives of the work reported in this dissertation, ^{568}DTPPKR^{573} peptide of ATP binding domain of SERCA is identified as the site of SERCA involved in the interaction. The trans membrane domain of Bcl-2 is not required for this interaction. However, apart from these identified domains, there might be other interacting domains of the two proteins which are not identified under the experiments reported here. Based on the chemical cross-linking experiments, the distance between the interface/interfaces of Bcl-2Δ21/SERCA complex can range from ~6-14Å. Mitsugumin-29 (Mg29) could also be involved in this Bcl-2Δ21/SERCA interactions. The association of SERCA with Bcl-2Δ21 is affected by aging.

2.5: References.

1. Brunner, J. (1993) New photolabeling and crosslinking methods, *Annu. Rev. Biochem. 62,* 483-514.
2. www.probes.com
3. Kluger, R. and Alagic, A. (2004) Chemical cross-linking and protein-protein interactions-a review with illustrative protocols, *Bioorg. Chem. 32(6),* 451-72.
4. Berggård, T., Linse, S., and James, P.(2007) Methods for the detection and analysis of protein-protein interactions, *Proteomics 7(16),* 2833-2842.
5. Vodovozova, E.L. (2007) Photoaffinity labeling and its application in structural biology, *Biochemistry (Mosc).72(1),* 1-20.
6. Phizicky, E.M., and Fields, S. (1995) Protein-protein interactions: methods for detection and analysis, *Microbiol. Rev. 59(1),* 94-123.

7. Trakselis, M.A., Alley, S.C., and Ishmael, F.T. (2005) Identification and mapping of protein-protein interactions by a combination of cross-linking, cleavage, and proteomics, *Bioconjug. Chem.16(4),* 741-750.
8. Dormán, G., and Prestwich, G.D. (1994) Benzophenone photophores in biochemistry, *Biochemistry 33(19),* 5661-5673.
9. www.piercenet.com
10. Vasilescu, J., and Figeys, D. (2006) Mapping protein-protein interactions by mass spectrometry, *Curr. Opin. Biotechnol. 17(4),* 394-399.
11. Leszyk, J., Tao, T., Nuwaysir, L.M., and Gergely, J. (1998) Identification of the photocrosslinking sites in troponin-I with 4-maleimidobenzophenone labelled mutant troponin-Cs having single cysteines at positions 158 and 21, *J. Muscle Res. Cell Motil. 19(5),* 479-490.
12. Burkitt, W.I., Derrick, P.J., Lafitte, D., and Bronstein, I. (2003) Protein-ligand and protein-protein interactions studied by electrospray ionization and mass spectrometry, *Biochem. Soc. Trans. 31(Pt 5),* 985-989.
13. Bennett, K.L., Kussmann, M., Björk, P., Godzwon, M., Mikkelsen, M., Sørensen, P., and Roepstorff, P. (2000) Chemical cross-linking with thiol-cleavable reagents combined with differential mass spectrometric peptide mapping--a novel approach to assess intermolecular protein contacts, *Protein Sci. 9(8),* 1503-1518.
14. Sinz, A. (2003) Chemical cross-linking and mass spectrometry for mapping three-dimensional structures of proteins and protein complexes, *J. Mass Spectrom. 38(12),* 1225-1237.
15. Schulz, D.M., Ihling, C., Clore, G.M., and Sinz, A. (2004) Mapping the topology and determination of a low-resolution three-dimensional structure of the calmodulin-melittin complex by chemical cross-linking and high-resolution FTICRMS: direct demonstration of multiple binding modes, *Biochemistry 43(16),* 4703-4715.
16. Dihazi, G.H., and Sinz, A. (2003) Mapping low-resolution three-dimensional protein structures using chemical cross-linking and Fourier transform ion-cyclotron resonance mass spectrometry, *Rapid Commun. Mass Spectrom. 17(17),* 2005-2014.
17. Kalkhof, S., Ihling, C., Mechtler, K., and Sinz, A. (2005) Chemical cross-linking and high-performance Fourier transform ion cyclotron resonance mass spectrometry for protein interaction analysis: application to a calmodulin/target peptide complex, *Anal. Chem. 77(2),* 495-503.
18. Sinz, A. (2005) Chemical cross-linking and FTICR mass spectrometry for protein structure characterization, *Anal. Bioanal. Chem. 381(1),* 44-47.
19. Sinz, A. (2006) Chemical cross-linking and mass spectrometry to map three-dimensional protein structures and protein-protein interactions, *Mass Spectrom. Rev. 25(4),* 663-682.
20. Schilling, B., Row, R.H., Gibson, B.W., Guo, X., and Young, M.M. (2003) MS2Assign, automated assignment and nomenclature of tandem mass spectra of chemically crosslinked peptides, *J. Am. Soc. Mass Spectrom. 14(8),* 834-850.
21. Gao, Q., Xue, S., Doneanu, C.E., Shaffer, S.A., Goodlett, D.R., and Nelson, S.D. (2006) Pro-CrossLink. Software tool for protein cross-linking and mass spectrometry, *Anal. Chem. 78(7),* 2145-2149.
22. Egger, D., and Bienz, K. (1994) Protein (western) blotting, *Mol. Biotechnol.1(3),* 289-305.

23. Dremina, E.S., Sharov, V.S., Kumar, K., Zaidi, A., Michaelis, E.K., and Schöneich, C. (2004) Anti-apoptotic protein Bcl-2 interacts with and destabilizes the sarcoplasmic/endoplasmic reticulum Ca2+-ATPase (SERCA), *Biochem. J. 383(Pt 2),* 361-370.
24. Fernandez, J.L., Rosemblatt, M., and Hidalgo, C. (1980) Highly purified sarcoplasmic reticulum vesicles are devoid of Ca2+-independent ('basal') ATPase activity, *Biochim. Biophys. Acta. 599(2),* 552-568.
25. Dremina, E.S., Sharov, V.S., and Schöneich, C. (2006) Displacement of SERCA from SR lipid caveolae-related domains by Bcl-2: a possible mechanism for SERCA inactivation, *Biochemistry 45(1),* 175-184.
26. Lanzetta, P.A., Alvarez, L.J., Reinach, P.S., and Candia, O.A. (1979) An improved assay for nanomole amounts of inorganic phosphate, *Anal. Biochem. 100(1),* 95-97.
27. Petros, A.M., Medek, A., Nettesheim, D.G., Kim, D.H., Yoon, H.S., Swift, K., Matayoshi, E.D., Oltersdorf, T., and Fesik, S.W. (2001) Solution structure of the antiapoptotic protein bcl-2, *Proc. Natl. Acad. Sci. U. S. A. 98(6),* 3012-3017. Epub 2001 Feb 27.
28. Zhang, Z., Lapolla, S.M., Annis, M.G., Truscott, M., Roberts, G.J., Miao, Y., Shao, Y., Tan, C., Peng, J., Johnson, A.E., Zhang, X.C., Andrews, D.W., and Lin, J. (2004) Bcl-2 homodimerization involves two distinct binding surfaces, a topographic arrangement that provides an effective mechanism for Bcl-2 to capture activated Bax, *J. Biol. Chem. 279(42),* 43920-43928.
29. McIntosh, D.B., Clausen, J.D., Woolley, D.G., MacLennan, D.H., Vilsen, B., and Andersen, J.P. (2003) ATP binding residues of sarcoplasmic reticulum Ca2+-ATPase, *Ann. N. Y. Acad. Sci. 986,*101-105.
30. Abu-Abed, M., Mal, T.K., Kainosho, M., MacLennan, D.H., and Ikura, M. (2002) Characterization of the ATP-binding domain of the sarco(endo)plasmic reticulum Ca(2+)-ATPase: probing nucleotide binding by multidimensional NMR, *Biochemistry 41(4),* 1156-1164.
31. Shimuta, M., Komazaki, S., Nishi, M., Iino, M., Nakagawara, K., and Takeshima, H. (1998) Structure and expression of mitsugumin29 gene, *FEBS Lett. 431(2),* 263-267.

Chapter 3:

Effect of Bcl-2Δ21 mutants on the interaction with SERCA.

3.1 Introduction to the analytical strategies.

3.1.1: Mutants of Bcl-2Δ21.

The *in vitro* studies of SERCA/Bcl-2 interactions described in Chapter 2 include photo cross-linking of the BH1 domain of Bcl-2Δ21 with SERCA using Benzophenone-4-maleimide (BPM), the cross-linking reagent, attached to Cys158 of wild type (WT) Bcl-2Δ21. Since the Cys158 is located in the hydrophobic groove of Bcl-2Δ21 (*1,2*), the labeling with BPM was difficult. To overcome this problem "Cys-mutants" of Bcl-2Δ21 were generated. In these Cys-mutants, the highly exposed Ser residues, based on the NMR structure of Bcl-2 (*1*), were substituted with Cys, while rather buried Cys158, the only one Cys residue of Bcl-2Δ21, was substituted with Ser. In addition to the Cys-mutants, the G145E mutation, which has been reported to completely diminish the anti- apoptotic activity of human Bcl-2 (*3*), was also selected for the SERCA/ Bcl-2Δ21 interaction studies. Site-directed mutagenesis was utilized to generate the mutants of Bcl-2Δ21, using a synthetic oligonucleotide primer(s) which is complementary to the DNA sequence of the protein to be mutated but consists of an internal mismatch corresponding to the necessary mutation (*4*). These mutants of Bcl-2Δ21 would be helpful in the identification of the domains/residues of Bcl-2Δ21 which are critical for the interaction with SERCA, one of the main objectives of the project.

3.1.2: Sucrose Density Gradient (SDG) fractionation of SR membranes.

Sucrose Density Gradient (SDG) fractionation can be used to fractionate cellular extracts based on the buoyant densities of the different particles in the sample. A gradient of sucrose is prepared in a centrifuge tube containing the sample to be fractionated by gently overlaying sucrose solutions of decreasing concentrations on top of each other so that the highest concentration is at the bottom of the tube. Upon centrifugation, the particles of the sample travel through the gradient and stop when their density matches that of the surrounding sucrose. The fractions of the gradient are removed carefully and further analyzed (*5*).

It has been shown previously, using SDG fractionation of purified SR vesicles in the presence and absence of Bcl-2Δ21, that the localization of SERCA in the SR membrane and thereby in the sucrose gradient, is changed by Bcl-2Δ21 (*6*). In this study SDG fractionation is used to examine the effect of the mutants of Bcl-2Δ21 to induce this translocalization of SERCA.

3.1.3: Ca^{2+}-ATPase activity assay.

The Ca^{2+}-ATPase activity assay is used to see the effect of the three mutants of Bcl-2Δ21 on the ATP hydrolysis activity of SERCA. The inorganic phosphate (P_i) released by the hydrolyzed ATP is colorimetrically measured as a complex of the phosphomolybdate-malachite green (*7, 8*). The complex absorbs at 660 nm and the intensity of the complex is proportional to the amount of P_i/hydrolyzed ATP in the sample. Both total and basal ATPase activities of the purified SR vesicles were

measured and the basal activity is subtracted from the total activity to obtain the Ca^{2+} dependent ATPase activity of the sample. Measured activity using this method is the Ca^{2+} dependent ATPase activity of SERCA since it has been shown before that this activity can be completely inhibited by the addition of thapsigargin, a well known inhibitor of SERCA (*9*).

3.1.4: Immunoprecipitation and GST- Bcl-2Δ21 binding assay.

Immunoprecipitation and the GST-Bcl-2Δ21 (where GST stands for Glutathione-S-Transferase) binding assay are two classical methods used for the detection of protein-protein interactions (*10-13*). The strategy involved is to affinity purify a protein/protein complex from a mixture using an antibody or any other affinity tag. The basic immunoprecipitation experiment includes the addition of the antibody to a mixture of proteins such as a cell lysate followed by the precipitation of the protein/protein complex bound to the antibody. Then the protein/protein complex is dissociated from the antibody and analyzed. In the experiments reported here, monoclonal Bcl-2 antibody is used to immunoprecipitate Bcl-2Δ21 from a mixture of Bcl-2Δ21/SR and the precipitated proteins are analyzed for any Bcl-2Δ21 bound proteins of the SR. In the GST-Bcl-2Δ21 binding assay, the GST tagged fusion protein is used to fish the proteins out of the SR which interact with Bcl-2Δ21. Commercially available glutathione-agarose beads can be used to purify Bcl-2Δ21 bound proteins of SR due to the affinity of GST for glutathione.

3.1.5: Photo cross-linking of mutants of Bcl-2Δ21with SERCA.

The importance of photo cross-linking in the studies of protein interactions is described in Chapter 2 under Section 2.1.1. The photo cross-linking ability of the mutants of Bcl-2Δ21 with SERCA was compared using the same photo cross-linking reagent BPM, used in the cross-linking experiments of wild type Bcl-2Δ21.

3.2: Materials and methods.

3.2.1: Site directed mutagenesis of Bcl-2Δ21.

The mutagenic oligonucleotide primers, 5'-AGG GAC GGG GTG AAC TGG GAG AGG ATT GTG GCC TTC TTT GAG-3', 5'-TTT GAG TTC GGT GGG GTC ATG TCA GTG GAG AGC GTC AAC-3', 5'-AAG TAC ATC CAT TAT AAG CTG TGT CAG AGG GGC TAC GAG TGG-3' and 5'-CTG TAC GGC CCC TGC ATG CGG CCT CTG-3' for G145E, C158S, S24C and S205C mutations of Bcl-2Δ21 respectively were designed and ordered from Integrated DNA Technologies, Inc., Coralville, IA. Plasmid DNA was isolated from *E. coli* host strain containing the pGEX3T vector of GST-Bcl-2Δ21 fusion protein. The mutagenesis reactions were performed using the Quick-change Multi Site-Directed Mutagenesis Kit (catalog no.200514, Stratagene, La Jolla, CA) according to the protocol provided with the kit. The Polymerase Chain Reaction (PCR) is used to synthesize mutant DNA strands starting with purified plasmid DNA and synthetic oligonucleotide primers. The PCR process was completed using a thermal cycler (Mastercycler personal, Eppendorf Scientific, Inc., New York, U.S.A.). After the transformation process, mutant plasmid

DNA was isolated from several clones and the DNA samples were submitted to Northwoods DNA, Inc. Solway, MN for DNA sequencing.

3.2.2: Protein expression and purification.

The successful clones containing G145E, S24C/C158S and S205C/C158S mutations were selected for protein expression and purification. The protein expression and purification procedure is described in Chapter 2 under Section 2.2.1 and this procedure yielded ca. 150 μg of G145E mutant and 25 μg each of S24C/C158S and S205C/C158S mutants per liter of LB medium as measured by a Coomassie Plus protein assay (Pierce, Rockford, IL). Purified proteins were subjected to SDS-PAGE, analyzed by western blotting (WB) with Bcl-2 antibody, and also using mass spectrometry after in-gel tryptic digestion.

3.2.3: Ca^{2+}-ATPase activity assay in the presence of Bcl-2Δ21 mutants.

Prior to the measurement of the activity of SERCA, the SR samples were incubated with WT and the mutants of Bcl-2Δ21 as follows. Three SR samples were prepared by diluting the concentrated SR vesicle suspension (ca. 20 mg of SR protein/mL) in STE buffer (7.5 mM Tris (pH 8.0), 150 mM NaCl, and 3 mM EDTA), the buffer used for purification and storage of Bcl-2Δ21, so that the contribution from the SR storage buffer to the final reaction mixture is <5%. The final concentration of SR proteins in these samples was 1 mg/mL. WT and the G145E mutant of purified Bcl-2Δ21 were added separately into two of these diluted SR

samples. The concentration of Bcl-2Δ21 (WT or G145E) in these two samples was 0.5 mg/mL. The third sample was the control reaction without Bcl-2Δ21. All three samples were incubated in 1.5 mL Eppendorf tubes at 37^{o}C using a dry thermostat without agitation. Aliquots of each sample were used to measure the activity as explained in the next paragraph. Protease inhibitor PMSF (1 mM) was used in each sample to prevent proteolytic degradation. Two similar experiments were performed using S24C/C158S or S205C/C158S in place of the G145E mutant. The final concentrations of Bcl-2Δ21 (WT or Cys-mutants) and SR proteins in these experiments were 0.4 mg/mL and 0.8 mg/mL, respectively.

The Ca^{2+} dependent ATPase activity assay was performed according to the procedure previously reported (*9*). Briefly, total and basal ATPase activities of the above mentioned SR samples were measured at 25°C over time using the colorimetric assay for inorganic phosphate (P_i). The Ca^{2+} dependent ATPase activity of the samples was calculated by subtracting the basal activity, measured in the presence of EGTA, from the total activity, measured in the presence of $CaCl_2$. Measured activity using this method is the Ca^{2+} dependent ATPase activity of SERCA since it has been shown previously that this activity can be completely inhibited by the addition of thapsigargin, a well known inhibitor of SERCA (*9*).

3.2.4: Sucrose Density Gradient (SDG) fractionation of SR in the presence of Bcl-2Δ21 mutants.

Prior to the SDG fractionation, the SR samples were incubated with WT and the three mutants of Bcl-2Δ21 as follows: Four 20 μg samples of concentrated SR vesicle suspension (ca. 20 mg of SR protein/mL) were diluted in STE buffer so that the contribution from the SR storage buffer to the final medium is <5%. The final concentration of SR proteins in these samples was 0.3 mg/mL. Purified WT and Cys-mutants (S24C/C158S and S205C/C158S) of Bcl-2Δ21 (10 μg each) were added separately into three of these diluted SR samples. The fourth sample was the control reaction without Bcl-2Δ21. All four samples were incubated in 1.5 mL Eppendorf tubes at 37°C for two hours using a dry thermostat without agitation. Protease inhibitor PMSF (1 mM) was used in each sample to prevent proteolytic degradation. In another similar experiment, G145E mutant was used in place of the Cys-mutants.

After incubation, samples were subjected to SDG fractionation using the reported procedure (*6*). After the fractionation, the first 2 mL fraction from the top of the gradient of each sample was discarded. In the experiment with Cys-mutants, four fractions (two 1 mL fractions and two 3.5 mL fractions) and, in the experiment with the G145E mutant, eight fractions (six 1 mL fractions and two 1.5 mL fractions) were collected from the top to the bottom of the gradient. The fractions of each sample were analyzed by western blotting with SERCA antibody after SDS-PAGE. For the western blot analysis, 12.5 μL, 18.7 μL and 43.7 μL were used from 1mL, 1.5 mL and 3.5 mL fractions, respectively.

3.2.5: Immunoprecipitation and GST- Bcl-2Δ21 binding assay.

For the GST-Bcl-2Δ21 binding assay, 100 μg of SR were solubilized in 150 μL of lysis buffer (10 mM Tris (pH 7.4), 10 mM EDTA, 1% Nonidet P40, 1 mM PMSF and protease inhibitors (Roche Diagnostics)). This was incubated with 10 μg of GST-Bcl-2Δ21 (WT or mutants) for 2 h at 4°C. As a control, another 100 μg of SR were solubilized in 150 μL of lysis buffer and incubated without GST-Bcl-2Δ21. The samples were incubated with 30 μL (packed volume) of pre-washed glutathione-agarose beads for another 2 h at 4°C. The beads were spun down at 10000g and washed three times with lysis buffer and another three times with STE. STE (30 μL) was added and boiled for 5 min with sample buffer (2% SDS, 10% glycerol, 125 mM Tris pH 6.8) followed by western blot analysis after SDS-PAGE.

For immunoprecipitation, 50 μg of SR were solubilized in 150 μL of lysis buffer and precleared with 30 μL of pre-washed Protein A-agarose beads (Sigma, St. Louis, MO) for 15 min at 4^{o}C. After removing the beads by centrifugation, the supernatant was incubated, first with 8μg of Bcl-2Δ21 (WT or mutants) for 1 h at 4^{o}C and second, with 5 μL of Bcl-2 antibody for another 1 h at 4^{o}C. Then 30 μL of pre-washed Protein A-agarose beads were added to each sample. After 2 h of incubation at 4^{o}C, the Protein A-agarose beads with bound immunocomplex were spun down, washed three times with lysis buffer and three times with STE and re-suspended in 30 μL of STE buffer. Finally the samples were boiled with sample buffer and analyzed by western blotting after SDS-PAGE.

3.2.6: Comparison of WT and Cys-mutants of Bcl-2Δ21 in cysteine derivatization:

The wild type (with or without 0.2% SDS) and the two Cys-mutants of Bcl-2Δ2 with final concentrations of 1 μM each were incubated with 20 μM ThioGlo1 for 1 h at 37°C in 200 mM phosphate buffer (pH 7.4). 1 ml of each of these samples was used to measure the fluorescence of ThioGlo1-cysteine adducts, at excitation and emission wavelengths of 379 nm and 513 nm, respectively. A Shimadzu RF5000U fluorescence spectrophotometer was used for measurements.

3.2.7: Photo cross-linking of Bcl-2Δ21 mutants with SERCA using BPM.

BPM labeling of Bcl-2Δ21 and the photo cross-linking reactions were performed as described in Chapter 2 under Sections 2.2.4 and 2.2.7. Both wild type and the three mutants of Bcl-2Δ21 were used in the experiment.

3.2.8: Details of SDS-PAGE and Western Blotting.

Samples boiled with the sample buffer were separated on precast 4-20% gradient gels from Bio-Rad Laboratories (Hercules, CA) or Invitrogen (Carlsbad, CA) using tris-glycine running buffer. For MS analysis, the gels were stained with Coomassie Blue protein staining reagent. For WB analysis, the gels were electroblotted onto 0.45 μm polyvinylidinedifluoride (PVDF) membrane (Millipore, Bedford, MA) and an ECL detection kit (GE Healthcare, UK) was used to visualize the spots according to the manufacturer's procedure.

3.3: Results and Discussion.

3.3.1: Mutants of Bcl-2Δ21.

As mentioned previously, due to the difficulty in BPM labeling of Cys158, which is located in a hydrophobic groove of Bcl-2Δ21, the Cys-mutants were generated by converting well exposed Ser residues into Cys. The rather buried Cys158, the only Cys residue of Bcl-2Δ21, was converted to Ser. Even though attempts were made to mutate several Ser residues the first mutagenesis trial resulted in only two successful S→C/C→S substitutions, S24C/C158S and S205C/C158S. The DNA sequencing data clearly show the presence of the two Cys-mutant clones (S24C/C158S, S205C/C158S) and also the third mutant G145E, among the DNA samples analyzed. These clones were used for protein expression and purification. In addition to the DNA sequencing data, the S205→C and G145E mutations could also be verified using ESI-Ion trap-MS. Scheme 3.1 shows the amino acid sequence of the wild type Bcl-2Δ21 indicating the mutation sites of the mutants.

```
1                 10                  20                  30                  40
MAHAGRTGYD NREIVMKYIH YKLSQRGYEW DAGDVGAAPP
41
GAAPAPGIFS SQPGHTPHPA ASRDPVARTS PLQTPAAPGA
81
AAGPALSPVP PVVHLTLRQA GDDFSRRYRR DFAEMSSQLH
121
LTPFTARGRF ATVVEELFRD GVNWGRIVAF FEFGGVMCVE
161
SVNREMSPLV DNIALWMTEY LNRHLHTWIQ DNGGWDAFVE
201
LYGPSMRPLF DFSWLSLK
```

SCHEME 3.1: Amino acid sequence of wild type Bcl-2Δ21: the mutation sites are indicated in red.

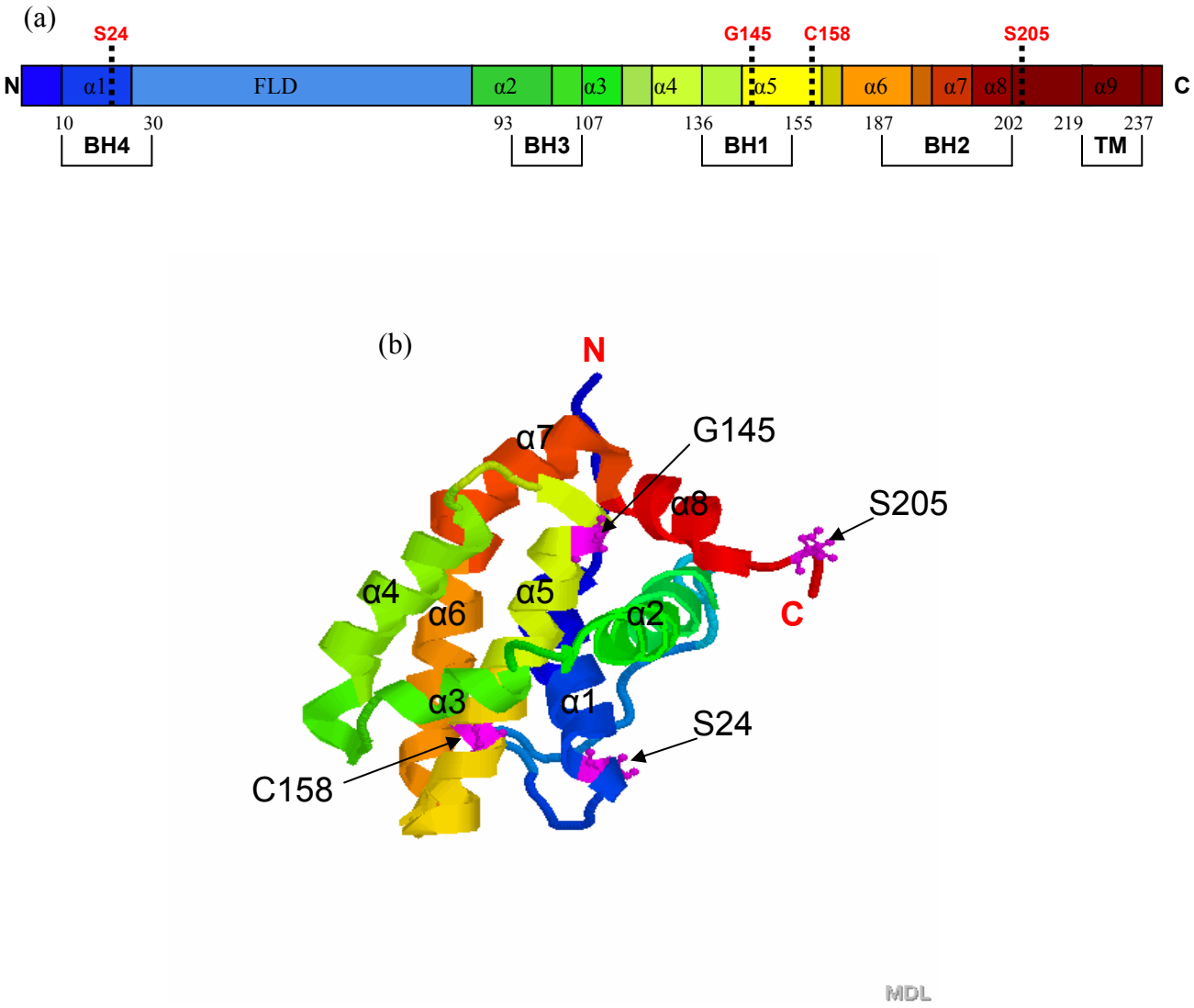

FIGURE 3.1: Mutants of Bcl-2Δ21: (a) Schematic showing different regions of the Bcl-2 molecule; the mutation sites are labeled in red; nine alpha helices (α1-α9), the flexible loop domain (FLD), four Bcl-2 homology domains (BH1-BH4) and trans membrane domain (TM) are indicated along with the starting and ending residue numbers of each domain (*14*). (b) 3-D structure of Bcl-2 indicating the location of the mutation sites (Picture was generated using PDB file 1G5M with Molecular Visualization Resources of Molviz.org)

The Figure 3.1 shows the mutation sites in a schematic diagram and also with respect to the 3-D structure of Bcl-2. In S24C/C158S, the S→C substitution site, Ser24, is located in α1 of the BH4 domain. Even though this N terminal region has been identified as an essential region for apoptosis inhibition by Bcl-2, the S24 in particular is not an essential residue as revealed by studies based on S24→G conversion (*15*). Therefore the S24→C mutation should not have any effect on the activity of Bcl-2Δ21. On the other hand the S205→C mutation in the S205C/C158S mutant is located right next to C terminal end of the BH2 domain. The conversion of S205→C also should not have any effect on the activity of Bcl-2Δ21 since the truncated form, Bcl-$2_{(1\text{-}203)}$ is still active in cell protection (*16*). Since the oxidation of C158 has been reported to have no effect on the action of Bcl-2Δ21 on SERCA inactivation (*9*), the C158→S substitution is also expected to have no effect on the activity of Bcl-2Δ21. The fourth mutation site, G145 on the other hand, is a highly conserved residue in the Bcl-2 family and also it has been identified as a critical residue in anti-apoptotic action of Bcl-2. The G145E mutant has been reported to completely diminish anti-apoptotic activity of human Bcl-2 (*2, 3*). Therefore the G145E mutant is expected to show no/less effect on SERCA inactivation.

After the purification of the three mutant proteins of Bcl-2Δ21 (G145E, S24C/C158S and S205C/C158S), the concentrations were determined by Coomassie Plus protein concentration assay. As revealed by the assay, the amount of G145E mutant produced is about two times that of the WT whereas that of the two Cys-mutants is about 1/3 of the WT level. These differences are probably due to some

alterations in hydrophobicity of the molecule caused by the mutations. The hydrophobicity should be lower in G145E while it should be higher in the two Cys-mutants with respect to the WT molecule. As seen in the western blot (Figure 3.2) all three mutants and the WT protein have the same affinity for the anti Bcl-2 antibody. The less intense band below the 25 kDa mark can be assumed to be a hydrolytic and/or proteolytic product of Bcl-2Δ21.

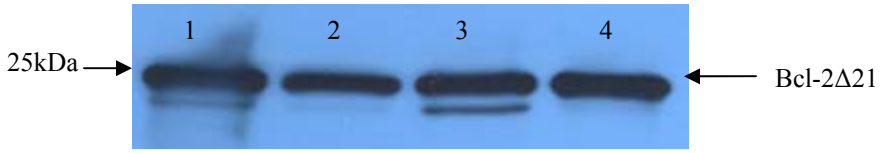

FIGURE 3.2: Wild type and mutants of Bcl-2Δ21 analyzed by western blotting with Bcl-2 antibody: 1-wild type, 2- S24C/C158S, 3-S205C/C158S, and 4-G145E of Bcl-2Δ21.

3.3.2: Effect of mutants of Bcl-2Δ21 on Ca^{2+}-ATPase activity of SERCA.

Even though the two Cys-mutants were generated primarily targeting the cross-linking experiments, they were used in the activity assay experiments along with G145E mutant, to study their effect on SERCA inactivation. Samples of SR were co-incubated with the WT or mutants of Bcl-2Δ21 prior to the activity measurements. A molar ratio of 2:1 (Bcl-2Δ21: SERCA) was used since complete inactivation of SERCA was reported after 2 hours of co-incubation at this ratio (*6,9*). Also some important control experiments have been reported previously, confirming that this SERCA inactivation is specifically caused by Bcl-2Δ21(*9*). Figures 3.3 and

3.4 show the variation of Ca^{2+}-ATPase activity of SERCA over time, indicating how the three mutants affect SERCA activity.

Since G145E is a loss-of-function mutant of human Bcl-2 as reported in a study using mammalian cell lines (*3*), one could expect to see no/smaller effect on SERCA inactivation from this mutant compared to WT Bcl-2Δ21. As expected, G145E mutant did not change the activity of SERCA significantly even after 4 hours of incubation (Figure 3.3). This clearly demonstrates that the G145 of Bcl-2Δ21 is a critical hot spot for the inactivation of SERCA.

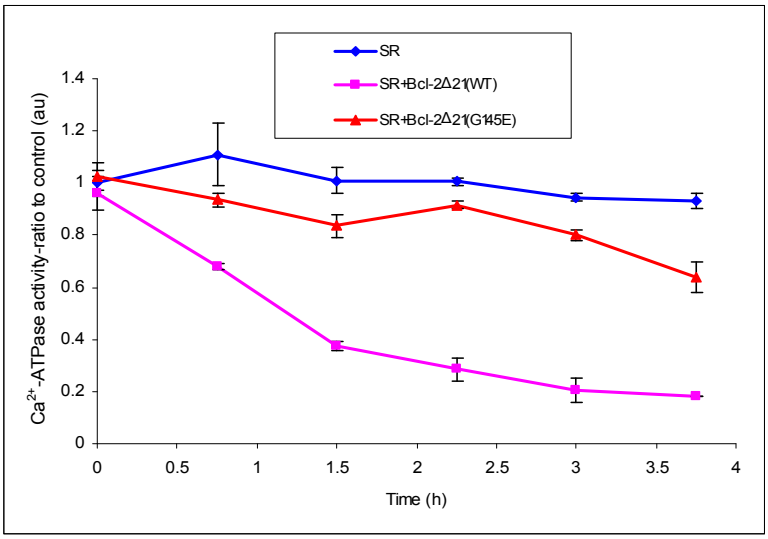

FIGURE 3.3: Effect of the G145E mutant of Bcl-2Δ21 on the activity of SERCA: The graph shows the Ca^{2+}-ATPase activity (ratio to control) over time, without Bcl-2Δ21(blue line), in the presence of WT (purple line) and the G145E mutant (red line) of Bcl-2Δ21.

The two Cys-mutants were expected to show a similar effect as the WT Bcl-2Δ21 on the inactivation of SERCA. Interestingly and surprisingly the two Cys-mutants acted as gain-of-function mutants and SERCA was inactivated to a higher extent than with WT Bcl-2Δ21 (Figure 3.4). Complete inactivation of SERCA is observed even after 1 ½ hours of co-incubation with the Cys-mutants.

Considering all three mutants together, the more hydrophobic Cys-mutants are more efficient while the less hydrophobic G145E mutant shows less SERCA inactivation, suggesting that hydrophobicity of the Bcl-2Δ21 molecule is important for SERCA/Bcl-2Δ21 interactions. Hydrophobicity of Bcl-2Δ21 might facilitate association with SERCA and/or incorporation of Bcl-2Δ21 into the SR membrane thus inactivating SERCA faster.

(a)

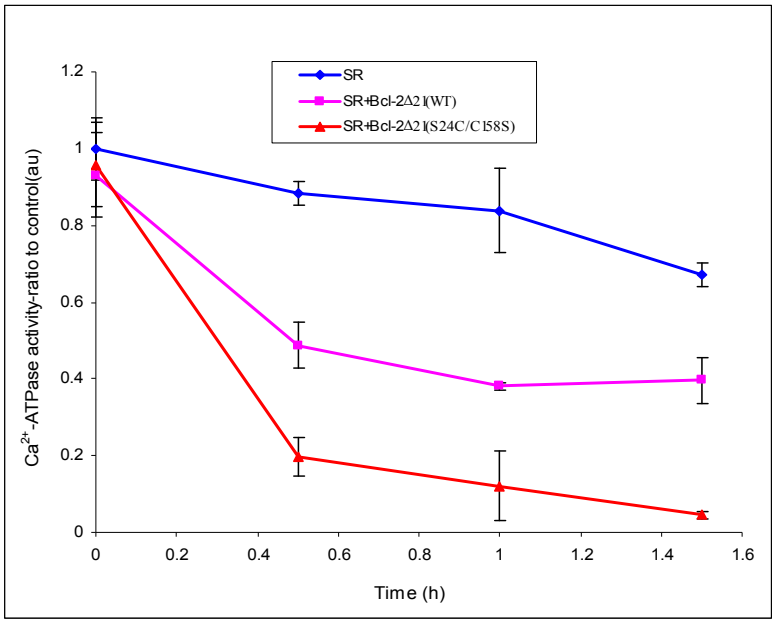

(b)

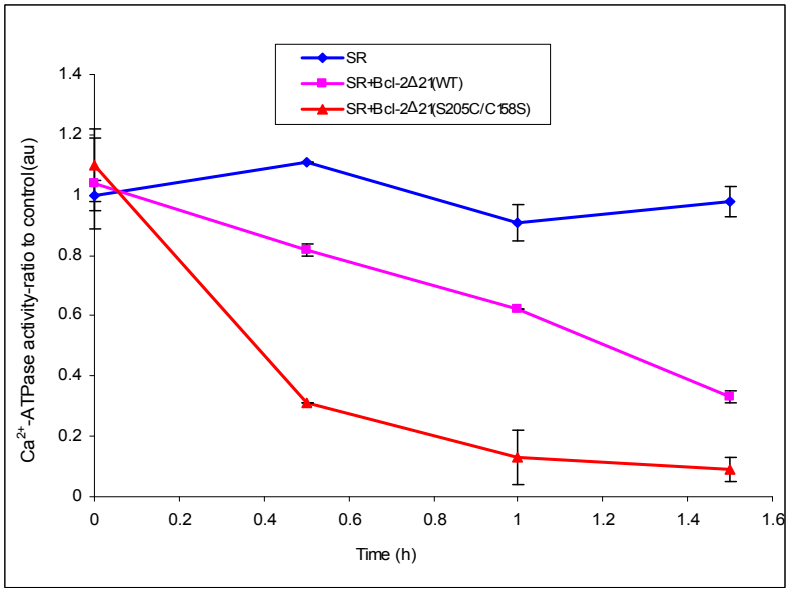

FIGURE 3.4: Effect of the Cys-mutants of Bcl-2Δ21 on the activity of SERCA: (a) Effect of S24C/C158S; (b) Effect of S205C/C158S; The graphs show the Ca^{2+}-ATPase activity (ratio to control) over time, without Bcl-2Δ21(blue lines), in the presence of WT (purple lines) and the Cys-mutants (red lines) of Bcl-2Δ21.

3.3.3: Effect of mutants of Bcl-2Δ21 on Sucrose Density Gradient (SDG) fractionation of SR.

Using SDG fractionation, it was shown previously by Dremina et al that SERCA is localized in Caveolae-Related Domains (CRD) of the SR membrane (*6*). The location of this CRD fraction is indicated in the simulated sucrose gradient in Figure 3.5.

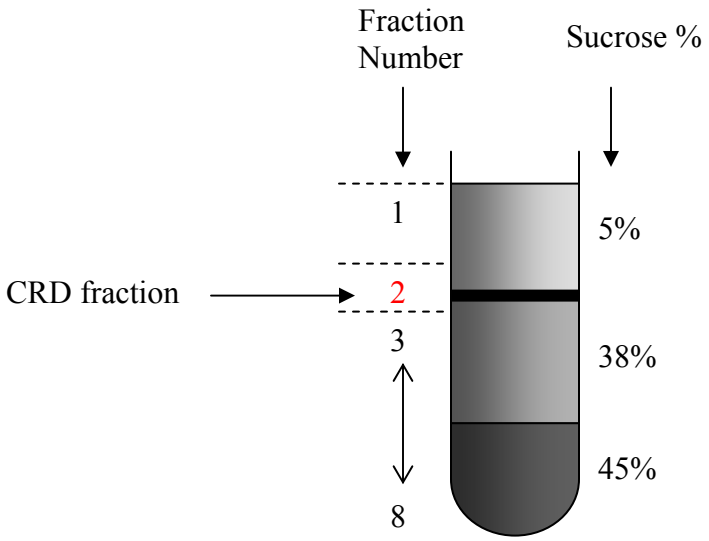

FIGURE 3.5: Simulated sucrose gradient after fractionation of SR: CRD fraction (number 2) is localized between 5% and 38% sucrose.

After the co-incubation with SR, Bcl-2Δ21 is incorporated into CRD, colocalized with SERCA and also induces translocation of SERCA from CRD. Partial unfolding of SERCA was also seen along with the inactivation and translocation (*6, 9*). Figure 3.6 is a schematic showing the location of SERCA in the SR/ER membrane before and after the incubation with Bcl-2Δ21.

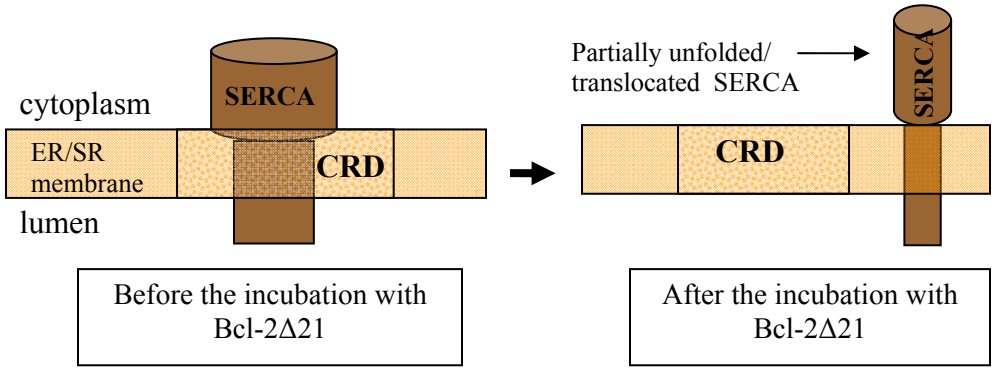

FIGURE 3.6: Location of SERCA in SR/ER membrane: before and after the incubation with Bcl-2Δ21.

The three mutants of Bcl-2Δ21 were compared with WT for their ability to induce translocation of SERCA from the CRD of the ER/SR membrane. The SR samples were incubated with Bcl-2Δ21 (WT or the three mutants) before the SDG fractionation. The location of SERCA within the gradient after SDG fractionation was determined using western blotting with a SERCA antibody. These western blots are shown in Figure 3.7. The results with the two Cys-mutants are shown in the Figure 3.7-a while Figure 3.7-b shows the results for the G145E mutant. Lane 2 of each sample represents the CRD fraction. The SR samples without Bcl-2Δ21 show almost all SERCA in the low density CRD fraction (Lane 2 of Figure 3.7-a(i) and b(i)) whereas the SR samples with WT Bcl-2Δ21 show SERCA even in the high density bottom fraction (Lane 4 of Figure 3.7-a(ii) and Lane 8 of b(ii)). This observation is consistent with previously published data, i.e. when SERCA is inactivated by Bcl-2Δ21, it is translocated from CRD to a different membrane environment and therefore

SERCA can be seen even in the high density bottom fraction of the sucrose gradient (*6*).

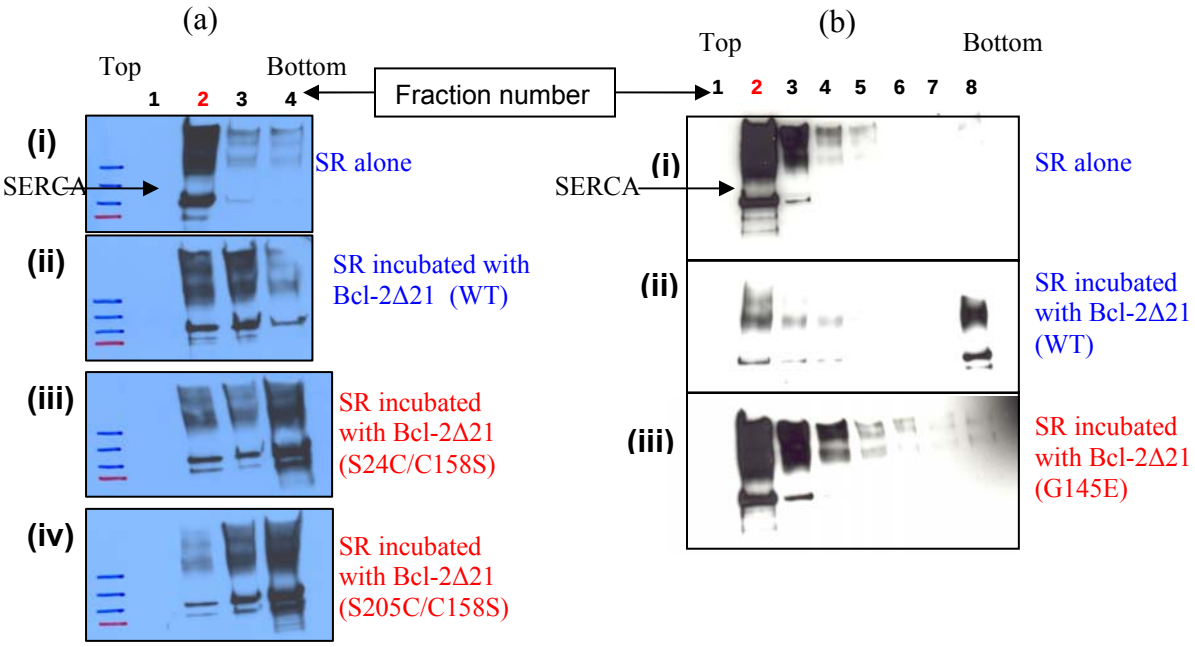

FIGURE 3.7: Effect of mutants of Bcl-2Δ21 on Sucrose Density Gradient (SDG) fractionation of SR: SDG fractions probed with SERCA antibody; (a) Experiment with the Cys-mutants; (i) SR alone, (ii)SR incubated with WT, (iii) SR incubated with S24C/C158S and (iv) SR incubated with S205C/C158S. (b) Experiment with G145E mutant; (i) SR alone, (ii) SR incubated with WT, (iii) SR incubated with G145E.

Since the two Cys-mutants showed higher SERCA inactivation, one could expect to see translocation of more SERCA from the CRD of the SR membrane. If this is true the samples incubated with the Cys-mutants should show less SERCA in the low density CRD fraction and more SERCA in the high density bottom fraction, compared to the sample incubated with the wild type Bcl-2Δ21. As expected, bottom

fractions of the SR samples incubated with Cys-mutants (Lane 4 of Figure 3.7-a (iii) and (iv)) show more SERCA. The G145E mutant, on the other hand, showed less SERCA inactivation and hence no/less translocation of SERCA with the G145E mutant can be expected and, if this is true, the sample incubated with the G145E mutant should indicate more SERCA in the low density CRD fraction and less SERCA in the high density bottom fraction, compared to the sample incubated with the wild type Bcl-2Δ21. As seen in the Figure 3.7-b, the SR sample incubated with G145E mutant shows more SERCA in the CRD fraction and no/less SERCA in the bottom fraction (compare Lanes 2 and 8 of Figure 3.7-b (iii)). These results further confirm the correlation between SERCA inactivation and translocation, the more inactivation the more translocation.

3.3.4: Association of SERCA with mutants of Bcl-2Δ21; Using GST-Bcl-2Δ21 binding assay and immunoprecipitation.

To compare the ability of Bcl-2Δ21 mutants to associate with SERCA, a GST-Bcl-2Δ21 binding assay and immunoprecipitation (IP) was employed. Figure 3.8-a shows the binding assay samples probed with Bcl-2 antibody. In addition to the 50kDa GST-Bcl-2Δ21 band, a degradation product of the fusion protein is seen. Further the WB shows less fusion protein of S24C/C158S mutant (Lane 2 in a) suggesting relatively lower stability of this mutant and this affects the comparison of this Cys-mutant with the others for their binding ability with SERCA. However, WT, S205C/C158S and G145E samples show almost the same amount of fusion protein

(Lanes 1, 3 and 4 in Figure 3.8-a) and therefore those three can be compared with each other for their binding ability with SERCA.

The SERCA antibody WB of the binding assay samples is shown in Figure 3.8-b. Since all three mutant samples show the SERCA band (Lanes 5, 6, 7 in Figure 3.8-b), fusion proteins of the three mutants of Bcl-2Δ21 can directly bind with SERCA. However, the S205C/C158S sample shows less SERCA (Lane 6 in b) while the G145E sample shows more SERCA (Lane 7 in b) compared to the WT sample (Lane 4 in b). Since, irreversible inactivation of SERCA is faster with the S205C/C158S mutant, availability of less native SERCA for association with Bcl-2Δ21 can be suggested. Also the opposite argument explains the more intense SERCA band seen with the G145E mutant. The control sample, without GST-Bcl-2Δ21 shows no SERCA (Lane 3 in b) confirming there is no affinity of SERCA for glutathione-agarose beads. Further, it has been reported previously that GST itself has no affinity for SERCA (*9*). Therefore SERCA seen in the binding assay samples is due to the association with Bcl-2Δ21. However, there might be some other unidentified protein/proteins in the SR helping this SERCA/ Bcl-2Δ21 association.

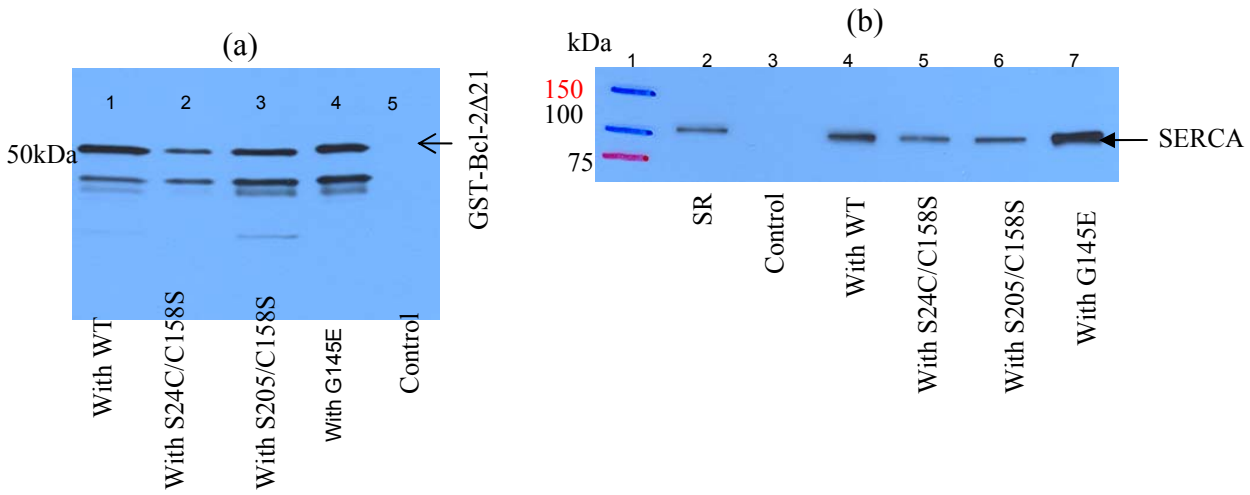

FIGURE 3.8: Association of SERCA with mutants of Bcl-2Δ21; Using GST-Bcl-2Δ21 binding assay: (a) western blot with Bcl-2 antibody; 1-with WT, 2-with S24C/C158S, 3-with S205C/C158S and 4-with G145E of GST-Bcl-2Δ21. 5-control sample without GST-Bcl-2Δ21. (b) western blot with SERCA antibody; 1-molecular weight marker, 2-fraction of purified SR vesicles, 3-control sample without GST-Bcl-2Δ21, 4-with WT, 5-with S24C/C158S, 6-with S205C/C158S and 7-with G145E of GST- Bcl-2Δ21.

Immunoprecipitation using Bcl-2 antibody was also employed to further confirm the ability of Bcl-2Δ21 mutants to directly associate with SERCA. Figure 3.9-a shows IP samples in the WB with Bcl-2 antibody. As seen with the GST-Bcl-2Δ21 binding assay, the IP sample of S24C/C158S shows less Bcl-2Δ21 (Lane 3 in Figure 3.9-a) further confirming that this mutant is relatively more susceptible to degradation during the hours of incubation. WT and the other two mutants, S205C/C158S and G145E, are almost the same in stability and show similar amounts of Bcl-2Δ21 in the samples (Lanes 2, 4 and 5 in Figure 3.9-a).

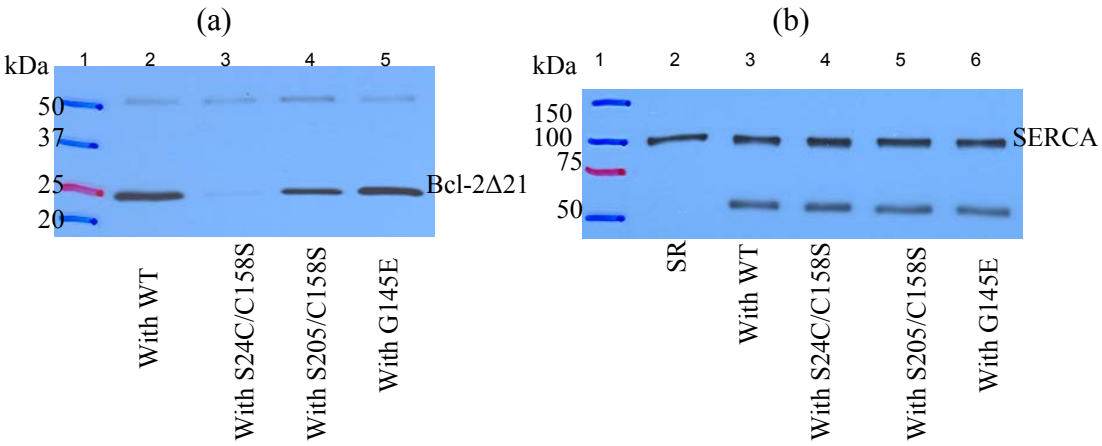

FIGURE 3.9: Association of SERCA with mutants of Bcl-2Δ21; Using immunoprecipitation: (a) western blot with Bcl-2 antibody; 2-with WT, 3-with S24C/C158S, 4-with S205C/C158S and 5-with G145E of Bcl-2Δ21. (b) western blot with SERCA antibody; 2-fraction of purified SR vesicles, 3-with WT, 4-with S24C/C158S, 5-with S205C/C158S and 6-with G145E of Bcl-2Δ21.

The WB with SERCA antibody (Figure 3.9-b) shows SERCA with all four samples further confirming that, not only the WT but also the three mutants are capable of directly binding to SERCA. However, the intensities of the SERCA bands with both WT and the mutants are the same and do not show a pattern identical to the GST-Bcl-2Δ21 binding assay samples (Lanes 3, 4, 5, 6 of Figure 3.9-b). During IP, both Bcl-2Δ21 antibody and SERCA are competing with each other for association with Bcl-2Δ21. Furthermore, the irreversible inactivation of SERCA caused by interaction with Bcl-2Δ21 could lower the amount of native SERCA available for IP. For these reasons, the amount of SERCA immunoprecipitated does not accurately reflect the relative affinity of the three Bcl-2Δ21 mutants for the association with

SERCA. The band at 50kDa in the western blots of immunoprecipitates is probably due to non-specific binding of Bcl-2 antibody and SERCA antibody with the light chain of the Bcl-2 antibody used for IP.

3.3.5: Comparison of WT and Cys-mutants of Bcl-2Δ21 in cysteine derivatization:

As mentioned earlier, the two Cys-mutants, S24C/C158S and S205C/C158S, were generated primarily for photo cross-linking experiments. Since S24 and S205 are well exposed residues, higher efficiency in cysteine derivatization is expected with the C24 and C205 of the two Cys-mutants. As expected the two Cys-mutants are more susceptible efficient than wild type to cysteine derivatization as revealed by ThioGlo1-Cysteine adduct formation (Figure 3.10). However, compared to the wild type Bcl-2Δ21 with added SDS, the mutants show only about a 10% increase in labeling efficiency (Figure 3.11). Therefore BPM derivatization of the Cys-mutants, for photo cross-linking experiments, was also achieved in the presence of 0.05% SDS in order to have more BPM labeled molecules. After the BPM labeling reaction, the added SDS was removed from the reaction mixture by dialysis before cross-linking with SERCA.

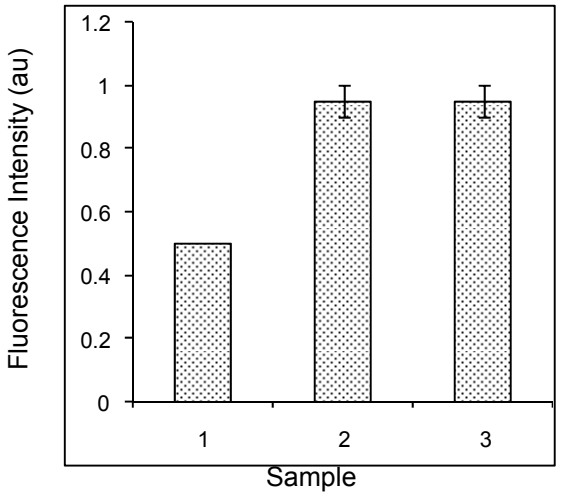

FIGURE 3.10: Comparison of the Cys-mutants with wild type Bcl-2Δ21 (without SDS) for cysteine derivatization, as determined by ThioGlo1-Cystein adduct formation: (1)-Wild type, (2)-S24C/C158S and (3)-S205C/C158S of Bcl-2Δ21.

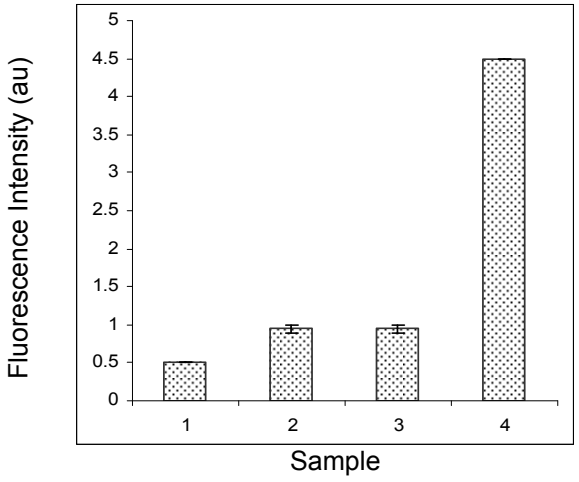

FIGURE 3.11: Comparison of the Cys-mutants with wild type Bcl-2Δ21 (with SDS) for cysteine derivatization, as determined by ThioGlo1-Cystein adduct formation: (1)-Wild type (without SDS), (2)-S24C/C158S and (3)-S205C/C158S and (4)Wild type (with SDS).

3.3.6: Mutants of Bcl-2Δ21 in photo cross-linking with SERCA.

Figures 3.12 and 3.13 are the western blots with Bcl-2 and SERCA antibodies, respectively, of the photo cross-linked samples. In the WB of the Bcl-2 antibody (Figure 3.12), the wild type Bcl-2Δ21 clearly shows (Lanes 2 and 3 of Figure 3.12) two bands at 135kDa and 160kDa corresponding to the two cross-linked products of 1:1 and 2:1 molar ratio of Bcl-2Δ21: SERCA, respectively. The photo cross-linking of wild type Bcl-2Δ21 with SERCA is discussed in Chapter 2 under Section 2.3.4. Since the Cys158 of the BH1 domain is the site of cross-linking reagent in the wild type Bcl-2Δ21, it was concluded that the BH1 domain of the hydrophobic groove of Bcl-2Δ21 is in direct contact with SERCA.

When Bcl-2Δ21 mutants are considered, even though the G145E mutant shows loss-of-function on SERCA inactivation, it shows clear cross-linked products and also homodimers with intensities comparable to the WT (compare Lane 9 with Lane 3 of Figure 3.12). As with WT Bcl-2Δ21, the site of cross-linking in the G145E mutant is also Cys158. Therefore the cross-linking results with the G145E mutant further support the suggestion that the SERCA interaction surface of Bcl-2Δ21 involves the BH1 domain. As mentioned before, Bcl-2Δ21 homodimerization involves two binding surfaces, the acceptor and the donor surfaces. It is known that G145 is located in the middle of the acceptor surface of Bcl-2Δ21 homodimers (*17*). The lower intensity of the dimer (50 kDa band) of the G145E mutant compared to the WT (compare Lane 8 with Lane 2 of Figure 3.12) indicates some negative effect on homodimerization by the G145E mutant. However it is interesting to notice

comparable levels of homodimers of both the WT and G145E mutant in the presence of the SR. Even though the G145E mutant lowers homodimerization ability, the availability of SR vesicle membrane compensates for it. The SR/BPM control sample shows no bands in the WB (Lane 10 of Figure 3.12) confirming the absence of any non-specific binding of Bcl-2 antibody with SR proteins.

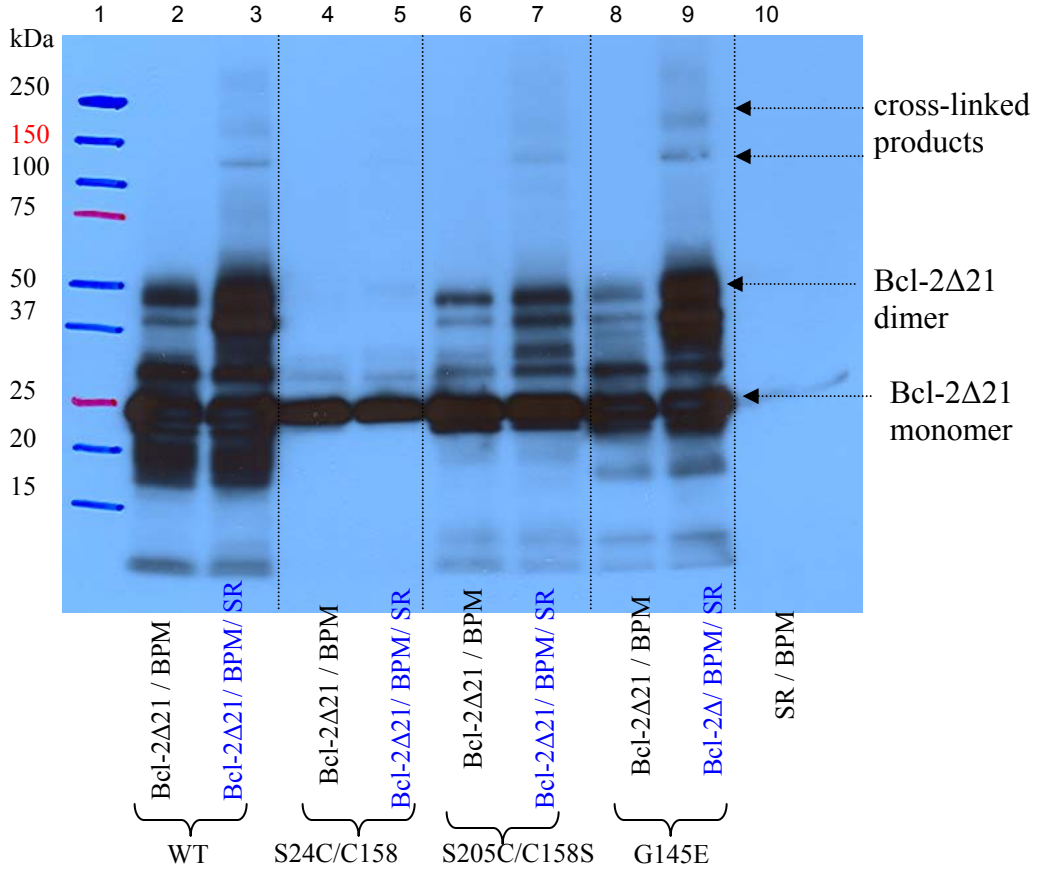

FIGURE 3.12: Bcl-2 antibody western blot of photo cross-linked samples: Lanes 3, 5, 7 and 9 are samples of Bcl-2Δ21/BPM/SR of WT, S24C/C158S, S205C/C158S and G145E of Bcl-2Δ21, respectively. Lanes 2, 4, 6 and 8 are the corresponding control samples of Bcl-2Δ21/BPM. Lane 10 is the SR/BPM control sample. Lane 1 is the molecular weight marker.

The fast inactivation of SERCA by the two Cys-mutants would affect the cross-linking with SERCA and therefore the cross-linking results would not be comparable with that of the wild type results. As revealed by the binding assay and IP experiments the S24C/C158S mutant is less stable and degrades faster. Consistent with this observation, the photo cross-linking sample of the S24C/C158S mutant shows less monomer compared to the other samples (Figure 3.12; compare the band at 25 kDa of Lanes 4 and 5 with others). However, the S24C/C158S mutant samples clearly show the absence of the cross-linked products and homodimers. The absence of cross-linked bands would indicate that the site of cross-linking reagent in this mutant, Cys24, and hence the BH4 domain, is not sufficiently close to the SERCA interaction surface. On the other hand, since the inactivation and translocation of SERCA by this mutant is much faster, there might not be enough Bcl-2Δ21-associated SERCA available for cross-linking during UV irradiation. Even though BH4 is a part of the Bcl-2 donor surface for homodimerization (*17*), Cys24 in particular might not be sufficiently close to covalently link with the other S24C/C158S molecule of the homodimer.

The S205C/C158S mutant, on the other hand, shows both cross-linked products and homodimers (Figure 3.12; Lanes 6 and 7). However the intensities of these bands are lower, relative to the WT bands. The cross-linking site, Cys205 in the S205C/C158S mutant is located closer to the BH2 domain, which is a part of the hydrophobic surface groove of Bcl-2Δ21. Therefore not only the BH1 domain (as seen with the WT and the G145E mutant) but also the BH2 domain of Bcl-2Δ21

should be interacting with SERCA. Nevertheless the BH2 domain is a part of the acceptor surface of Bcl-2 homodimers (*17*) and therefore the appearance of the homodimers in the cross-linked sample is acceptable. As with S24C/C158S mutant, the argument based on fast SERCA inactivation, can be made here too, explaining the lower intensity of the cross-linked bands. This argument was facilitated by the finding that the incubation time of the SERCA/Bcl-2Δ21 mixture prior to the UV irradiation is critical for observation of cross-linked products. Clear cross-linked bands were seen only with 15 min of incubation and longer incubation times (45 min and 2 hours) did not show cross-linked products with both Cys-mutants (data not shown).

The SERCA antibody WB of the cross-linked samples is shown in Figure 3.13. It was noticed previously (Chapter 2) that the photo cross-linked sample of Bcl-2Δ21/BPM/SR of wild type protein and the SR/BPM control sample show identical results and therefore SERCA/Bcl-2Δ21 cross-linked bands could not be confirmed with SERCA antibody. Similar to the results with wild type Bcl-2Δ21, the results of the cross-linked samples of Bcl-2Δ21/BPM/SR of the three mutants (Lanes 3-6 in Figure 3.13) and also of the SR/BPM control sample (Lane 2 of Figure 3.13) are identical. Therefore the discussion about the SERCA antibody western blot of the photo cross-linked samples with wild type Bcl-2Δ21, is applicable here too (see Chapter 2, Section 2.3.4). Even though the same amount of protease inhibitor is used in all cross-linking samples, the two Cys-mutant samples show higher SERCA degradation (bands below 100 kDa in Lanes 4 and 5 in Figure 3.13). This could be

caused by relatively higher inactivation and translocation of SERCA by these Cys-mutants.

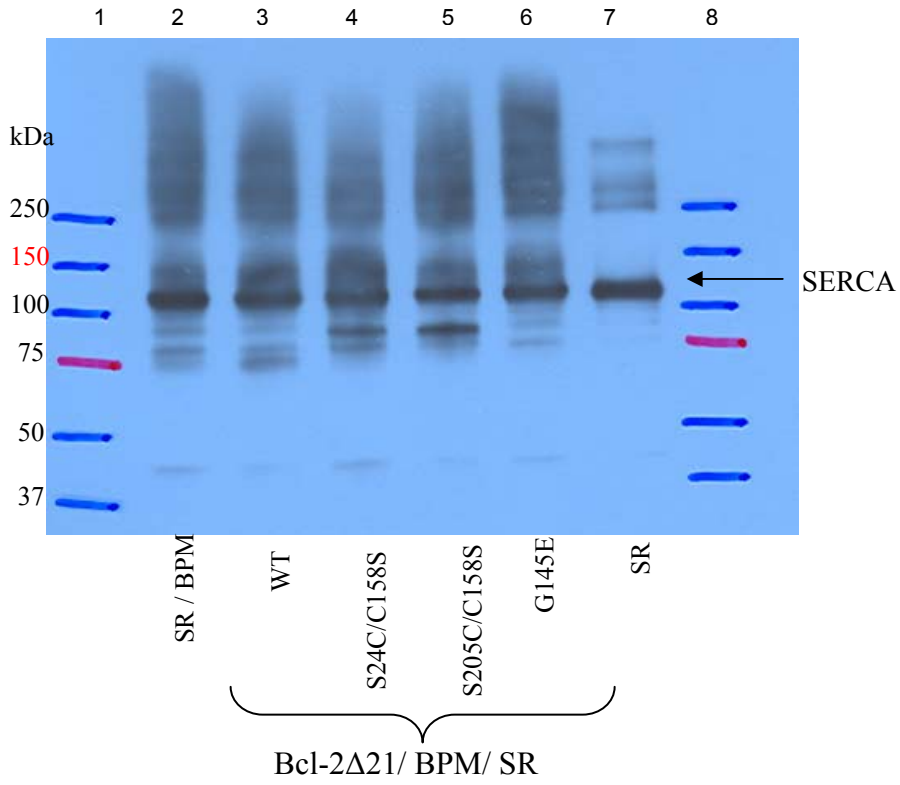

FIGURE 3.13: SERCA antibody western blot of photo cross-linked samples: Lanes 3, 4, 5 and 6 are samples of Bcl-2Δ21/BPM/SR of WT, S24C/C158S, S205C/C158S and G145E of Bcl-2Δ21, respectively. Lane 2 is the SR/BPM control sample without Bcl-2Δ2. Lane 7 is a fraction of purified SR vesicles. Lanes 1, 8 are the molecular weight marker.

3.4: Conclusions.

In conclusion, the experiments described in this chapter further confirm that Bcl-2Δ21 and SERCA can interact with both 1:1 and 2:1 (Bcl-2Δ21: SERCA) molar ratios. All three mutants of Bcl-2Δ21 (S24C/C158S, S205C/C158S and G145E) can directly associate with SERCA. The G145E mutant is a loss-of-function whereas the two Cys-mutants, S24C/C158S and S205C/C158S, are gain-of-function on SERCA inactivation and translocation. The conserved residue, G145, is a critical hot spot for Bcl-2Δ21-mediated inactivation and translocation of SERCA. Fulfilling the second objective of the work reported in this dissertation, the BH1and BH2 domains of Bcl-2Δ21 are identified as directly involved in the interactions with SERCA. The trans membrane domain of Bcl-2 is not required for this interaction.

3.5: References.

1. Petros, A.M., Medek, A., Nettesheim, D.G., Kim, D.H., Yoon, H.S., Swift, K., Matayoshi, E.D., Oltersdorf, T., and Fesik, S.W. (2001) Solution structure of the antiapoptotic protein bcl-2, *Proc. Natl. Acad. Sci. U. S. A. 98(6),* 3012-3017. Epub 2001 Feb 27.
2. Petros, A.M., Olejniczak, E.T., and Fesik, S.W. (2004) Structural biology of the Bcl-2 family of proteins, *Biochim. Biophys. Acta. 1644(2-3),* 83-94.
3. Yin, X.M., Oltvai, Z.N., and Korsmeyer, S.J. (1994) BH1 and BH2 domains of Bcl-2 are required for inhibition of apoptosis and heterodimerization with Bax, *Nature 369(6478),* 321-323.
4. Carter, P. (1986) Site-directed mutagenesis, *Biochem. J. 237(1),* 1-7.
5. Voet, D., Voet, J.G. and Pratt, C.W. (2002) *Fundamentals of Biochemistry* Upgrade edition, pp 106-107, John Wiley & Sons, Inc., U.S.A.
6. Dremina, E.S., Sharov, V.S., and Schöneich, C. (2006) Displacement of SERCA from SR lipid caveolae-related domains by Bcl-2: a possible mechanism for SERCA inactivation, *Biochemistry 45(1),* 175-184.
7. Chan, K.M., Delfert, D., and Junger, K.D. (1986) A direct colorimetric assay for Ca2+ -stimulated ATPase activity, *Anal. Biochem. 157(2),* 375-380.

8. Lanzetta, P.A., Alvarez, L.J., Reinach, P.S., and Candia, O.A. (1979) An improved assay for nanomole amounts of inorganic phosphate, *Anal. Biochem. 100(1),* 95-97.
9. Dremina, E.S., Sharov, V.S., Kumar, K., Zaidi, A., Michaelis, E.K., and Schöneich, C. (2004) Anti-apoptotic protein Bcl-2 interacts with and destabilizes the sarcoplasmic/endoplasmic reticulum Ca2+-ATPase (SERCA), *Biochem. J. 383(Pt 2),* 361-370.
10. Berggård, T., Linse, S., and James, P. (2007) Methods for the detection and analysis of protein-protein interactions, *Proteomics 7(16),* 2833-2842.
11. Kuroda, K., Kato, M., Mima, J., and Ueda, M. (2006) Systems for the detection and analysis of protein-protein interactions, Appl. Microbiol. Biotechnol. 71(2), 127-136.
12. Piehler, J. (2005) New methodologies for measuring protein interactions in vivo and in vitro, Curr. Opin. Struct. Biol. 15(1), 4-14.
13. Phizicky, E.M., and Fields, S. (1995) Protein-protein interactions: methods for detection and analysis, Microbiol. Rev. 59(1), 94-123.
14. Reed, J.C. (1997) Double identity for proteins of the Bcl-2 family, *Nature 387(6635),* 773-776.
15. Lee, L.C., Hunter, J.J., Mujeeb, A., Turck, C., and Parslow, T.G. (1996) Evidence for alpha-helical conformation of an essential N-terminal region in the human Bcl2 protein, *J. Biol. Chem. 271(38),* 23284-23288.
16. Vance, B.A., Zacharchuk, C.M., and Segal, D.M. (1996) Recombinant mouse Bcl-2(1-203). Two domains connected by a long protease-sensitive linker, *J. Biol. Chem. 271(48),* 30811-30815.
17. Zhang, Z., Lapolla, S.M., Annis, M.G., Truscott, M., Roberts, G.J., Miao, Y., Shao, Y., Tan, C., Peng, J., Johnson, A.E., Zhang, X.C., Andrews, D.W., and Lin, J. (2004) Bcl-2 homodimerization involves two distinct binding surfaces, a topographic arrangement that provides an effective mechanism for Bcl-2 to capture activated Bax, *J. Biol. Chem. 279(42),* 43920-43928.

Chapter 4:

Overall discussion, conclusions and future experiments.

4.1: Overall discussion and conclusions.

Bcl-2 regulated changes in the Sarco/Endoplasmic Reticulum (SR/ER) Ca^{2+} level have been subjected to investigation by various groups (*1-5*). Interaction of Bcl-2 with different ER proteins such as Inositol tris phosphate receptor (IP_3R) (*6*), and SERCA (*7-9*) was reported recently, attempting to answer the question "How does Bcl-2 regulate the SR/ER Ca^{2+} level?" It has been reported that both full length Bcl-2 and the truncated form, Bcl-2Δ21, can directly associate with and inactivate SERCA. Under normal conditions SERCA is mainly localized in low density Caveolae-Related Domains (CRD) of the SR/ER membrane. After association with Bcl-2, SERCA is translocated to a different high density region of the SR/ER membrane (*8, 9*). In the present study important characteristics of the SERCA/Bcl-2 interactions were unraveled including the identification of the critical residues/domains of the interface of the two proteins.

The wild type and also the three mutants, S24C/C158S, S205C/C158S and G145E of the truncated form of Bcl-2, Bcl-2Δ21 were used in the experiments. All anti-apoptotic proteins including Bcl-2 have nine alpha helices and four BH domains (BH1-4). They have a common hydrophobic surface groove formed by the BH1-3 domains which are important in heterodimerization with pro-apoptotic members (*10,*

11). The truncated form, Bcl-2Δ21, contains only eight alpha helices since it lacks the α9/TM domain.

Cross-linking was utilized to identify the sites/domains of SERCA/Bcl-2Δ21 interaction surface. This method has been used for decades in protein interaction studies. When the interface of interacting proteins are identified through cross-linking, the site of cross-linking reagent is a key factor. If it is too close to the interface or at a site, directly involved in the interaction, it might block the proteins interacting with each other. On the other hand if it is too far from the interface, even though the proteins are interacting, the reagent is not sufficiently close to crosslink the interaction partners. Benzophenone-4-maleimide (BPM), photo activatable cross-linking reagent used in this study is attached to Cys158 in the case of WT and also of the G145E mutant of Bcl-2Δ21. As previously reported the redox status of Cys158 does not affect the Bcl-2Δ21-mediated inactivation of SERCA (*8*). Therefore BPM attachment to Cys158 of Bcl-2Δ21 can be expected not to affect the SERCA/Bcl-2Δ21 association. In fact BPM treated Bcl-2Δ21 can effectively inactivate SERCA as revealed by a Ca^{2+}-ATPase activity assay. After photo cross-linking both WT and the G145E mutant show cross-linked products confirming that Cys158 is located closer to the SERCA/Bcl-2Δ21 interface. The Cys158 is located in the BH1 domain, one of the three domains of the hydrophobic surface groove of Bcl-2. Therefore the BH1 domain and hence the hydrophobic surface groove of Bcl-2 must be directly interacting with SERCA.

In the Cys-mutants, S24C/C158S and S205C/C158S, the site of BPM activation is Cys24 and Cys 205, respectively. Cys24 is located in BH4 domain while Cys205 is right next to the C-terminal end of the BH2 domain of Bcl-2Δ21. Based on the cross-linking results with the S24C/C158S mutant, the BH4 domain is not a partner of the SERCA/Bcl-2Δ21 interface whereas the cross-linking results of the S205C/C158S mutant suggest that the BH2 domain is a part of the SERCA/Bcl-2Δ21 interface.

Importantly, as evident from cross-linking results, both one or two molecules of Bcl-2Δ21 can interact with SERCA. In the SERCA-2Bcl-2Δ21 trimer, two molecules of Bcl-2Δ21 could react at two separate sites on SERCA or a homodimer of Bcl-2Δ21 could react as a single unit, with one site of SERCA. A very small fraction of cross-linked products is seen in agreement with a previously suggested transient interaction/weak binding constant of Bcl-2Δ21 with SERCA (*8,9*). Only a small fraction of associated SERCA/Bcl-2Δ21, preventing cell death, is reasonable in vivo, since inactivation of all or a larger fraction of SERCA by Bcl-2Δ21 could be death inducible rather than protecting.

G145 is a conserved residue in α5 of BH1, located at the bottom of the hydrophobic surface groove of Bcl-2 (*10-12*). This highly conserved G residue plays a crucial role in anti apoptotic activity of Bcl-2 as demonstrated by several mutations involving this residue. Decreased death repressor activity and the absence of heterodimerization with pro-apoptotic member Bax, was reported with ^{144}WGR^{146} into ^{144}AAA^{146}(where W-Tryptophan, G-Glycine, R-Arginine and A-Alanine),

G145A and G145E mutations in Bcl-2, and also with the equivalent mutation, G138A in Bcl-x_L, a structural homolog of Bcl-2 (*12*). The G145E mutations in the Bcl-2 homolog of *C.elegans*, CED-9, is reported as a gain-of-function mutation emphasizing the importance of the G145 of BH1 domain in apoptosis control (*13*).

It is reported here that this conserved G residue, G145 in the α5/BH1 domain of the hydrophobic surface groove of Bcl-2Δ21 is important in inactivation and translocation of SERCA. The G145E mutation of Bcl-2Δ21 diminished the inactivation and translocation of SERCA. Since this single site mutation cannot be tolerated, G145 of Bcl-2Δ21 must be a critical site for inactivation and translocation of SERCA. However, the mutant is still able to cross-link with SERCA through the cross-linking reagent at Cys158. This reveals that the surface of Bcl-2Δ21 of SERCA/Bcl-2Δ21 interface should contain several interaction sites and is not limited to G145.

Glycine has the smallest side chain, a hydrogen atom, with the smallest cross sectional area and it facilitates proper protein folding. As a highly conserved residue, G145 should be critical for proper topology of the hydrophobic surface groove of Bcl-2Δ21 and therefore it facilitates Bcl-2Δ21 controlled SERCA inactivation and translocation. The G→E mutation introduces a negatively charged, larger side chain into the hydrophobic groove of Bcl-2Δ21, changing the characteristics of the groove. Probably this G→E conversion might reduce the hydrophobicity of the molecule thus changing electrostatic and hydrophobic interactions between the side chains of the SERCA/Bcl-2Δ21 interface which are important in inactivation and translocation of

SERCA. Also we cannot exclude that, apart from G145, there might be other residues in BH1, BH2 and BH3 domains of the hydrophobic surface groove of Bcl-2Δ21 which are important in this interaction.

The two Cys-mutants, S24C/C158S and S205C/C158S, on the other hand are gain-of-function on SERCA inactivation and translocation. Since C→S and S→C replacements in the mutants are isosteric, this gain-of-function cannot be caused by any alterations in steric effects. Rather these mutations might change the hydrogen bond network of Bcl-2Δ21, changing the overall structure of the protein. This structural change would facilitate the interaction of the hydrophobic surface groove of Bcl-2Δ21 with SERCA. Further this structural change in S24C/C158S mutant might affect the stability of the protein making it more susceptible to proteolytic/hydrolytic degradation.

To date more than 10 different isoforms of SERCA have been identified (*14*). SERCA inserts its Ca^{2+} transport function through the well known E1/E2 model. The high Ca^{2+} affinity E1 conformation of SERCA changes to the low affinity E2 conformation while actively transporting Ca^{2+} ions from the cytoplasm into the ER (*15-17*). SERCA is a trans-membrane protein. Its cytoplasmic head piece contains six subdomains. These are the N-terminal stalk domain (residues 1-40), the β-strand domain (residues 131-238), the phosphorylation domain (residues 328-505), the ATP binding domain (residues 505-680), the hinge domain (residues 681-738) and the C-terminal region (residues 902-994). The stalk domain connects the head piece to the transmembrane domain. The phosphorylation domain and the ATP binding domain

together form the active site for ATP hydrolysis (*18, 19*). Inter domain interactions between these cytosolic domains, specifically between the ATP binding and phosphorylation domains are important in the Ca^{2+} transport mechanism of SERCA (*20, 21*).

The SERCA peptide, ^{568}DTPPKR^{573}, cross-linked to the Cys158/BH1 domain of Bcl-2Δ21, as identified from mass spectrometry, is located at the cytoplasmic ATP binding domain. More importantly it is located right next to ^{560}RCLALA^{565}, one of the conserved motifs in SERCA (*22*). Furthermore, it has been found previously, using a fragment of SERCA (residues 357-600) containing the ATP binding domain, that Thr569 was among the residues whose backbone conformation was changed upon nucleotide binding, as measured using NMR spectroscopy (*23*). Therefore Thr569 and hence ^{568}DTPPKR^{573} could be directly involved in ATP binding during the catalytic cycle of SERCA. Bcl-2Δ21 might directly but transiently interact with the ATP binding domain of SERCA thus blocking the cross-talk between the ATP binding and the phosphorylation domains, which is required for SERCA activity. As reported previously, the SERCA/Bcl-2Δ21 interaction does not change the ATP binding affinity of the domain (*9*). Interaction of Bcl-2Δ21 with ^{568}DTPPKR^{573} would not necessarily change the affinity of the domain for ATP since more than one amino acid residue is supporting the binding process (*23-27*). Apart from this ATP binding domain, Bcl-2Δ21 might interact with other domains of SERCA which were not identified in this study.

Other SR proteins which act in concert with SERCA in SR-calcium regulation (*28*) and also yet unidentified Bcl-2Δ21 and SERCA binding proteins can be involved in this SERCA/Bcl-2Δ21 interaction. Protective action of HSP70 (where HSP stands for Heat Shock Protein) on inactivation of SERCA by Bcl-2Δ21 has been reported (*29*). As suggested by our GST-Bcl-2Δ21 binding assay, photo cross-linking and mass spectrometric data, Mitsugumin-29 (Mg29) could be another involved protein. Mg29 is a recently identified protein in the triad-junction of skeletal muscle (*30*). It is essential for proper SR membrane structure and hence for proper function of skeletal muscle (*31*). It can interact functionally with Rynodine Receptor (RyR), a calcium release channel in the SR membrane, leading to apoptotic cell death (*32*). Its interaction with the Store Operated Calcium channel (SOC), a channel in plasma membrane which mediates extracellular Ca^{2+} entry into the cytoplasm, has also been reported (*33*). In addition to other possible Bcl-2Δ21 and SERCA binding proteins, some other factors which cannot be produced *in-vitro* could also be participating in the SERCA/Bcl-2Δ21 interactions.

Apart from the direct interaction, Bcl-2Δ21 might inactivate SERCA through some other indirect mechanisms. Truncated Bcl-2Δ21, which lacks membrane anchoring trans-membrane domain, is reported to have membrane insertion characteristics (*34, 35*) suggesting that Bcl-2Δ21 might inactivate SERCA indirectly through interactions with membrane lipids. As mentioned earlier, SERCA is mainly located at CRD of SR membrane and is translocated from CRD after interaction with Bcl-2Δ21(*9*). Cholesterol and Sphingolipids fall under the main lipids in CRD (*36*).

GM1, a glycosphingolipid highly concentrated in CRD is known to inhibit SERCA activity by changing the cytosolic part of SERCA into a less compact form (*37*) and this conformational change might lead to translocation of SERCA. Bcl-2Δ21 might interact with GM1 in a favorable manner supporting the GM1-mediated inactivation and conformational change of SERCA.

In conclusion, the work reported in this dissertation further supports the previously suggested direct association of Bcl-2Δ21 with SERCA causing inactivation and translocation of SERCA (*8, 9*). Based on the cross-linking studies the two proteins can interact in both 1:1 and 2:1 (Bcl-2Δ21: SERCA) molar ratios. Fulfilling the major objectives of the project, the BH1 and BH2 domains, and hence the hydrophobic surface groove of Bcl-2Δ21 were identified as directly involved in the interactions with SERCA. The BH1 domain of Bcl-2Δ21 interacts with the ^{568}DTPPKR^{573} peptide of the ATP binding domain of SERCA. Based on the chemical cross-linking experiments, the distance between the interface/interfaces of Bcl-2Δ21/SERCA complex can range from ~6-14Å. Even though all three mutants, S24C/C158S, S205C/C158S and G145E of Bcl-2Δ21 studied can directly associate with SERCA, the G145E mutant is a loss-of-function whereas the two Cys-mutants, S24C/C158S and S205C/C158S, are gain-of-function on SERCA inactivation and translocation. Therefore the conserved residue G145 is a critical hot spot for the Bcl-2Δ21-mediated inactivation and translocation of SERCA. Mitsugumin-29 (Mg29) could also be involved in Bcl-2Δ21/SERCA interactions. The association of SERCA with Bcl-2Δ21 is affected by aging.

4.2: Future Experiments.

Some suggested experiments that would further support the studies on SERCA/Bcl-2 interactions are described below. Preliminary data of some initial experiments are also presented.

4.2.1: Improvement of mass spectrometric identification of cross-linked peptides.

As mentioned above the SERCA peptide, ^{568}DTPPKR^{573} of the ATP binding domain was identified cross-linked to Cys158 of wild type Bcl-2Δ21 through the photo cross-linking reagent, Benzophenone-4-maleimide (BPM). However, since the MS/MS of the cross-linked SERCA-Bcl-2Δ21 dipeptide was not found in ESI-FTICR-MS data, the exact cross-linking site within the peptide of SERCA could not be confirmed. The reason for this is the lower abundance of cross-linked products in the sample and the problem can be overcome by using a method to enrich the sample with cross-linked products. Affinity purification is commonly used in this regard. Ni^{2+} affinity purified cross-linked products of His_6-Bcl-2Δ17, explained in Chapter 2, can be analyzed by mass spectrometry after in-gel/in-solution tryptic digestion of the vacuum-concentrated fraction of interest. This would improve the MS data and the MS/MS of the cross-linked products would be seen. Alternatively a photo cross-linking reagent with an affinity tag such as biotin can be used in cross-linking reactions so that the cross-linked peptides can be affinity purified after the tryptic digestion using streptavidin-conjugated beads before the MS analysis (*38*).

Use of a cleavable cross-linking reagent such as PEAS (Scheme 4.1) is another way of making the MS analysis of cross-linked products easier (*39, 40*). The R group of PEAS indicated in Scheme 4.1 is transferred to Cys158 of Bcl-2Δ21 through a disulfide-exchange reaction. Upon photo activation, Bcl-2Δ21 is covalently linked to SERCA. Cleavage of the disulfide bond within the linker transfers the R group to SERCA. The MS data of the tryptic digests are analyzed for the peptide of SERCA modified with R and the MS/MS of this peptide would reflect the exact site of cross-linking.

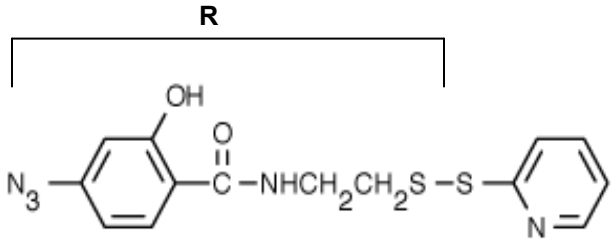

SCHEME 4.1: *N*-((2-pyridyldithio)ethyl)-4-azidosalicylamide (PEAS) (www.probes.com): The R group can be transferred to Cys158 of Bcl-2Δ21 through a disulfide-exchange reaction.

In a preliminary photo cross-linking reaction using PEAS (following the same reaction steps as with BPM, mentioned in Chapter 2), bands that can be considered as cross-linked products of Bcl-2Δ21 were seen with the Bcl-2 antibody (data not shown). However the samples are not good enough for MS analysis, since smeared lanes are seen even with the Bcl-2Δ21/PEAS control sample and therefore the reaction conditions should be further optimized. Once the reaction conditions are

optimized to observe clear cross-linked products in the western blots, the in-gel digests can be analyzed by MS. Since the MS data is searched for a single peptide of SERCA modified with R, not a cross-linked dipeptide as with BPM (see Chapter 2), the data analysis is relatively easier after cross-linking with PEAS.

4.2.2: Effect of W188 of Bcl-2Δ21 on inactivation and translocation of SERCA.

W188 is another conserved residue located in the BH2 domain of Bcl-2. W188A mutation has been reported to completely diminish the anti apoptotic activity of human Bcl-2 (*11, 12*). Therefore W188A would be another important mutant of Bcl-2Δ21 on the inactivation and translocation of SERCA. The W188A mutant has already been generated in the lab using PCR-based site directed mutagenesis.

As revealed by some preliminary experiments, the W188A mutant of Bcl-2Δ21 can inactivate and also translocate SERCA from the Caveolae-Related Domains (CRD) of the SR membrane. The Ca^{2+}-ATPase activity assay in the presence of W188A mutant shows a significant decrease in the enzymatic activity of SERCA (see Figure 4.1). When this mutant was used in an SDG fractionation experiment as explained in Chapter 3, SERCA is detected in almost all the fractions of the sucrose gradient compared to the control sample without Bcl-2Δ21 (compare (i) and (iii) of Figure 4.2). However since more degradation of SERCA is also seen with the same sample fractions containing W188A mutant, the inactivation and translocation of SERCA could be caused by some proteolytic enzymes co-purified during the purification of Bcl-2Δ21 (W188A). Therefore the results seen with this initial Ca^{2+}-

ATPase activity assay and SDG fractionation experiments are not very conclusive and the experiments should be repeated in the presence of more protease inhibitor.

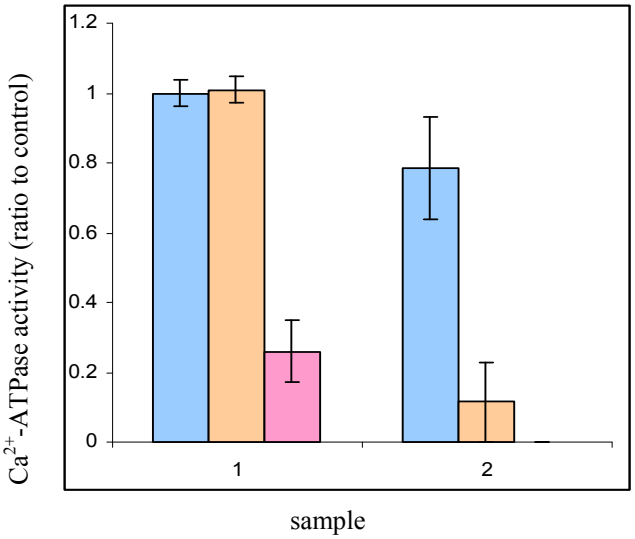

FIGURE 4.1: Effect of W188A mutant of Bcl-2Δ21 on Ca^{2+}-ATPase activity of SERCA: (●)-SR alone; (●)-SR mixed with wild type Bcl-2Δ21; (●)-SR mixed with W188A mutant of Bcl-2Δ21; 1-before incubation at 37 °C; 2-after 1h of incubation at 37 °C.

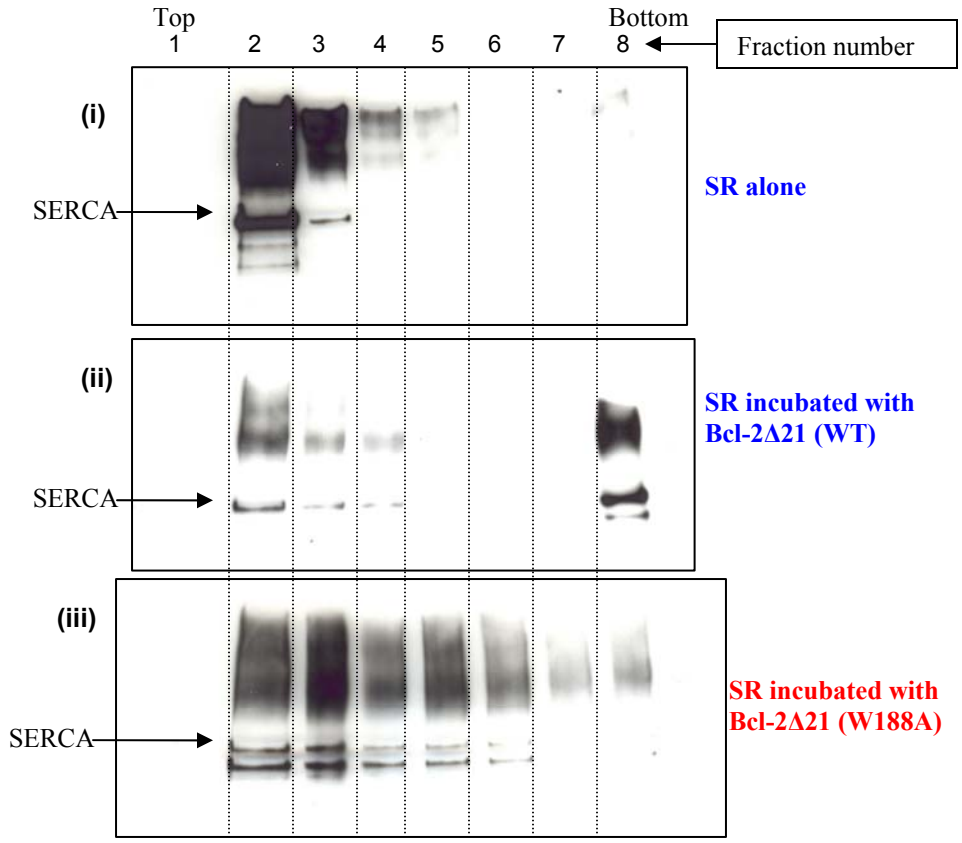

FIGURE 4.2: Effect of W188A mutant of Bcl-2Δ21 on Sucrose Density Gradient (SDG) fractionation of SR: SDG fractions probed with SERCA antibody; (i) SR alone, (ii) SR incubated with WT, (iii) SR incubated with W188A.

4.2.3: Other proteins involved in the interactions of SERCA/Bcl-2Δ21.

As suggested by the GST-Bcl-2Δ21 binding assay, photo cross-linking and mass spectrometric data described in the Chapter 2, Mitsugumin-29 (Mg29) could be one of the other proteins involved in this SERCA-Bcl-2Δ21 interaction. Using

purified Mg29 in immunoprecipitation and GST-Bcl-2Δ21 binding assay experiments would confirm the association of Mg29 with the SERCA/Bcl-2Δ21 complex.

Also since the protective action of HSP70 (Heat Shock Protein 70) on inactivation of SERCA by Bcl-2Δ21 has already beenreported (*29*), cross-linking experiments involving HSP70/SERCA and HSP70/Bcl-2Δ21 would be helpful in elucidating the architecture of the protein complex thereby understanding the associated function of HSP70 in regulation of SERCA/Bcl-2Δ21 interactions.

4.3: References.

1. Foyouzi-Youssefi, R., Arnaudeau, S., Borner, C., Kelley, W.L., Tschopp, J., Lew, D.P., Demaurex, N., and Krause, K.H. (2000) Bcl-2 decreases the free Ca2+ concentration within the endoplasmic reticulum, *Proc. Natl. Acad. Sci. U. S. A. 97(11),* 5723-5728.
2. Oakes, S.A., Opferman, J.T., Pozzan, T., Korsmeyer, S.J., Scorrano, L., Oakes, S.A., Opferman, J.T., Pozzan, T., Korsmeyer, S.J., and Scorrano, L. (2003) Regulation of endoplasmic reticulum Ca2+ dynamics by proapoptotic Bcl-2 family members, *Biochem. Pharmacol. 66(8),* 1335-1340.
3. Pinton, P., Ferrari, D., Rapizzi, E., Di Virgilio, F., Pozzan, T., and Rizzuto, R. (2001) The Ca2+ concentration of the endoplasmic reticulum is a key determinant of ceramide-induced apoptosis: significance for the molecular mechanism of Bcl-2 action, *EMBO J. 20(11),* 2690-2701.
4. Pinton, P., Ferrari, D., Magalhães, P., Schulze-Osthoff, K., Di Virgilio, F., Pozzan, T., and Rizzuto, R. (2000) Reduced loading of intracellular Ca(2+) stores and downregulation of capacitative Ca(2+) influx in Bcl-2-overexpressing cells, *J. Cell Biol. 148(5),* 857-862.
5. Lam, M., Dubyak, G., Chen, L., Nuñez, G., Miesfeld, R.L., and Distelhorst, C.W. (1994) Evidence that BCL-2 represses apoptosis by regulating endoplasmic reticulum-associated Ca2+ fluxes, *Proc. Natl. Acad. Sci. U. S. A. 91(14),* 6569-6573.
6. Chen, R., Valencia, I., Zhong, F., McColl, K.S., Roderick, H.L., Bootman, M.D., Berridge, M.J., Conway, S.J., Holmes, A.B., Mignery, G.A., Velez, P., and Distelhorst, C.W. (2004) Bcl-2 functionally interacts with inositol 1,4,5-trisphosphate receptors to regulate calcium release from the ER in response to inositol 1,4,5-trisphosphate. *J. Cell Biol. 166(2),* 193-203.
7. Kuo, T.H., Kim, H.R., Zhu, L., Yu, Y., Lin, H.M., and Tsang, W. (1998) Modulation of endoplasmic reticulum calcium pump by Bcl-2, *Oncogene 17(15),* 1903-1910.

8. Dremina, E.S., Sharov, V.S., Kumar, K., Zaidi, A., Michaelis, E.K., and Schöneich, C. (2004) Anti-apoptotic protein Bcl-2 interacts with and destabilizes the sarcoplasmic/endoplasmic reticulum Ca2+-ATPase (SERCA), *Biochem. J. 383(Pt 2),* 361-370.
9. Dremina, E.S., Sharov, V.S., and Schöneich, C. (2006) Displacement of SERCA from SR lipid caveolae-related domains by Bcl-2: a possible mechanism for SERCA inactivation, *Biochemistry 45(1),* 175-184.
10. Zhang, Z., Lapolla, S.M., Annis, M.G., Truscott, M., Roberts, G.J., Miao, Y., Shao, Y., Tan, C., Peng, J., Johnson, A.E., Zhang, X.C., Andrews, D.W., and Lin, J. (2004) Bcl-2 homodimerization involves two distinct binding surfaces, a topographic arrangement that provides an effective mechanism for Bcl-2 to capture activated Bax, *J. Biol. Chem. 279(42),* 43920-43928.
11. Petros, A.M., Olejniczak, E.T., and Fesik, S.W. (2004) Structural biology of the Bcl-2 family of proteins, *Biochim. Biophys. Acta. 1644(2-3),* 83-94.
12. Yin, X.M., Oltvai, Z.N., and Korsmeyer, S.J. (1994) BH1 and BH2 domains of Bcl-2 are required for inhibition of apoptosis and heterodimerization with Bax, *Nature 369(6478),* 321-323.
13. Hengartner, M.O., and Horvitz, H.R. (1994) Activation of C. elegans cell death protein CED-9 by an amino-acid substitution in a domain conserved in Bcl-2, *Nature 369(6478),* 318-320.
14. Periasamy, M., and Kalyanasundaram, A. (2007) SERCA pump isoforms: their role in calcium transport and disease, *Muscle Nerve. 35(4),* 430-442.
15. MacLennan, D.H., Rice, W.J., and Green, N.M. (1997) The mechanism of Ca2+ transport by sarco(endo)plasmic reticulum Ca2+-ATPases, *J. Biol. Chem. 272(46),* 28815-28818.
16. Lancaster, C.R. (2002) A P-type ion pump at work, *Nat. Struct. Biol. 9(9),* 643-645.
17. Toyoshima, C., Nomura, H., and Sugita, Y. (2003) Structural basis of ion pumping by Ca(2+)-ATPase of sarcoplasmic reticulum, *FEBS Lett. 555(1),* 106-110.
18. Toyoshima, C., Nakasako, M., Nomura, H., and Ogawa, H. (2000) Crystal structure of the calcium pump of sarcoplasmic reticulum at 2.6 Å resolution, *Nature 405(6787),* 647-655.
19. Martonosi, A.N., and Pikula, S. (2003) The structure of the Ca2+-ATPase of sarcoplasmic reticulum, *Acta. Biochim. Pol. 50(2),* 337-365.
20. Hua, S., Ma, H., Lewis, D., Inesi, G., and Toyoshima, C. (2002) Functional role of "N" (nucleotide) and "P" (phosphorylation) domain interactions in the sarcoplasmic reticulum (SERCA) ATPase, *Biochemistry 41(7),* 2264-2272.
21. Ma, H., Lewis, D., Xu, C., Inesi, G., and Toyoshima, C. (2005) Functional and structural roles of critical amino acids within the"N", "P", and "A" domains of the Ca2+ ATPase (SERCA) headpiece, *Biochemistry 44(22),* 8090-8100.
22. McIntosh, D.B., Clausen, J.D., Woolley, D.G., MacLennan, D.H., Vilsen, B., and Andersen, J.P. (2003) ATP binding residues of sarcoplasmic reticulum Ca2+-ATPase, *Ann. N. Y. Acad. Sci. 986,*101-105.
23. Abu-Abed, M., Mal, T.K., Kainosho, M., MacLennan, D.H., and Ikura, M. (2002) Characterization of the ATP-binding domain of the sarco(endo)plasmic reticulum Ca(2+)-ATPase: probing nucleotide binding by multidimensional NMR, *Biochemistry 41(4),* 1156-1164.
24. Ma, H., Lewis, D., Xu, C., Inesi, G., and Toyoshima, C. (2005) Functional and structural roles of critical amino acids within the"N", "P", and "A" domains of the Ca2+ ATPase (SERCA) headpiece, *Biochemistry 44(22),* 8090-8100.

25. McIntosh, D.B., Clausen, J.D., Woolley, D.G., MacLennan, D.H., Vilsen, B., and Andersen, J.P. (2003) ATP binding residues of sarcoplasmic reticulum Ca2+-ATPase, *Ann. N. Y. Acad. Sci. 986,*101-105.
26. Clausen, J.D., McIntosh, D.B., Vilsen, B., Woolley, D.G., and Andersen, J.P. (2003) Importance of conserved N-domain residues Thr441, Glu442, Lys515, Arg560, and Leu562 of sarcoplasmic reticulum Ca2+-ATPase for MgATP binding and subsequent catalytic steps. Plasticity of the nucleotide-binding site, *J. Biol. Chem. 278(22),* 20245-20258.
27. Hua, S., Ma, H., Lewis, D., Inesi, G., and Toyoshima, C. (2002) Functional role of "N" (nucleotide) and "P" (phosphorylation) domain interactions in the sarcoplasmic reticulum (SERCA) ATPase, *Biochemistry 41(7),* 2264-2272.
28. Rossi, A.E., and Dirksen, R.T. (2006) Sarcoplasmic reticulum: the dynamic calcium governor of muscle, *Muscle Nerve. 33(6),* 715-731.
29. Dremina, E.S., Sharov, V.S., and Schöneich, C. (2006) HSP70 Protection Against the Inactivation of SERCA by Anti-Apoptotic Protein Bcl-2: aPossible Link Between Apoptosis, Oxidative Stress and Aging, *Free Radical Biol. Med. 41(1),* S80.
30. Shimuta, M., Komazaki, S., Nishi, M., Iino, M., Nakagawara, K., and Takeshima, H. (1998) Structure and expression of mitsugumin29 gene, *FEBS Lett. 431(2),* 263-267.
31. Nishi, M., Komazaki, S., Kurebayashi, N., Ogawa, Y., Noda, T., Iino, M., and Takeshima, H. (1999) Abnormal features in skeletal muscle from mice lacking mitsugumin29, *J. Cell Biol. 147(7),* 1473-1480.
32. Pan, Z., Hirata, Y., Nagaraj, R.Y., Zhao, J., Nishi, M., Hayek, S.M., Bhat, M.B., Takeshima, H., and Ma, J. (2004) Co-expression of MG29 and ryanodine receptor leads to apoptotic cell death: effect mediated by intracellular Ca2+ release, *J. Biol Chem. 279(19),* 19387-19390.
33. Pan, Z., Yang, D., Nagaraj, R.Y., Nosek, T.A., Nishi, M., Takeshima, H., Cheng, H., and Ma, J. (2002) Dysfunction of store-operated calcium channel in muscle cells lacking mg29, *Nat. Cell Biol. 4(5),* 379-383.
34. García-Sáez, A.J., Mingarro, I., Pérez-Payá, E., and Salgado, J. (2004) Membrane-insertion fragments of Bcl-xL, Bax, and Bid, *Biochemistry 43(34),* 10930-10943.
35. Schendel, S.L., Xie, Z., Montal, M.O., Matsuyama, S., Montal, M., and Reed, J.C. (1997) Channel formation by antiapoptotic protein Bcl-2, *Proc. Natl. Acad. Sci. U. S. A. 94(10),* 5113-5118.
36. Smart, E.J., Graf, G.A., McNiven, M.A., Sessa, W.C., Engelman, J.A., Scherer, P.E., Okamoto, T., and Lisanti, M.P. (1999) Caveolins, liquid-ordered domains, and signal transduction, *Mol. Cell Biol. 19(11),* 7289-7304.
37. Wang, Y., Tsui, Z., and Yang, F. (1999) Antagonistic effect of ganglioside GM1 and GM3 on the activity and conformation of sarcoplasmic reticulum Ca(2+)-ATPase, *FEBS Lett. 457(1),* 144-148.
38. Ahrends, R., Kosinski, J., Kirsch, D., Manelyte, L., Giron-Monzon, L., Hummerich, L., Schulz, O., Spengler, B., and Friedhoff, P. (2006) Identifying an interaction site between MutH and the C-terminal domain of MutL by crosslinking, affinity purification, chemical coding and mass spectrometry, *Nucleic Acids Res. 34(10),* 3169-3180.
39. Cai, K., Itoh, Y., and Khorana, H.G. (2001) Mapping of contact sites in complex formation between transducin and light-activated rhodopsin by covalent crosslinking: use of a photoactivatable reagent, *Proc. Natl. Acad. Sci. U. S. A. 98(9),* 4877-4882.

40. Ebright, Y.W., Chen, Y., Kim, Y., and Ebright, R.H. (1996) S-[2-(4-azidosalicylamido)ethylthio]-2-thiopyridine: radioiodinatable, cleavable, photoactivatible cross-linking agent, *Bioconjug. Chem. 7(3),* 380-384.

Chapter 5:

Unresolved Issues related to the SERCA/ Bcl-2Δ21 Investigation.

In the Scientific Method of experimental investigations, an experiment should be reported with all the relevant observations. The relevant observations include not only the things noticed in a successful experiment but also the problems encountered. All the problems encountered throughout the course of the project are summarized here.

5.1: Derivatization of Cys158 of Bcl-2Δ21 using Benzophenone-4-maleimide (BPM).

The very first problem encountered was the difficulty in BPM labeling of the Cys158 of the wild type Bcl-2Δ21 for photo cross-linking experiments. Since the Cys158 is buried in the interior of the molecule, BPM derivatization under the native conditions was not successful and hence more time was spent figuring out the optimum denaturing conditions for the BPM labeling reaction. The successful removal of the denaturing agent from the medium before the cross-linking reaction, so that there is no effect from excess denaturing agent on the association of SERCA/Bcl-2Δ21, was also challenging.

In order to verify the presence of BPM labeled Bcl-2Δ21, ESI-IonTrap-MS was utilized at the first place after the in-gel tryptic digestion. However the peptide of Bcl-2Δ21 with BPM-Cys158 could not be found in the MS data even after repeated trials using different enzymatic digestion conditions (such as in-solution digestion,

different ratios of trypsin: Bcl-2Δ21, digestion in the presence of Ca^{2+} which is a co-factor for trypsin) and also using a longer time for on-line chromatographic separation of tryptic peptides. Finally the BPM labeling of the Cys158 could be confirmed using ESI-FTICR-MS.

5.2: Photo and chemical cross-linking reactions.

More time than expected was spent in optimizing cross-linking reaction conditions. The photo cross-linking experiment was repeated again and again, changing one variable at a time, until the optimum time for co-incubation of SERCA/Bcl-2Δ21 prior to the UV irradiation, the ratio of SERCA: Bcl-2Δ21, the UV irradiation time and also the UV intensity were established. The failure to confirm the photo cross-linked products in the western blot with SERCA antibody was another problem.

The purified Sarcoplasmic Reticulum (SR) membrane, the source of SERCA, contains a number of other proteins with apparent molecular weights identical to SERCA, Bcl-2Δ21 and also to the size of cross-linked products. This was a major problem in cross-linking experiments which caused some ambiguity in the identification of cross-linked products of SERCA/Bcl-2Δ21 in the western blots. For the same reason the Coomassie Blue stained gels of cross-linked samples did not help at all in identification of the cross-linked bands and identical bands were seen even with the control sample without Bcl-2Δ21. However the presence of the SR membrane assures the native conformation of the trans-membrane protein, SERCA. If

SERCA were separated from the SR membrane, it should be incorporated into a synthetic membrane prior to each experiment and that would make the cross-linking experiment lengthier and more complex.

Chemical cross-linking experiments, using amine and thiol reactive heterobifunctional chemical cross-linking reagents (Chapter 2), also caused some problems. Bcl-2Δ21 modified with the linker first, followed by the addition of SR, did not show any cross-linked products of Bcl-2Δ21. Possibly the modification of the amine groups of Bcl-2Δ21 by the linker prevents the association with SERCA. However when the reaction was performed starting with SR; i.e., the linker is added to SR first followed by the addition of Bcl-2Δ21, resulted in the cross-linked bands (see Chapter 2).

5.3: Mass spectrometric analysis of cross-linked products.

As mentioned earlier, since the purified Sarcoplasmic Reticulum (SR) membrane, the source of SERCA, contains number of other proteins, the cross-linked samples are always contaminated with these other unnecessary proteins. Therefore, relatively more efficient in-solution enzymatic digestion could not be involved and in-gel digestion which causes an extensive sample loss in each step was utilized. Even though the 1D-SDS-PAGE helped to some extent in separation of the cross-linked products from other SR proteins, the gel bands of interest were still contaminated with other proteins which are identical to the size of the cross-linked products. These other proteins are relatively highly abundant in the gel band and suppress the low

abundant cross-linked peptides during the MS run. The presence of these other proteins in the digest made the identification of the cross-linked peptides within the MS data more difficult.

Even though there are several software tools are developed to date for protein cross-linking studies, one that identifies peptides cross-linked through the photo cross-linking reagent, BPM was not available at least by the time of the MS data analysis of the cross-linked samples. Therefore the MS data were analyzed manually looking for the cross-linked peptides of SERCA and Bcl-2Δ21. This tedious, time consuming manual search was a major difficulty in the project.

5.4: Mutants of Bcl-2Δ21.

Due to the difficulty in BPM labeling of the Cys158 of the wild type Bcl-2Δ21, for photo cross-linking experiments, the two double-cysteine mutants, S117C and S205C, of Bcl-2Δ21 were generated. However these mutants did not result in successful photo cross-linking reactions. Probably the presence of two Cys residues (Cys158 and Cys117/Cys 205) in the molecule caused some unfavorable homo oligomerization of Bcl-2Δ21 molecules. Therefore production of four single-cysteine mutants (S24C/C158S, S205C/C158S, S117C/C158S and S167C/C158S) was attempted. Only two mutations were successful (S24C/C158S and S205C/C158S) and the other two failed (S117C/C158S and S167C/C158S). Expression of four other mutants (G145E, W188A, I14G and I 19G), which have been identified as loss-of-function mutants on anti-apoptotic activity of Bcl-2Δ21, was attempted hoping to

study their effect on the SERCA/Bcl-2Δ21 interactions. However, only two mutagenesis reactions (G145E, W188A) were successful.

The other difficulty associated with the mutants was the purification of enough proteins for experiments. Both the Cys-mutants, S24C/C158S and S205C/C158S, and also W188A of Bcl-2Δ21 yielded a very small amount of proteins from 1L of Luria-Bertani (LB) medium, compared to the wild type protein. Therefore, to have sufficient proteins for each experiment, each of these mutants was purified from bacteria grown in at least 2-3L of LB medium.